AD-A058 636 VIRGINIA UNIV CHARLOTTESVILLE DEPT OF ENVIRONMENTAL --ETC F/G 8/3
ANALYSIS OF SPATIAL AND TEMPORAL SHORELINE VARIATIONS ALONG THE--ETC(U)
SEP 78 R DOLAN, B HAYDEN, W FELDER, J HEYWOOD N00014-75-C-0480
UNCLASSIFIED TR-19 NL

1 OF 2
AD
A058636

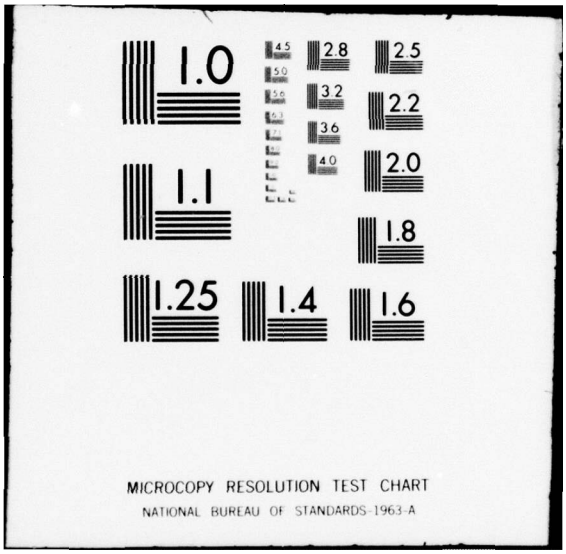
1.0
1.1
1.25
1.4
1.6
1.8
2.0
2.2
2.5
2.8
3.2
3.6
4.0
4.5
5.0
5.6
6.3
MICROCOPY RESOLUTION TEST CHART
NATIONAL BUREAU OF STANDARDS-1963-A

CLASSIFICATION OF COASTAL ENVIRONMENTS

TECHNICAL REPORT 19

(12)

ANALYSIS OF SPATIAL AND TEMPORAL SHORELINE VARIATIONS ALONG THE UNITED STATES ATLANTIC COAST

LEVEL II

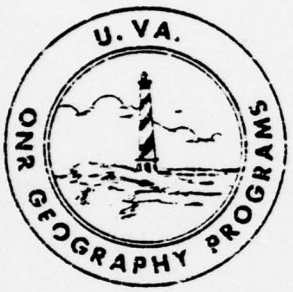

Robert Dolan
Bruce Hayden
Wilson Felder
Jeffrey Heywood
Phyllis Ross

Department of Environmental Sciences
University of Virginia

SEPTEMBER, 1978

OFFICE OF NAVAL RESEARCH

GEOGRAPHY PROGRAMS

N00014-75-C-0480 - TASK #NR389 170

APPROVED FOR PUBLIC RELEASE

DISTRIBUTION UNLIMITED

CLASSIFICATION OF COASTAL ENVIRONMENTS

TECHNICAL REPORT 19

ANALYSIS OF SPATIAL AND TEMPORAL SHORELINE VARIATIONS ALONG THE UNITED STATES ATLANTIC COAST

Technical rept.

134 p.

Robert Dolan,
Bruce Hayden,
Wilson Felder,
Jeffrey Heywood
Phyllis Ross

Department of Environmental Sciences
University of Virginia
Charlottesville

SEPTEMBER, 1978

OFFICE OF NAVAL RESEARCH

GEOGRAPHY PROGRAMS

N00014-75-C-0480 - TASK #NR389 170

APPROVED FOR PUBLIC RELEASE

DISTRIBUTION UNLIMITED

TECHNICAL REPORT No. 19

CONTENTS

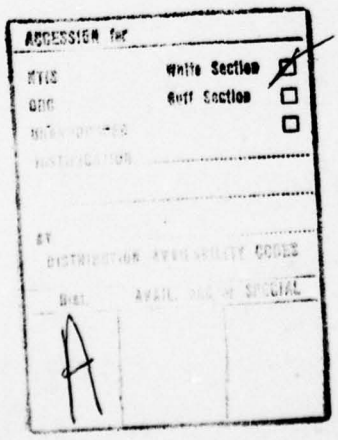

A NEW PHOTOGRAMMETRIC METHOD FOR DETERMINING SHORELINE EROSION

Robert Dolan, Bruce Hayden, and Jeffrey Heywood

Department of Environmental Sciences
University of Virginia
Charlottesville, Virginia 22903

Reprint from *Coastal Engineering* 2(1978)21-39

ANALYSIS OF COASTAL EROSION AND STORM SURGE HAZARDS

Robert Dolan, Bruce Hayden, and Jeffrey Heywood

Department of Environmental Sciences
University of Virginia
Charlottesville, Virginia 22903

Reprint from *Coastal Engineering* 2(1978)51-53

Coastal Engineering, 2 (1978) 41—53

ANALYSIS OF COASTAL EROSION AND STORM SURGE HAZARDS

ROBERT DOLAN, BRUCE HAYDEN and JEFFREY HEYWOOD

Department of Environmental Sciences, University of Virginia, Charlottesville, Va. (U.S.A.)

(Received July 18, 1977; accepted December 2, 1977)

ABSTRACT

Dolan, R., Hayden, B. and Heywood, J., 1978. Analysis of coastal erosion and storm surge hazards. Coastal Eng., 2: 41—53.

Prediction of shoreline erosion and storm-surge penetration is essential for coastal planning and management in the United States. Historical aerial photography provides the best data base for information that can be used in establishing hazard zones along and across the coast. In this paper we summarize a new methodology for deriving risk probabilities. The method is tested and applied along a highly developed (90 km) reach of the New Jersey coast.

INTRODUCTION

Along the Atlantic coast of North America hurricanes and severe winter storms are responsible for frequent and sometimes dramatic landscape modification. In addition to the physical and ecological changes that occur, private land holdings are destroyed, communication and transportation facilities are disrupted, and the loss of life is not uncommon. In spite of the obvious hazards, development has proceeded at a rapid pace (Fig. 1).

To marine scientists and coastal engineers, the shore zone has long been recognized as an element of a highly dynamic physical system. The information base essential for good planning and management includes the current state of this system and its rates of change through time. Information of this type is now required in the United States for various sections of the National Environmental Policy Act of 1969, the Coastal Zone Management Act of 1972 and 1976, the National Flood Insurance Act of 1968, and the Flood Disaster Protection Act of 1973.

DATA COLLECTION

The analysis of shoreline dynamics for the purposes of establishing coastal hazard zones requires repetitive sampling of the shoreline and storm-surge penetration line, both spatially and temporally. Information of this type can

Fig. 1. Coastal development at Ocean City, Maryland.

be obtained from: (1) ground surveys; (2) maps and charts; and (3) aerial photographs. Based upon our research, we are convinced that the use of metric aerial photography is the best and most feasible data source for a nation-wide mapping effort. For this reason we have developed an Orthogonal Grid Address System (OGAS) to systematize the analysis of shorezone dynamics and to provide a uniform data base for establishing hazard zones.

The OGAS method provides for the rapid and systematic acquisition of shoreline information from historical aerial photographs at 100-m intervals along the coast (Dolan et al., 1978). Comparison of the data derived from different years permits the definition of statistical properties of shoreline change, storm-surge penetration, and the risks and hazards associated with development within these zones. The value of defining the statistical variability of beach profile data was emphasized recently by Hale (1977).

In brief, standard 1:5,000 scale base maps of the study region are prepared. These maps are produced by photo-enlargement of $7\frac{1}{2}$ min series United States Geological Survey topographic maps (1:24,000), which provides an area 3,500 m by 2,100 m. The frame of each base map is oriented with the long axis parallel to the coastline and positioned over the active portion of the coast. One long edge, lying entirely over the ocean, serves as the base line from which all measurements are made.

The historical aerial photographs are then enlarged to the exact scale of the base map through the use of a reflecting projector. On a transparent over-

lay placed over the base map, the shoreline and the storm-penetration line are traced from the projection. These tracings prepared from 1:5,000-scale projections of the sequence of historical photographs constitute the raw cartographic data base from which subsequent measurements are made. In this study, the shoreline is operationally defined as the high-water line. The storm-surge penetration line is defined as the line that separates the active, non-vegetated sand areas from the areas of continuous stands of grass and shrub.

On each tracing a transparent grid is overlaid — the grid is rectilinear with 100-m spacings. Any coastal location is thus specified by base map number and co-ordinates of the grid. The position of the shoreline and other lines of interest, with respect to the base map base line is then measured to the nearest 5 m. These data are punched on IBM cards for subsequent analyses (Dolan et al., 1978).

RESULTS

Among the several information sets generated by the OGAS program is a graph of the mean rate of change of shoreline calculated over all time periods and plotted with an envelope of ± one standard deviation (Fig. 2). This is a very useful graph for determining areas along the coast which have been subjected to the greatest change. It visually presents a measure of the erosion rates, stable areas, and areas along the coast that are more vulnerable to erosion. Numerical values for the mean and standard deviation at each of the 100-m transects are listed. The standard deviation lines are of additional value because they couple the historical trend with episodic changes associated with extreme storm events.

These statistics, as with any statistics of natural systems, must be applied with caution. Although there is a wealth of geological information to confirm that shoreline change has been underway for many coasts of the world on a more or less continuous basis for centuries, aerial photography is available for only three or at most four decades. The resulting statistics are thus based upon samples of short periods of a much longer trend. One must therefore assume that the past 30 to 40 years of shoreline change is representative of the longer trend, and thus indicative of the future. Complementary information from other disciplines, including oceanography, climatology, and geomorphology can be important in establishing confidence in the statistics.

In addition, the selection of individual photographic flights can bias the statistics. In our analysis, for example, we included among our five sets of photography a flight taken soon after the Ash-Wednesday storm of 1962 (125-year return interval). This storm alone is responsible for a considerable amount of statistical variance in our data set.

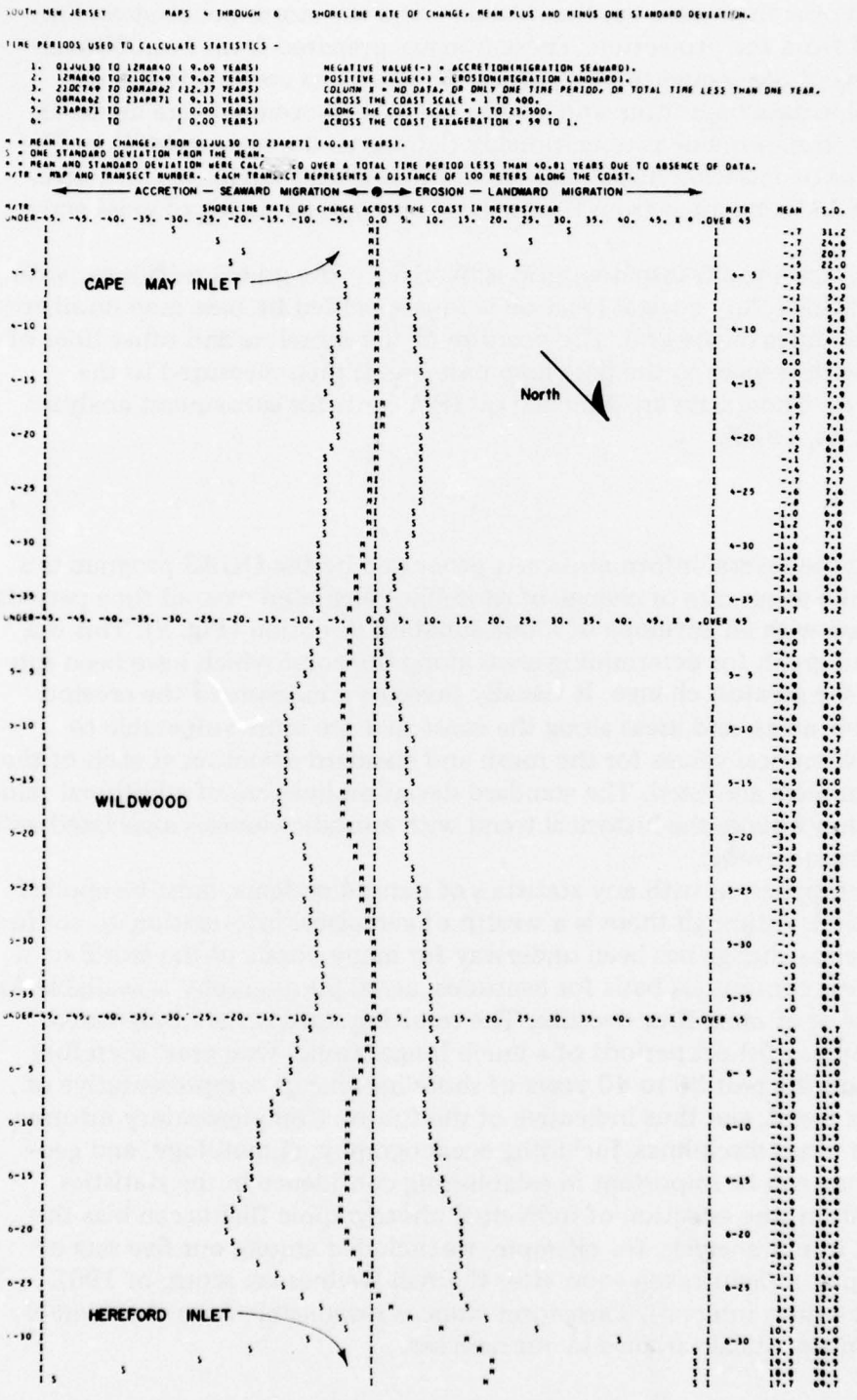

Fig. 2. Graph showing mean rate of change of shoreline ± one standard deviation for the southern New Jersey coast from Cape May Inlet to Hereford Inlet (1930—1971).

APPLICATION

Three separate lines are related to the question of risks and hazards in the shorezone (Fig. 3): (1) the shoreline; (2) the landward limit of the major destruction zone; and (3) the landward limit of the surge damage zone. Since each of these lines vary in position over time, the risk or probability

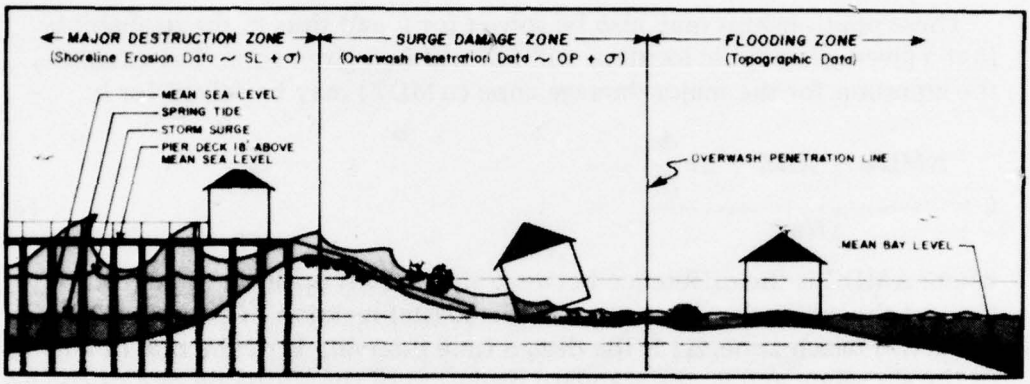

Fig. 3. Hazard zones across the coast.

that a place or point will fall within one of the zones defined by these lines likewise varies over time. These probabilities can be estimated from the data base provided by the OGAS program.

Future positions of the shoreline and the landward limits of the major destruction and surge damage zones (Fig. 3) may be calculated for specified time intervals and desired probability levels. The information required for these calculations is: (1) the rate of shoreline change (ds/dt); (2) the standard deviation of shoreline change rates (σ_s); (3) the rate of change of the storm-surge penetration line (dv/dt); and (4) the standard deviation of the rate of change of storm-surge penetration line (σ_v).

The landward limit of the shoreline (ΔS) for a design time interval (Δt) specified for a given probability level (p) is given by:

$$\Delta S\Big]_{\Delta t,p} = \Delta t\left(\frac{ds}{dt} + k\sigma_s\right) \tag{1}$$

where k is the number of standard deviations appropriate to the specified probability level.

The landward limit of the major damage zone (ΔMDZ) for a design time interval (Δt) specified for a given probability level (p) is given by:

$$\Delta \mathrm{MDZ}\Big]_{\Delta t,p} = \mathrm{ABZ} + \Delta t\left(\frac{ds}{dt} + k\sigma_s\right) \tag{2}$$

where ABZ is the width of the existing active beach zone. In other applica-

tions and if data are available, temporal variation of ABZ may be incorporated into eq. 2.

The landward limit of the surge damage zone (ΔSDZ) for a design time interval (Δt) specified for a given probability level (p) is given by:

$$\Delta \mathrm{SDZ}\Big]_{\Delta t, p} = \Delta t \left(\frac{dv}{dt} + k\sigma_v \right) \tag{3}$$

These relationships may also be solved for k and thus p, the probability that a given geographic location will fall within a given zone. For example, the equation for the major damage zone (ΔMDZ) may be solved for k:

$$k = \frac{\Delta \mathrm{MDZ} - \mathrm{ABZ} - \Delta t \dfrac{ds}{dt}}{\Delta t(\sigma_s)} \tag{4}$$

where ΔMDZ is the difference between the current position of landward limit of the major damage zone and the coastal location of concern; ABZ is the active beach zone, Δt is the design time interval, ds/dt the rate of change of the shoreline and σ_s the standard deviation of the shoreline rate of change. Once k is calculated, the probability may be found. Using solutions of this type the probability for any location may be calculated.

The relationship between probability levels (p) and equivalent k values is:

p:	0.99	0.95	0.90	0.85	0.80	0.75	0.70	0.65	0.60	0.55	0.50
k:	2.33	1.65	1.28	1.04	0.84	0.67	0.52	0.39	0.25	0.13	0.00

Since k is merely the number of δ desired, thus p is accordingly specified.

THE NEW JERSEY COAST

Under sponsorship of the Federal Flood Insurance Program of the Department of Housing and Urban Development, we conducted a demonstration project using the OGAS program along the New Jersey coast. Changes in the position of the shoreline and storm-surge penetration line were mapped from Cape May to Little Egg Inlet, a distance of 90 km (Fig. 4), from five sets of aerial photography spanning the period from 1930 to 1971.

The New Jersey coastline is not an unbroken reach; it is segmented into eight individual "islands" by a series of inlets. Our analysis shows that rates of change in both the shoreline and storm-surge penetration line for islands *IV* and *VI* (Fig. 5) have very low variance along the coast, so the means can serve as good predictors. In contrast, the means for islands *II*, *VII*, and *VIII* give poor estimates because the variation is high; islands *III* and *V* have modest variation. Thus it is clear that island averages are not necessarily the best choices for establishing risk and hazard zones along the New Jersey coast and that stratification into smaller segments would be preferable.

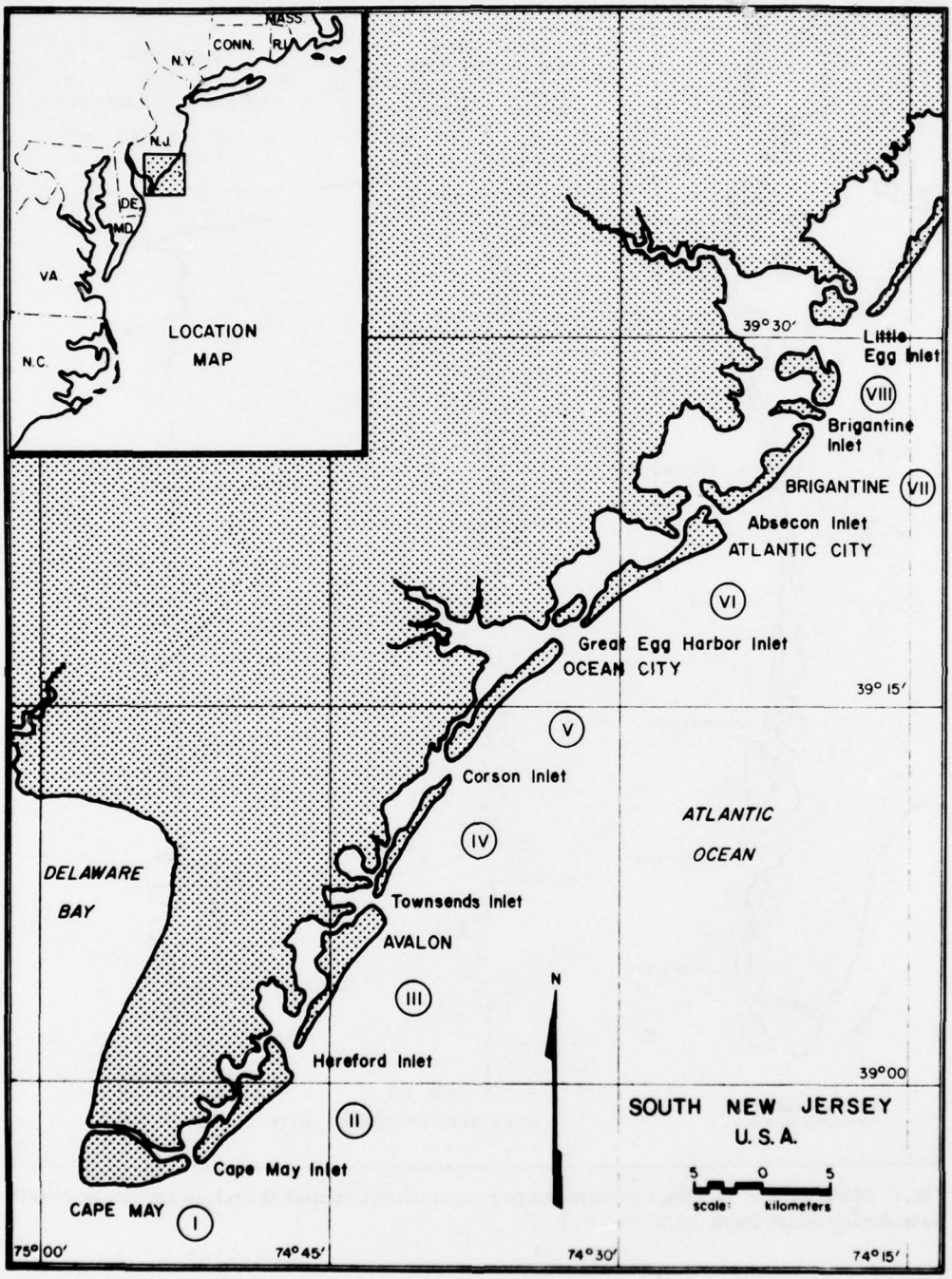

Fig. 4. The southern coast of New Jersey, U.S.A.

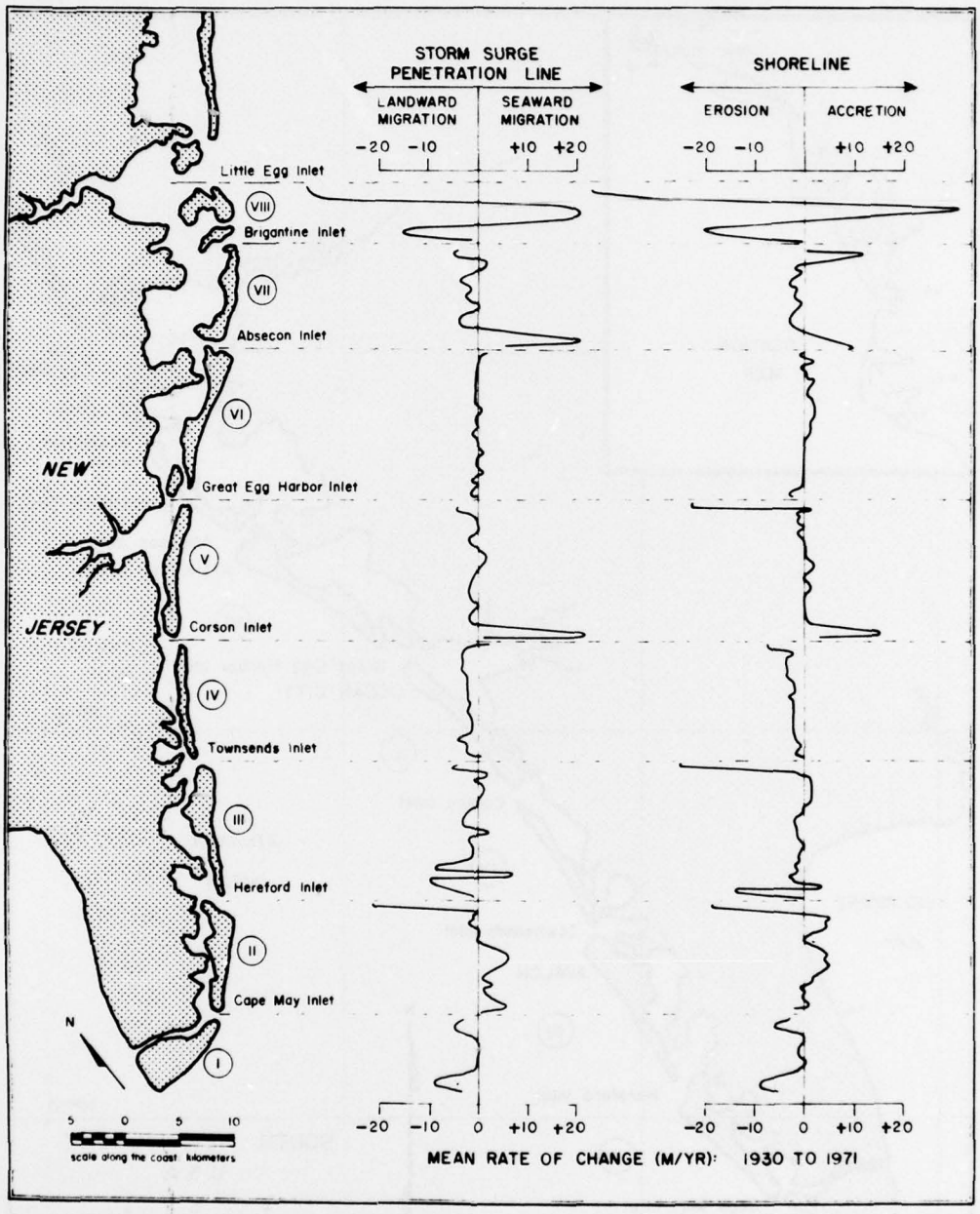

Fig. 5. Mean rate of change in storm-surge penetration line and shoreline for the southern New Jersey coast from 1930 to 1971.

Sample calculations for formulas 1 and 3 are provided in Tables I, II, III, and IV for each of the eight islands included in the New Jersey demonstration study — changes in position of the defining lines of the various hazard zones are given. Table I presents data for the mean (p = 0.5) shoreline posi-

TABLE I

Forecasted mean shoreline position (in m) relative to current shoreline ($p = 0.5; k = 0$)*

Island number	Forecasted position for: Δt = 30 yr.	Δt = 66 yr.
I	−90	−198
II	+27	+59
III	−21	−46
IV	−75	−165
V	+18	+40
VI	+21	+46
VII	+18	+40
VIII	+81	+178

*Probability that the shoreline will be at or seaward of the distance given. A plus sign denotes a seaward direction of change (accretion), and a minus sign indicates a landward direction of change (erosion).

TABLE II

Forecasted shoreline position (in m) relative to current shoreline ($p = 0.84; k = 1.0$)*

Island number	Forecasted position for: Δt = 30 yr.	Δt = 66 yr.
I	−177	−389
II	−129	−284
III	−102	−224
IV	−108	−238
V	−72	−158
VI	−9	−20
VII	−111	−244
VIII	−528	−1,162

*Probability that the shoreline will be at or seaward of the distance given. A plus sign denotes a seaward direction of change (accretion), and a minus sign indicates a landward direction of change (erosion).

tion for 30 and 66 years hence. In Table II the probability constraint is raised to 0.84, or one chance in seven that the shoreline will be landward of the line defined. Tables III and IV provide equivalent information for the landward limit of the surge damage zone.

DISCUSSION: THE BASE LINE PROBLEM

The risk of ocean front flooding storm-surge damage decreases inland from the shoreline, but the shoreline is not a fixed feature of the coast. Recession

TABLE III

Forecasted mean position of the landward limit of the storm-surge damage zone relative to current storm-surge penetration line ($p = 0.5; k = 0$)*

Island number	Forecasted mean position (in m) for: Δt = 30 yr.	Δt = 66 yr.
I	−81	−178
II	+36	+79
III	−42	−92
IV	−60	−132
V	+15	+33
VI	0	0
VII	+48	+106
VIII	+138	+304

*Probability that the storm-surge penetration line will be at or seaward of the distance given. A plus sign denotes seaward migration, and a minus sign indicates landward migration.

TABLE IV

Forecasted landward limit (in m) of storm-surge damage zone relative to current storm-surge penetration line ($p = 0.84; k = 1.0$)*

Island number	Forecasted limit for: Δt = 30 yr.	Δt = 66 yr.
I	−168	−370
II	−105	−231
III	−171	−376
IV	−102	−224
V	−108	−238
VI	−24	−53
VII	−159	−350
VIII	−264	−581

*Probability that the storm-surge penetration line will be at or seaward of the distance given. A plus sign denotes seaward migration, and a minus sign indicates landward migration.

and accretion occur throughout the year as the beach responds to waves, tides, and sea level changes, so the manner in which the risk decreases inland from the shoreline varies in time. Therefore, the best base line for establishing specific hazard zones is the line with the least variation on time scales of less than the annual summer—winter climatic cycle, yet sensitive to longer term variation in the shoreline caused by changes in sea level or loss of sediment.

On maps and charts the shoreline is usually defined by mean high water or mean sea level. Neither of these lines are recognizable in the field or on aerial

photographs. As such they are not suitable for base lines upon which to define the risks of coastal hazards.

Of the several linear features of the shorezone, aerial photo interpretors have relied upon the high water line (HWL) as the best delineator of the shoreline. Under most conditions this line is relatively stable over the tidal cycle (Stafford, 1968), and for the purposes of field surveys, the HWL is clearly recognizable for several hours following high tide. In addition, the HWL is the most consistently recognizable linear feature of the shoreface on aerial photographs. While the HWL is relatively constant over the tidal cycle, it is subject to the following variations which must be recognized and planned for.

High tide variation

Over the course of the lunar month the height of tidal maxima varies between the extreme high spring tide maximum and the extreme low neap tide maximum. The position of the HWL on the beach face varies accordingly. Appropriate selection of the survey time within the lunar cycle or adjustment using tide tables is adequate correction for this variation.

Wave height variation

The distance of wave run-up on the beach face is in part determined by wave height. The higher the breaking wave the greater is the run-up. The impact of this contribution can be minimized by restricting survey periods to surf conditions of less than some specified height. Such a restriction eliminates survey on days of storm wave condition.

Beach slope variations

Beach slopes vary over time especially during and immediately following storms when large amounts of sediment are exchanged between the beach and the offshore. Variations in beach slope also are evident over the annual cycle. This variation in HWL due to temporal beach slope variation may be accounted for by: (a) eliminating surveys immediately following storm events; and (b) by seasonal survey time with and without required adjustments.

SUMMARY

Mean rates of change in shoreline and storm-surge penetration line for the eight islands of the southern 90 km of the New Jersey coast are summarized in Table V; standard deviations of rates of change are also presented. The magnitude of both the trends and the extremes are evident; even within areas with an accretion trend (island VIII) there have been periods of erosion. Therefore, in order to establish meaningful zones, consideration of both the

TABLE V

*Mean rate of change and standard deviation of rate of change in shoreline and storm-surge penetration line for eight barrier islands on the southern New Jersey coast (All figures in m/yr.)**

Island number	Mean rate of change		Standard deviation of rate of change	
	shoreline	SSP line	shoreline	SSP line
I	−3.0	−2.7	2.9	2.9
II	+0.9	+1.2	5.2	4.7
III	−0.7	−1.4	2.7	4.3
IV	−2.5	−2.0	1.1	1.4
V	+0.6	+0.5	3.0	4.1
VI	+0.7	0	1.0	0.8
VII	+0.6	+1.6	4.3	6.9
VIII	+2.7	+4.6	20.3	13.4

*A plus sign denotes seaward migration, and a minus sign indicates landward migration.

averages and the variances is essential. Given these statistics for the shoreline and the line of storm-surge penetration, probabilities of the various hazards may be derived.

The problems of risks and hazards in coastal environments differ from the equivalent flood plain problems because of secular variation due to shoreline change. This precludes estimates of storm-surge return intervals for assigning hazard probabilities. Accordingly, given a location on the coast, the hazard due to a "one-hundred-year storm" increases systematically with time on an eroding coast. Since there may be several causes for shoreline change, the problem cannot be resolved by further investigation of storm frequencies and magnitudes. The only alternative is empirical evaluations of historical data. To insure that an adequate information base is available, a systematic photo reconnaissance of the coast should be initiated. As the sample size in erosion studies increases, confidence levels in the derived statistics will improve.

Our investigation also resulted in this final observation. In those areas along the New Jersey coast that have been engineered to stabilize the shoreline (groins) and to prevent storm-surge penetration (seawalls), the mean rates of change have been greatly reduced — one meter or less per year in many areas; however, in these same areas, the standard deviations of the rates of change are high. This suggests that although the engineering works have succeeded in stabilizing the shoreline system, when extreme storms do occur, damage is often greater within the stabilized areas. Thus, the hazard of systematic erosion damage is decreased, but the risk of episodic storm damage due to storm-surge penetration is increased.

ACKNOWLEDGEMENTS

We wish to give special acknowledgement to our research assistant, Ms. Kathy Schroeder, who performed the aerial photograph interpretation for the historical erosion and storm-surge penetration data. The research was made possible through funding from the Department of Housing and Urban Development, NASA-Goddard Space Flight Center, and The National Park Service. Aerial photography for the New Jersey study was provided by the New Jersey Office of Shore Protection. Finally we wish to thank the Chesapeake Bay Ecological Program Office for providing services and imagery essential to the development of our method of measuring coastal change.

REFERENCES

Dolan, R., Hayden, B. and Heywood, J., 1978. A new photogrammetric method for determining shoreline erosion, Coastal Eng., 2:

Hale, J.S., 1977. Coastal sediments, Los Angeles county. Coastal Sediments '77, Fifth Symposium of the Waterway, Port, Coastal and Ocean Division of ASCE.

Stafford, D.B., 1968. Development and Evaluation of a Procedure for Using Aerial Photographs to Conduct a Survey of Coastal Erosion. Report prepared for State of North Carolina, Dept. of Civil Engineering, North Carolina State University, Raleigh, North Carolina. (Also unpublished PhD Thesis).

SPATIAL AND TEMPORAL ANALYSES OF SHORELINE VARIATIONS

Bruce Hayden, Robert Dolan, and Wilson Felder

Department of Environmental Sciences
University of Virginia
Charlottesville, Virginia 22903

Submitted for publication in *Coastal Engineering*
August 3, 1978

SPATIAL AND TEMPORAL ANALYSES OF SHORELINE VARIATIONS

Bruce Hayden

Robert Dolan

Wilson Felder

Department of Environmental Sciences

University of Virginia

Charlottesville, Virginia

ABSTRACT

Using detailed data from historical aerial photography, high resolution (100-m) shoreline and storm surge penetration line rates-of-change and variance were calculated for 428 km of coast between New Jersey and Cape Lookout, North Carolina. Shoreline erosion rates along the U.S. mid-Atlantic coast average 0.6 m/yr but commonly vary ($\pm$ 1σ) along-the-coast from -3.6 m/yr to 2.4 m/yr and from -6.8 m/yr to 5.6 m/yr on a decade to decade basis.

Spatial and temporal variances in shoreline change rates make the design of coastal experiments and systematic monitoring programs difficult. The precision of measurements of the rates of change of the shoreline and storm-surge penetration line decrease as the along-the-coast sampling interval increases. This decrease follows an hyperbolic tangent form of decline.

For the U.S. mid-Atlantic coast a sample spacing of 500 km will provide an estimate of the mean shoreline rate-of-change to within $\pm$ 0.25σ of the higher resolution (100-m) estimate. The average standard deviation of shoreline change rates for the U.S. mid-Atlantic Coast is $\pm$ 3.01 m/yr. Consequently, a 500-m sampling spacing will result in a precision of $\pm$ 0.75 m/yr for shoreline change. In addition to the hyperbolic tangent decline of measurement precision, along-the-coast periodicities in shoreline and storm-surge penetration line rates of change occur. Accordingly, unless the objective of the measurement program is to define these periodicities, a constant interval sampling should be avoided.

INTRODUCTION

We recently reported a new methodology for measuring historical changes in the shoreline and storm-surge penetration limit along sedimentary coasts (Dolan et al.,1978). Using an orthogonal coordinate system with transects spaced at 100-m intervals along-the-coast, we recorded to the nearest 5-m each point at which the shoreline and the storm-surge penetration (overwash) line intersected the across-the-shore transects along 428 km of the U.S. mid-Atlantic Coast (Fig. 1). This step was repeated up to seven times with aerial photographs dating from 1934 to 1977. The results yielded a continuum of high-resolution data beginning in New

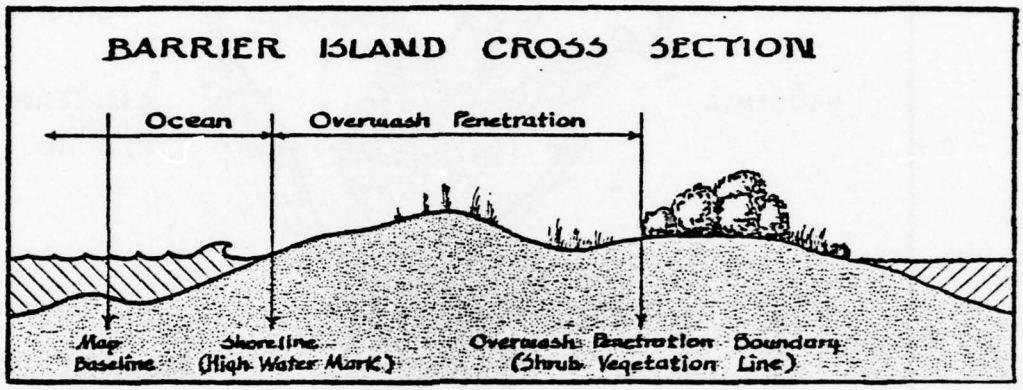

FIGURE 1 - DEFINITION OF SHORELINE (SL) AND STORM-SURGE (OVERWASH) PENETRATION LINE (SP)

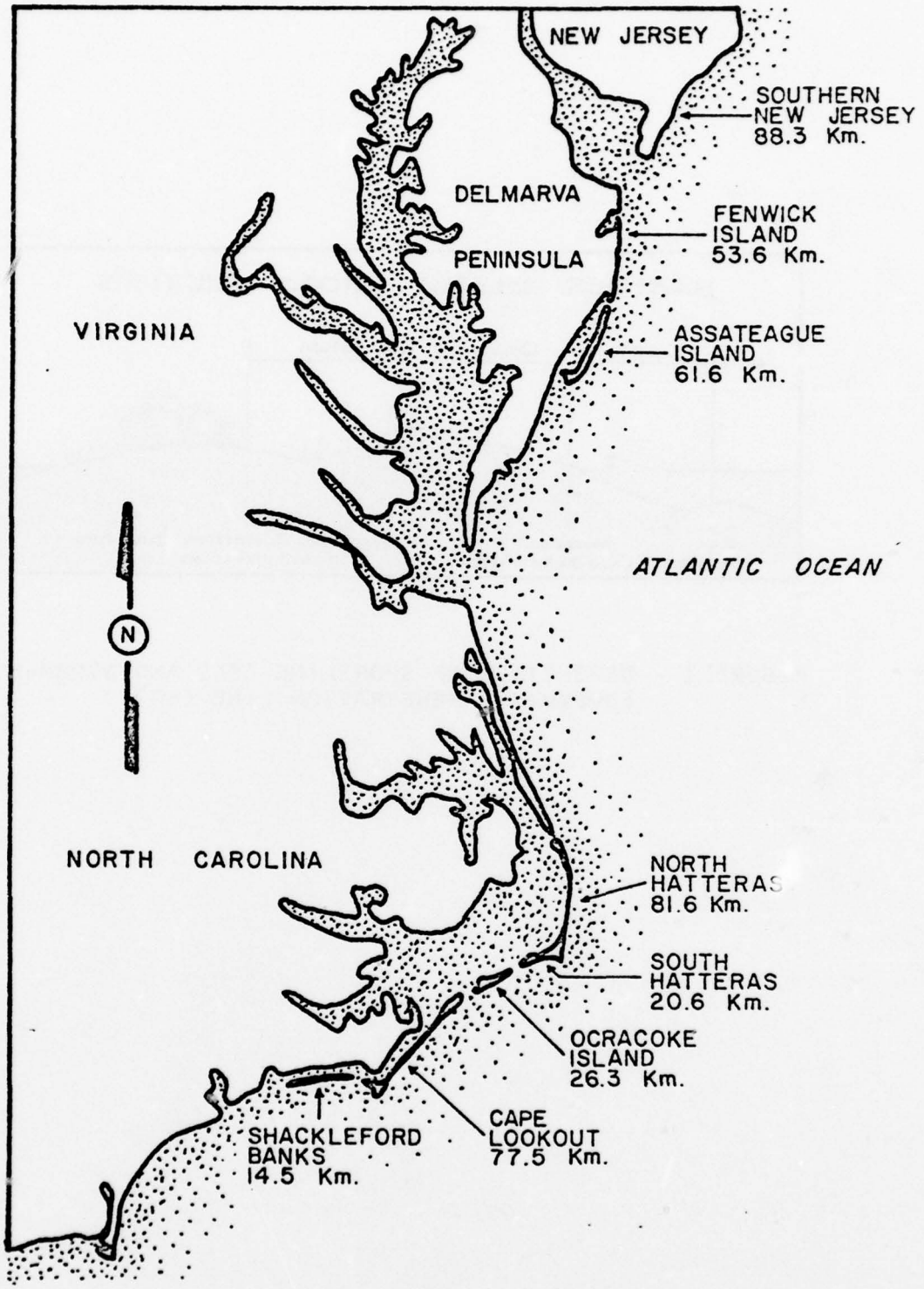

FIGURE 2 - LOCATION OF STUDY AREAS

Jersey and ending in North Carolina (Fig. 2). These data were analyzed to determine the spatial (along-the-coast) and temporal (decade-to-decade) persistence of the means and variances of the rates of shoreline change. The results provide fundamental information about the variation of sedimentary coasts which should prove of value in the design of experiments and development of systematic monitoring programs.

Two long-standing sampling questions are considered:

1) What are the relative magnitudes of the spatial and temporal variations of shoreline changes?

2) What is the effect of different sampling intervals on the statistical stability of measurements of shoreline change?

To answer these questions, we calculated the means and standard deviations of: 1) the rate of shoreline change ($\overline{SL}$), 2) the standard deviation of the rate of shoreline change (σSL), 3) the rate of change of the inland limit of storm-surge penetration ($\overline{SP}$), and 4) the standard deviation of this rate (σSP) for 14 barrier islands along the Atlantic coast. In addition, we determined the departures from the island-wide means and standard deviations which resulted with sampling intervals greater than 100 meters.

TABLE I

Spatial means (μ) and standard deviations (σ) of the long-term mean rates of change of the shoreline ($\overline{SL}$), the standard deviations of SL, the long-term mean rates of change of the storm surge penetration line ($\overline{SP}$), and the standard deviations of SP (m/yr). Negative sign indicates recession and a positive sign accretion. N indicates the sample size.

Temporal	$\overline{SL}$		σSL		$\overline{SP}$		σSP	
Spatial	μ	σ	μ	σ	μ	σ	μ	σ
Shackleford N = 123	-0.97	2.74	2.87	1.21	+5.36	4.08	19.79	12.07
Core Banks N = 392	-0.22	2.02	4.85	3.04	-0.26	2.06	7.64	5.31
Portsmouth N = 220	-0.96	0.80	16.40	8.14	+3.04	4.82	18.34	10.27
Ocracoke N = 239	+0.59	3.11	8.36	5.65	+24.16	23.63	32.46	27.44
S. Hatteras N = 175	+0.37	1.33	4.85	2.93	+4.71	2.15	6.36	3.20
N. Hatteras N = 600	-1.94	1.96	7.22	4.27	+4.96	7.04	16.08	10.58
Assateague N = 498	-1.63	1.96	5.67	3.55	+2.47	6.72	15.34	14.43
Fenwick N = 524	-0.58	1.20	3.32	0.95	+2.55	2.43	12.08	6.92
Cape May N = 90	-2.97	2.88	2.74	1.64	-2.72	2.91	10.06	7.09
Seven Mile B. N = 230	-0.60	7.92	11.23	15.52	+0.47	7.56	14.04	12.90
Ludlam N = 102	-2.28	1.40	2.85	1.45	-1.98	1.22	20.82	10.06
Peck Beach N = 123	+0.79	3.57	4.35	5.13	+0.60	4.15	13.11	5.41
Ventnor N = 135	+0.65	1.03	3.58	2.21	+0.01	0.81	8.32	12.11
Brigantine N = 101	+1.05	5.10	7.91	5.98	+1.70	6.90	9.50	0.75
Grand Means	-0.62	3.01	6.16	4.83	+3.22	5.95	14.57	9.95

MEANS AND VARIANCES

The means and standard deviations of the four variables ($\overline{SL}$, σSL, $\overline{SP}$, and σSP) for the 14 barrier islands comprising the 428 km study area are shown in Table I. For the average island within this reach, the long-term mean rate of shoreline change is 0.62 m/yr. The highest erosion rate was found at Cape May, New Jersey, (2.97 m/yr) and the highest accretion rate was on Brigantine Island, New Jersey, (1.05 m/yr). Variations in shoreline change rates within islands were in general as large and sometimes an order of magnitude larger than the island wide mean rates with an average value of $\pm$ 3.01 m/yr. Temporal variations of shoreline change rates averaged $\pm$ 6.16 m/yr, or an order of magnitude greater than the average rate of change.

Storm-surge penetrations over the last five decades have, in general, trended toward less penetration as indicated by the average "accretion" rate of this line (3.22 m/yr) (Table I). This accretion results not from an overall reduction in extreme storms (Hayden, 1976), but rather from the construction of barrier dunes and dikes and thus the retardation of storm-surge penetration. This accretion is particularly notable on Ocracoke Island (24.16 m/yr) where barrier dunes have resulted in a reduction of oceanic overwash and extensive shrub growth on the island (Schroeder, 1976).

In contrast Core Banks, an island with a natural dune system, has a landward recession rate of the storm-surge penetration limit which is essentially identical to that of the shoreline recession rate. Both the geographic variation ($\pm$ 5.95 m/yr) and the temporal variation ($\pm$ 14.57 m/yr) of the rates of change of storm-surge penetration line are large. Temporal variances exceed spatial variances by at least a factor of two for both the shoreline and the storm-surge penetration rates of change.

SAMPLING INTERVALS

Statistics presented in Table I are based on data with a sampling interval of 100 m. Larger sampling intervals should result in means which differ from the high resolution means. This difference, ($\Delta\mu$), has been calculated for each of the islands studied for all possible sampling intervals which are integer multiples of the original 100 m interval. Figure 3 shows the magnitudes of $\Delta\mu$ for varying sampling intervals and for the standard deviations of the long-term means of shoreline change (σSL) on the South Hatteras reach of the coast. In Figure 4 a similar plot is given for the mean rate of change of the storm-surge penetration line ($\overline{SP}$) on Core Banks. With the exception of four spikes in the curve for South Hatteras, which arise due to along-the-coast periodicities in σSL, the upper limit of $\Delta\mu$ defines a curve of the form

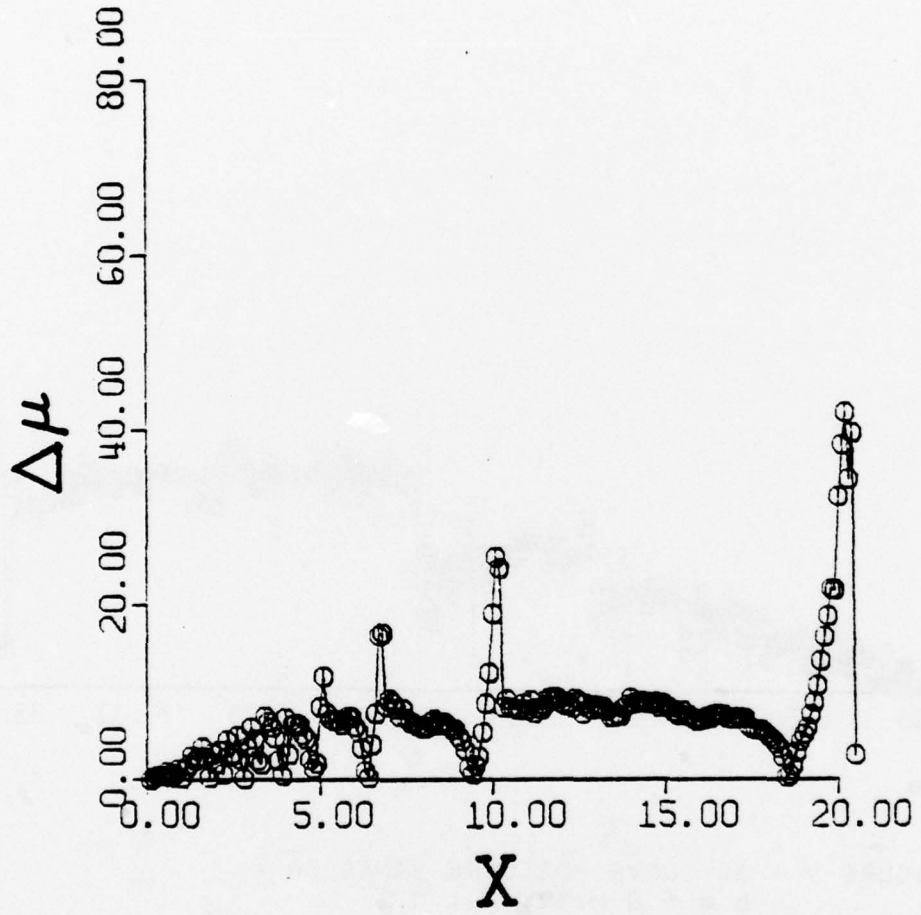

FIGURE 3 - Δμ CURVE FOR S. HATTERAS σSL
b = 8.0 M/YR, k = 0.4

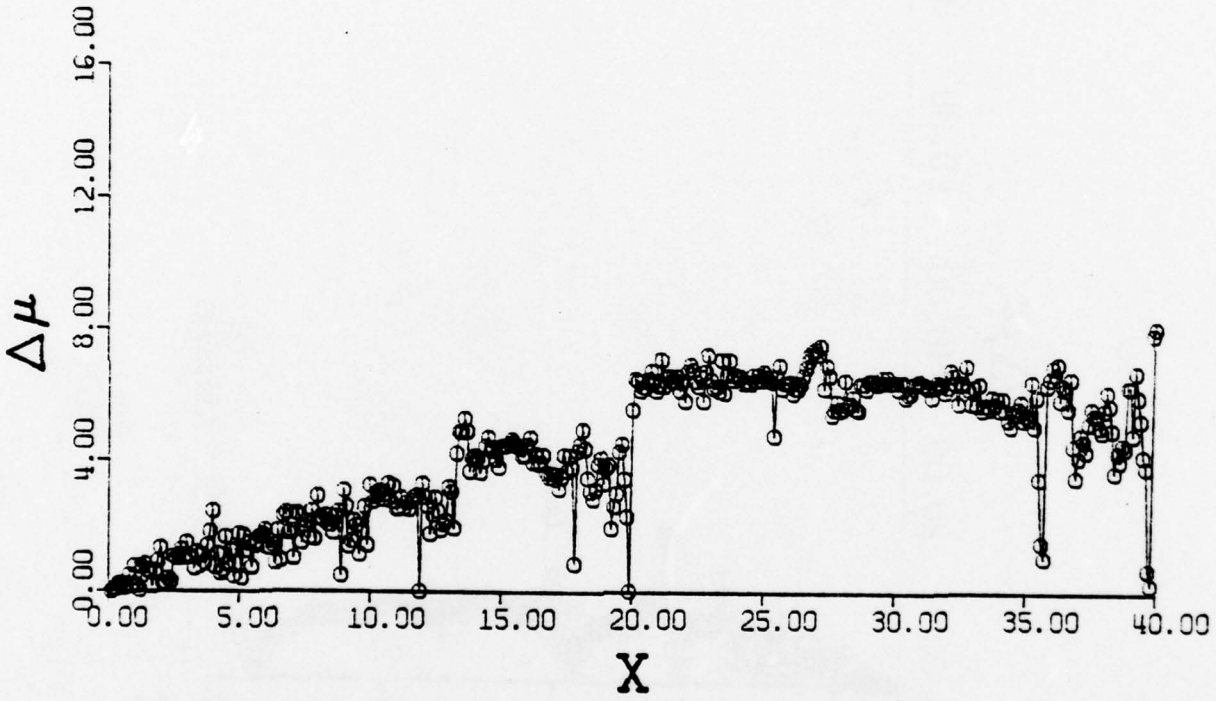

FIGURE 4 - Δμ CURVE FOR CORE BANKS $\overline{SP}$
b = 6.0 M/YR, k = 0.1

$$\Delta\mu = b\,tanh\ kx,$$

where b is the upper asymptotic bound of $\Delta\mu$, k determines the slope of the curve in the region near x = 0, and x is the sampling interval. In the case of the South Hatteras plot, b = 8.0 m/yr and k = 0.40. The Core Banks $\overline{SP}$ data indicate a value for b of 6.0 m/yr and a value for k of 0.10. Plots of $\Delta\mu$ prepared for each variable and each island are presented in the form of a table of b and k values from which the curves can be reconstructed (Table II).[1]

Since most coastal investigations call for sampling intervals smaller than 5 km, the portions of Figures 3 and 4 for sampling intervals $x \leq 5$ km are enlarged and reproduced in Figure 5a and 5b. In the case of the temporal standard deviation of shoreline change rates along South Hatteras (Fig. 5a), which averages $\pm$ 2.93 m/yr, a 1 km sampling interval would provide an estimate of this variable within 1σ of the high resolution mean. Along most reaches of the coast studied, variances are large and may be an order of magnitude greater than the mean. Therefore sampling interval choices may be more appropriately made on the basis of a small fraction of a standard deviation, for example, 0.25σ. The sampling interval for which $\Delta\mu = 0.25\sigma$ is here referred to as x'. The parameters b, k and x' thus define the along-the-coast statistical persistence of the data. Accordingly b, k, and x' values associated with the four variables are summarized in Tables II

---

[1]The original plots are presented in the appendix.

TABLE II

Persistence parameters b and k for barrier islands of the mid-Atlantic coast

Island Name	$\overline{SL}$		σSL		$\overline{SP}$		σSP	
	b	(k)	b	(k)	b	(k)	b	(k)
Shackleford	8.0	(.09)	8.0	(.12)	6.0	(.20)	*	*
Core Banks	1.0	(.20)	4.0	(.15)	6.0	(.10)	5.5	(.15)
Portsmouth	1.0	(.70	8.0	(.22)	11.0	(.20)	8.0	(.20)
Ocracoke	3.0	(.25)	6.0	(.15)	20.0	(.10)	25.0	(.05)
South Hatteras	2.0	(.40)	8.0	(.40)	4.0	(.20)	6.0	(.20)
North Hatteras	0.5	(.90)	3.0	(.08)	5.0	(.10	9.0	(.12)
Assateague	1.0	(.10)	2.0	(.40)	4.0	(.30)	20.5	(.40)
South Fenwick	2.5	(.08)	0.4	(.50)	0.6	(.50)	6.0	(.10)
North Fenwick	1.5	(.20)	0.5	(.50)	2.0	(.40)	7.0	(.20)
Cape May	*	*	*	*	*	*	5.5	(.40)
Seven Mile Bch.	2.0	(.90)	6.0	(.35)	2.0	(.50)	10.0	(.35)
Ludlam	5.0	(.20)	0.7	(.90)	1.8	(.20)	5.0	(.25)
Peck Beach	9.0	(.20)	4.0	(.20)	1.5	(.60)	3.0	(.25)
Ventnor	1.4	(.25)	2.5	(.20)	1.0	(.50)	4.5	(.30)
Brigantine	*	*	*	*	*	*	5.0	(.20)

*A $\Delta\mu$ value $\geq 0.25\sigma$ does not occur for any sampling interval; thus b and k could not be estimated.

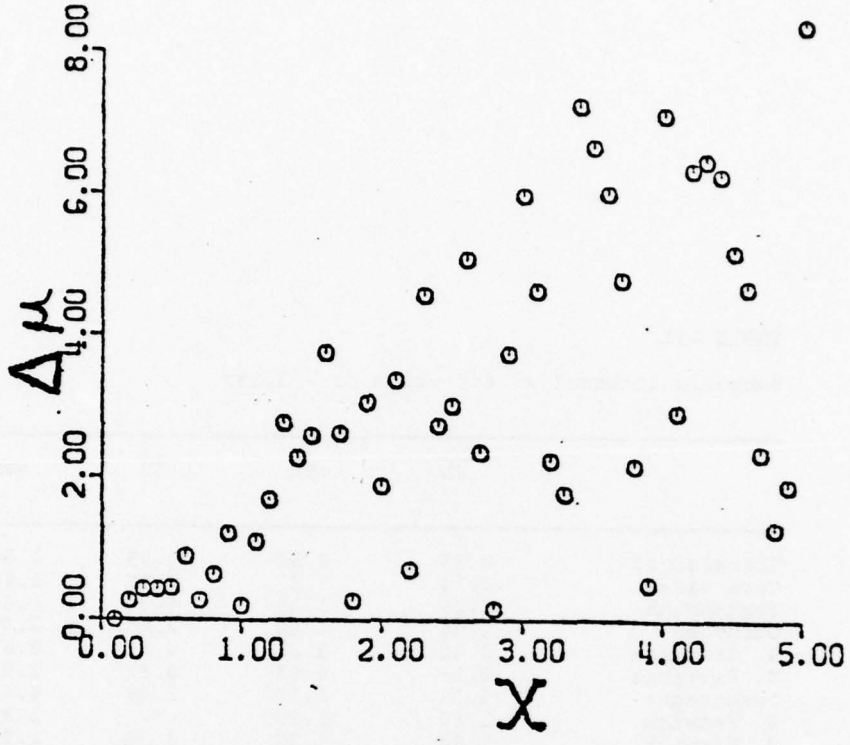

FIGURE 5A - PORTION OF FIG. 3 FOR SAMPLING INTERVALS $x \leq 5$ KM

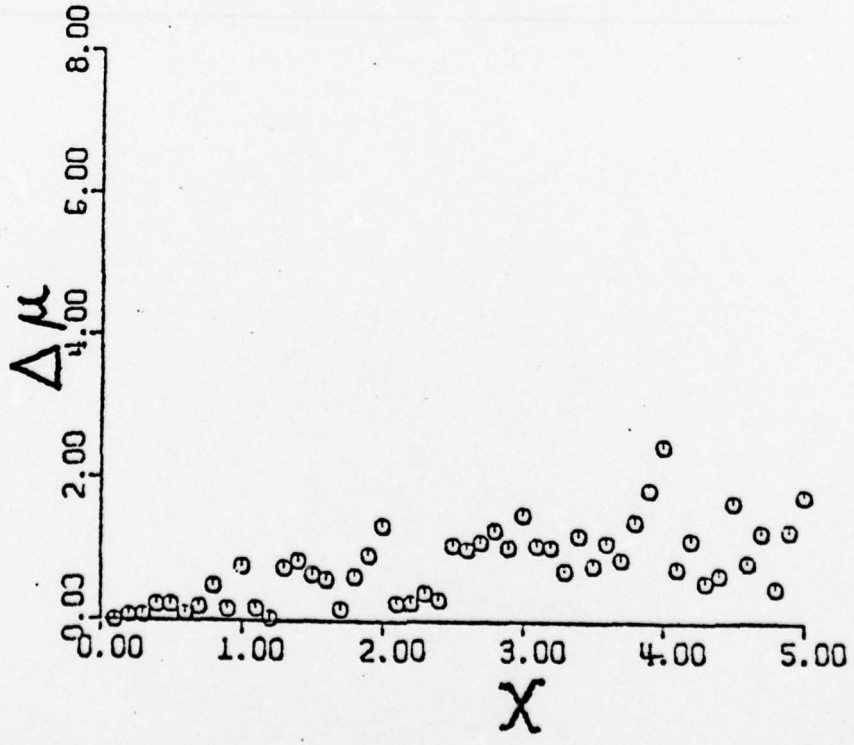

FIGURE 5B - PORTION OF FIG. 4 FOR SAMPLING INTERVALS $x \leq 5$ KM

TABLE III

Sampling interval x' for which $\Delta\mu = 0.25\sigma$

	$\overline{SL}$	σSL	$\overline{SP}$	σSP
Shackleford	0.95	0.32	0.85	1.50
Core Banks	2.74	1.27	0.86	1.64
Portsmouth	0.29	1.18	0.55	1.66
Ocracoke	1.06	1.60	3.04	2.06
S. Hatteras	0.42	0.23	0.67	0.67
N. Hatteras	2.16	4.63	3.66	1.51
Assateague	5.29	1.18	1.49	0.44
S. Fenwick	1.50	1.32	∞	2.96
N. Fenwick	1.00	1.02	3.29	1.26
Cape May	2.50	1.00	1.50	0.83
Seven Mile Beach	2.72	2.20	3.48	0.95
Ludlam	0.35	0.63	0.85	2.21
Peck Beach	0.50	1.66	1.41	1.94
Ventnor	0.74	1.11	0.41	2.71
Brigantine				0.19

and III for each barrier island studied. Given the functional (hyperbolic tangent) relationship between b and k, the standard deviation data given in Table I, and the value of x', adequate information for efficient sampling design is available in Table III for the mid-Atlantic coast, and should provide guidelines for other areas.

The representations given in Figures 3, 4, and 5 and the summarizations in Table I, II, and III also provide the information needed to address the question of spatial representativeness which we find to be constrained to no more than 1 km on either side of a site.

Variations in the position of the shoreline and in the position of the limit of storm-surge penetration are largely the result of extreme meteorological events. Accordingly, the statistics associated with change data are characterized by large variances. The major component of these variances is customarily thought of as fixed at the time scale of synoptic weather events. The data analyzed here are decadal in time scale, and the variance calculated is by most standards very large. Decade to decade variations in synoptic weather conditions reside not so much in the frequency of these events, as in their magnitude. While estimates of temporal variance are usually available, it appears to be three to four times larger than the spatial variance for a given reach of coast. Major departures from this rule not

withstanding, (Portsmouth, Ludlam, and Ventnor Islands), it seems to have general applicability. In view of the fact that temporal variances are found to exceed those along-the-coast, decadal shoreline change rate averages must be used with caution and with a wide margin for error. This result is illustrated in Table IV where the ratios of temporal to spatial variance for each of the islands studied are presented. In most cases this ratio exceeds unity by a substantial margin.

PERIODICITIES AND SAMPLING DESIGN

The $\Delta\mu$ versus sampling interval plot for Seven Mile Beach, New Jersey, (Fig. 6) clearly illustrates the problems encountered with sampling design for coastal reaches which have spikes in the $\Delta\mu$ curve. The mean rate of shoreline change (spatial) along this reach of coast is only 0.60 m/yr, however, the standard deviation of this mean is large (7.92 m/yr). If a sampling interval of 7.8 km were used along this reach the mean shoreline rate of change measured would be 21.95 m/yr or nearly 40 times greater than the 100 m interval mean. A slightly larger sampling interval of 8.0 km would result in a calculated mean of 0.70 m/yr, a very good estimate.

Spikes in the $\Delta\mu$ curve appear to be the result of periodicities in the shoreline and storm-surge line change data. Figure 6 clearly indicates that numerous periodicities

TABLE IV

Ratios of the temporal to spatial standard deviations of rates of change of the shoreline and the storm-surge penetration line

	$\mu(\sigma_{SL})/\sigma(\overline{SL})$	$\mu(\sigma_{SP})/\sigma(\overline{SP})$
Shackleford	1.05	4.86
Core Banks	2.40	3.71
Portsmouth	20.63	3.80
Ocracoke	2.69	1.34
S. Hatteras	3.66	2.96
N. Hatteras	3.68	2.28
Assateague	2.85	2.28
Fenwick	2.75	4.96
Cape May	0.95	3.46
Seven Mile Beach	1.42	1.86
Ludlam	2.04	17.17
Peck Beach	1.22	3.16
Ventnor	3.47	10.28
Brigantine	1.55	1.38
Grand Means	3.59	4.52

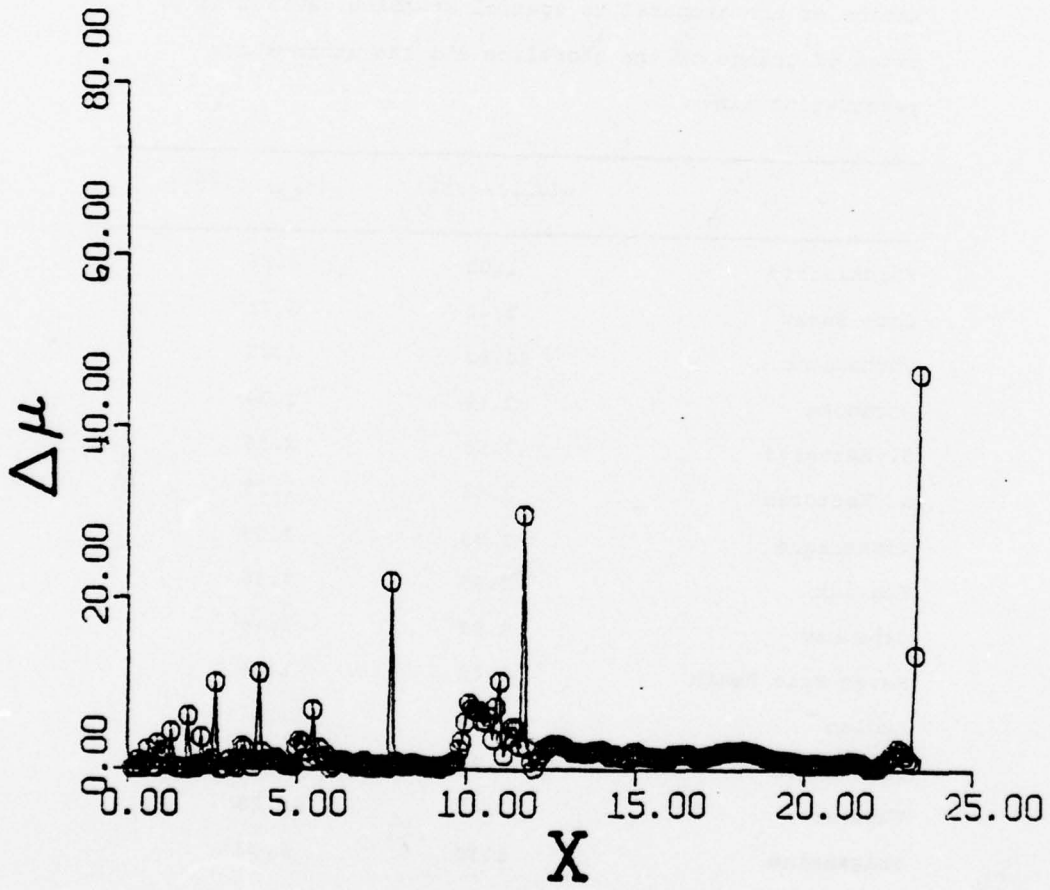

FIGURE 6 - Δμ CURVE FOR SEVEN MILE BEACH $\overline{SL}$

are present, and given the time period of the base data (1930's thru 1970's) they cannot be considered ephemeral features of the process data. In an earlier report (Dolan et al, 1978) we suggested that periodicities in $\overline{SL}$, σSL, $\overline{SP}$ and σSP data for the coastal reach between Cape Hatteras and Cape Lookout are the result of standing waves trapped between the two capes. When the coastal dynamics data are viewed as a data series of climatological form, the attribute of statistical stationarity applies and in the absence of knowledge of the underlying periodicities, a random sampling scheme is recommended.

CONCLUSIONS

Based on our analyses of rate of change data for both the shoreline and the limit of storm-surge penetration for more than 400 km of coast at 100-m intervals, we conclude the following:

1) Shoreline change rates on an island-wide basis vary from 3.0 m/yr erosion to 1.0 m/yr accretion with a mean for the study area of 0.6 m/yr.
2) Along-the-coast variations in shoreline and storm-surge penetration line change are as much as an order of magnitude larger than the mean rates.
3) Temporal variance of shoreline erosion is 3 to

4 times larger than the along-the-coast spatial variance, while temporal variance of storm-surge penetration change rates is 4 to 5 times larger than spatial variance.

4) For the islands studied, sampling at sites farther apart than 1.0 km provides little more precision than one sampling site for an entire island.

5) In general, sampling intervals of 2.5 km or less are required in order to specify island-wide means within $\pm$ 0.25σ of the high resolution mean.

6) Site specific (transect or profile) measures of shoreline or storm-surge penetration rates are representative of approximately $\pm$ 500-m along the coast.

7) Mid-Atlantic coast shorelines are characterized by a complex series of along-the-coast periodicities in shoreline dynamics and, in general, unless the objective is to define the periodicities, regular sampling intervals should be avoided.

8) Shoreface dynamics are highly variable in space and time, therefore mean rates of change are of little value unless accompanied by a specification of associated variance.

REFERENCES

Dolan, R., Hayden, B., and Heywood, J., 1978. A new photogrammetric method for determining shoreline erosion. Coastal Engineering 2:21-39.

Dolan, R., Hayden, B., and Heywood, J., 1978. Analysis of coastal erosion and storm-surge hazards. Coastal Engineering 2:41-53.

Hayden, B., 1976. Storm wave climates at Cape Hatteras, North Carolina: recent secular variations. Science 190:981-983.

Schroeder, P.M., Dolan, R., and Hayden, B., 1976. Vegetation changes associated with barrier-dune construction on the Outer Banks of North Carolina. Env. Management 1(2):105-114.

ACKNOWLEDGMENTS

This research is sponsored by Geography Programs, Office of Naval Research; the National Park Service; and National Aeronautics and Space Administration.

APPENDIX

Computer Generated Plots of Alongshore Persistence Data

This appendix contains material too voluminous to be included in the text proper but of sufficient value to be included as an appended section. The constants and coefficients of the hyperbolic tangent function for the decay of estimates of the means and standard deviations with increasing sampling interval for each island were given in the text. While these coefficients provide sufficient information for the reconstruction of the plots of $\Delta\mu$ versus sampling interval, the details of the original plots include additional information on the departures (periodicities) from the hyperbolic tangent decay. The original figures are included here. The table of contents of this appendix lists the figures included. The plots are ordered from 1 to 64 beginning with Shackleford Banks to the south and ending with Brigantine Island, New Jersey, to the north. For each island the plots are given in the following order: $\overline{SL}$, σSL, $\overline{SP}$, σSP. For each variable and each island two plots are given. The first gives the decay of $\Delta\mu$ for all possible sampling intervals larger than 100m. The second plot gives a high resolution plot of sampling intervals between 100m and 5000m.

These plots should be of value in both experimental design of subsequent shoreline dynamics studies and in shoreline monitoring programs for the mid-Atlantic coast.

APPENDIX

TABLE OF CONTENTS

22. North Hatteras Island, Shoreline Rate Standard Deviation (σSL)

23. North Hatteras Island, Mean Storm Surge Penetration ($\overline{SP}$)

24. North Hatteras Island, Storm Surge Penetration Standard Deviation (σSP)

25. Assateague Island, Shoreline Mean Rate ($\overline{SL}$)

26. Assateague Island, Shoreline Rate Standard Deviation (σSL)

27. Assateague Island, Mean Storm Surge Penetration ($\overline{SP}$)

28. Assateague Island, Little Tom's Cove to Smith Hammocks, Storm Surge Penetration Standard Deviation (σSP)

29. Assateague Island, Cherry Tree Hill to Fox Hill Level, Storm Surge Penetration Standard Deviation (σSP)

30. Assateague Island, Fox Hill Level to Ocean City Inlet, Storm Surge Penetration Standard Deviation (σSP)

31. Fenwick Island, South of Indian River Inlet, Shoreline Mean Rate ($\overline{SL}$)

32. Fenwick Island, North of Indian River Inlet, Shoreline Mean Rate ($\overline{SL}$)

33. Fenwick Island, South of Indian River Inlet, Shoreline Rate Standard Deviation (σSL)

34. Fenwick Island, North of Indian River Inlet, Shoreline Rate Standard Deviation (σSL)

35. Fenwick Island, South of Indian River Inlet, Mean Storm Surge Penetration ($\overline{SP}$)

36. Fenwick Island, North of Indian River Inlet, Mean Storm Surge Penetration ($\overline{SP}$)

37. Fenwick Island, South of Indian River Inlet, Storm Surge Penetration Standard Deviation (σSP)

38. Fenwick Island, North of Indian River Inlet, Storm Surge Penetration Standard Deviation (σSP)

39. South New Jersey, Cape May Shoreline Mean Rate ($\overline{SL}$)

40. South New Jersey, Cape May Shoreline Rate Standard Deviation (σSL)

41. South New Jersey, Cape May, Mean Storm Surge Penetration ($\overline{SP}$)

42. South New Jersey, Cape May, Storm Surge Penetration Standard Deviation (σSP)

43. South New Jersey, Seven Mile Beach, Shoreline Mean Rate ($\overline{SL}$)

44. South New Jersey, Seven Mile Beach, South of Hereford Inlet, Shoreline Rate Standard Deviation (σSL)

45. South New Jersey, Seven Mile Beach, North of Hereford Inlet, Shoreline Rate Standard Deviation (σSL)

46. South New Jersey, Seven Mile Beach, Storm Surge Penetration ($\overline{SP}$)

47. South New Jersey, Seven Mile Beach, South of Hereford Inlet, Storm Surge Penetration Standard Deviation (σSP)

48. South New Jersey, Seven Mile Beach, North of Hereford Inlet, Storm Surge Penetration Standard Deviation (σSP)

49. South New Jersey, Ludlam Beach, Shoreline Mean Rate ($\overline{SL}$)

50. South New Jersey, Ludlam Beach, Shoreline Rate Standard Deviation (σSL)

51. South New Jersey, Ludlam Beach, Mean Storm Surge Penetration ($\overline{SP}$)

52. South New Jersey, Ludlam Beach, Storm Surge Penetration Standard Deviation (σSP)

53. South New Jersey, Peck Beach, Shoreline Rate Standard Deviation ($\overline{SL}$)

54. South New Jersey, Peck Beach, Shoreline Rate Standard Deviation (σSL)

55. South New Jersey, Peck Beach, Mean Storm Surge Penetration ($\overline{SP}$)

56. South New Jersey, Peck Beach, Storm Surge Penetration Standard Deviation (σSP)

57. South New Jersey, Ventnor Island, Shoreline Mean Rate ($\overline{SL}$)

58. South New Jersey, Ventnor Island, Shoreline Rate Standard Deviation (σSL)

59. South New Jersey, Ventnor Island. Mean Storm Surge Penetration ($\overline{SP}$)

60. South New Jersey, Ventnor Island, Mean Storm Surge Penetration Standard Deviation (σSP)

61. South New Jersey, Brigantine Island, Shoreline Mean Rate ($\overline{SL}$)

62. South New Jersey, Brigantine Island, Shoreline Rate Standard Deviation (σSL)

63. South New Jersey, Brigantine Island, Mean Storm Surge Penetration ($\overline{SP}$)

64. South New Jersey, Brigantine Island, Storm Surge Penetration Standard Deviation (σSP)

SHACKLEFORD BANKS

MEAN SHORELINE RATE ($\overline{SL}$)

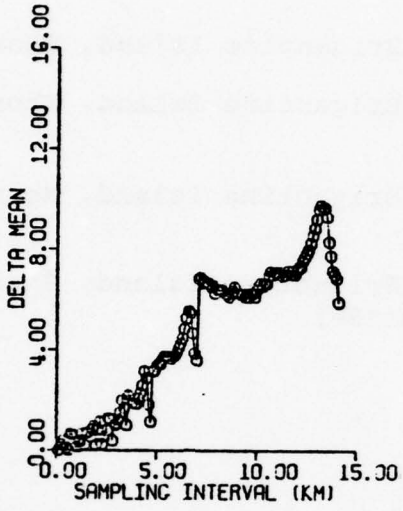

1A

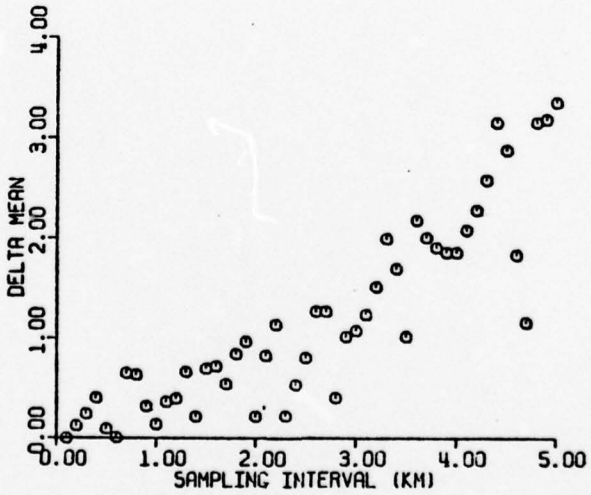

1B

SHACKLEFORD BANKS

SHORELINE RATE
STANDARD DEVIATION (σ_{SL})

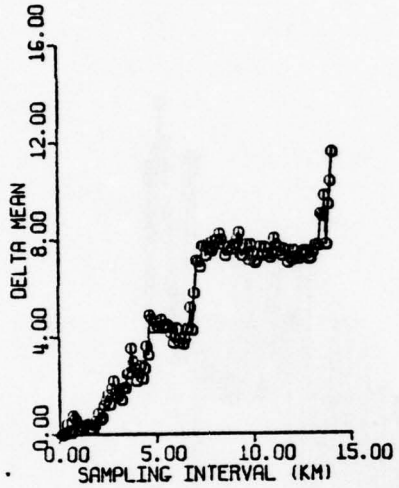

2A

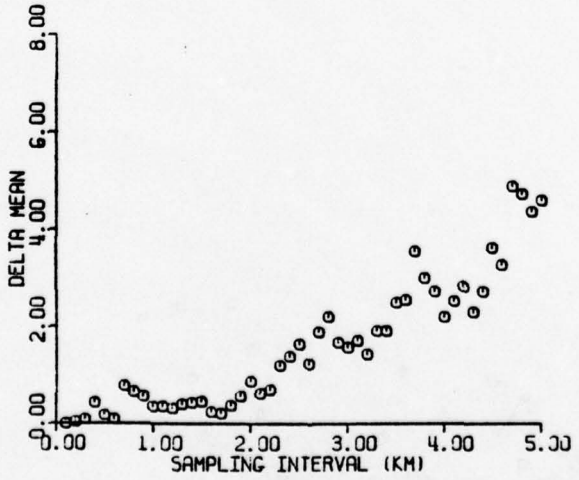

2B

SHACKLEFORD BANKS

MEAN STORM SURGE PENETRATION ($\overline{SP}$)

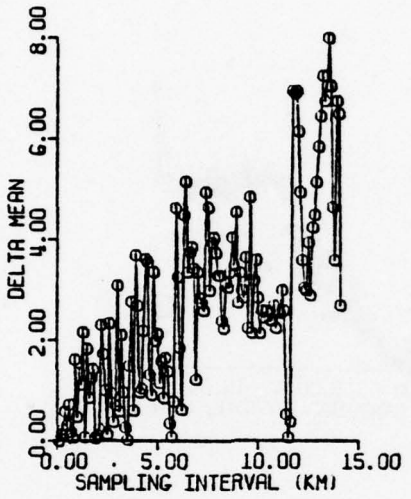

3A

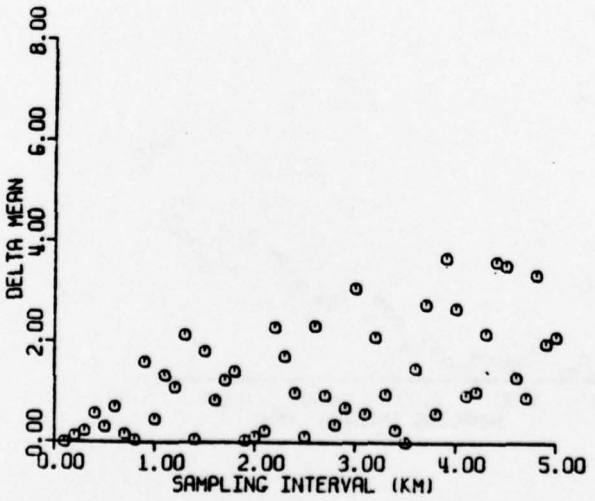

3B

SHACKLEFORD BANKS

STORM SURGE PENETRATION STANDARD DEVIATION (σSP)

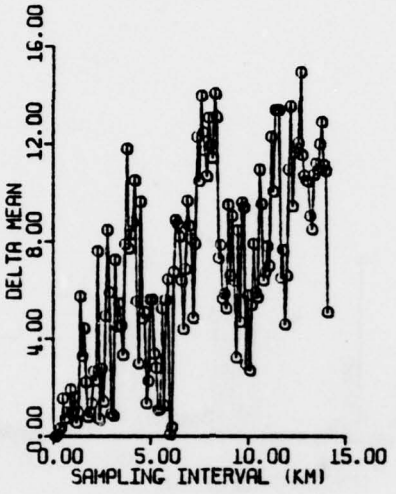

4A

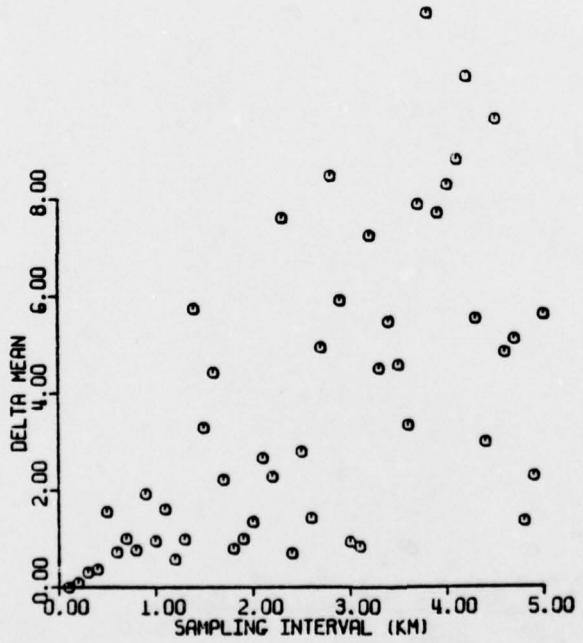

4B

PORTSMOUTH ISLAND

MEAN SHORELINE RATE ($\overline{SL}$)

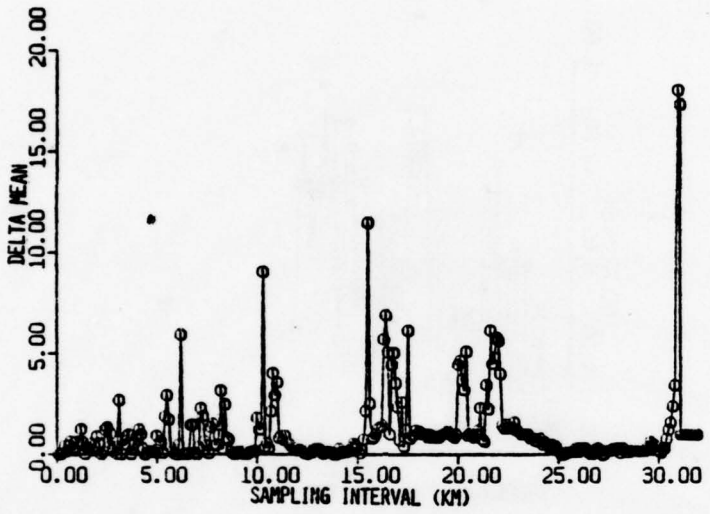

5A

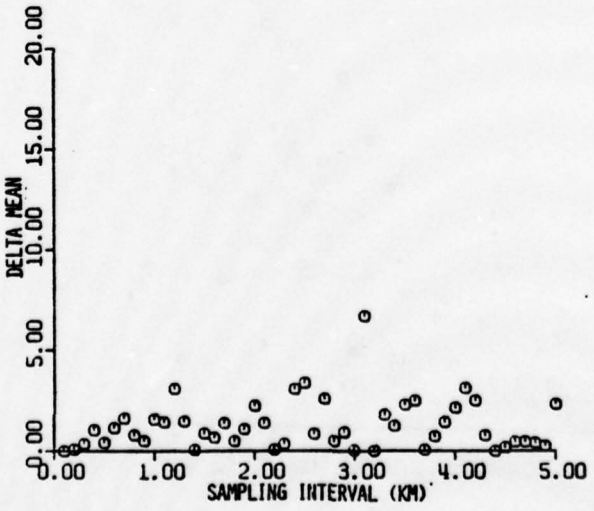

5B

PORTSMOUTH ISLAND

SHORELINE RATE
STANDARD DEVIATION (σ_{SL})

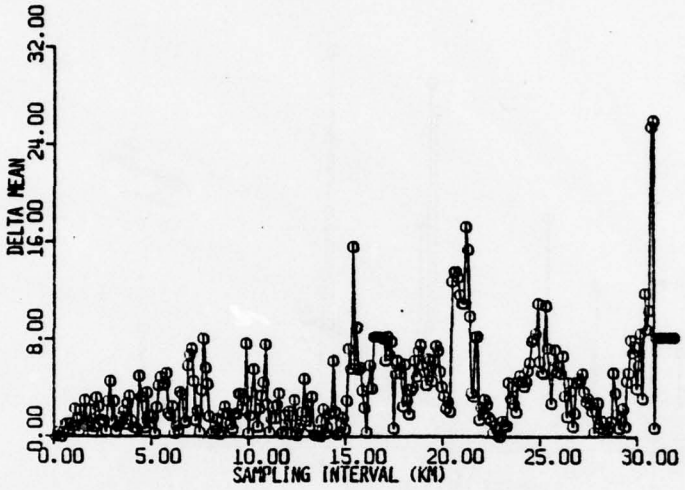

6A

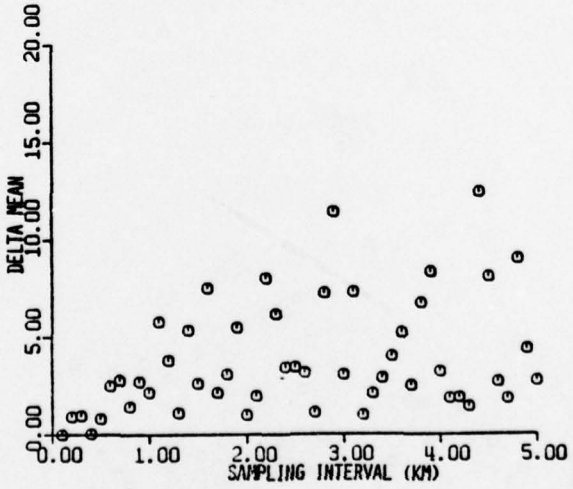

6B

PORTSMOUTH ISLAND

MEAN STORM SURGE PENETRATION ($\overline{SP}$)

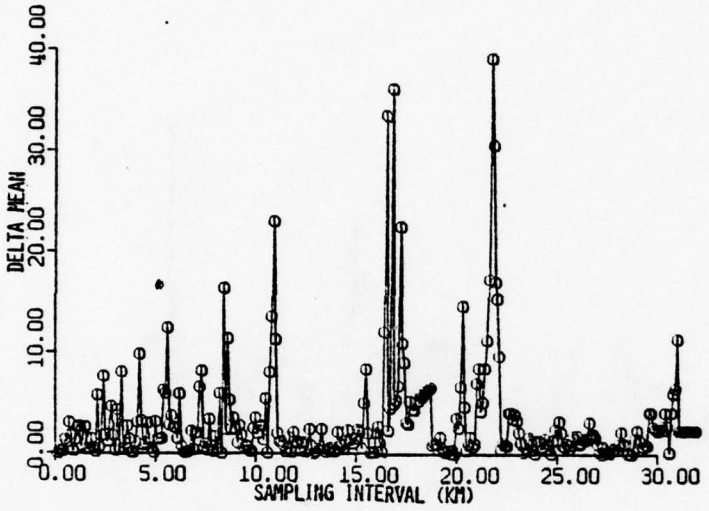

7A

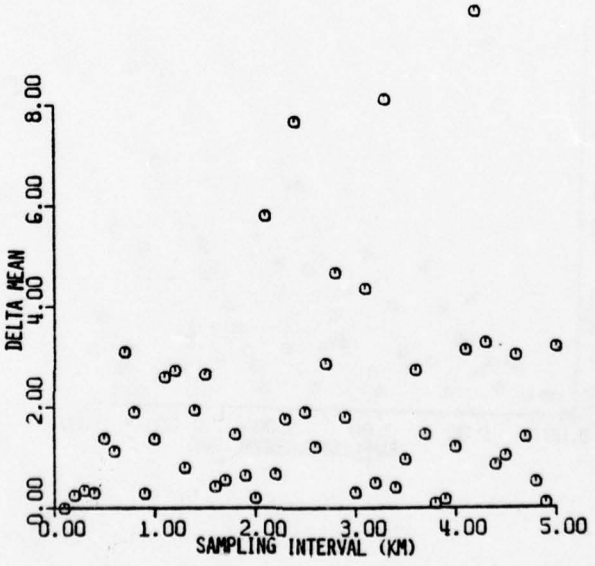

7B

PORTSMOUTH ISLAND

STORM SURGE PENETRATION STANDARD DEVIATION (σ_{SP})

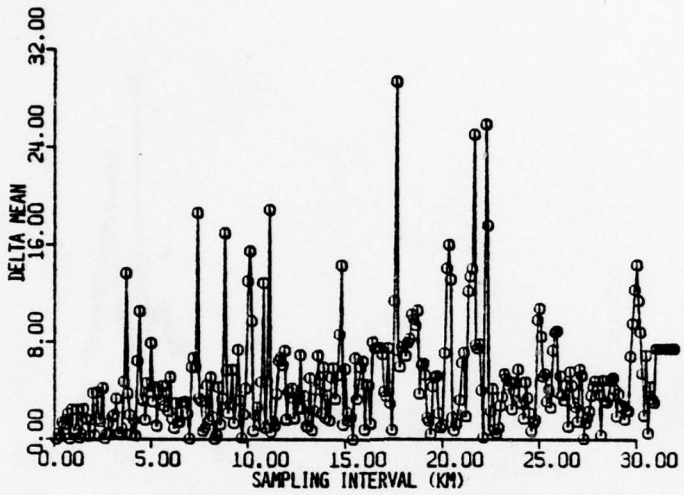

8A

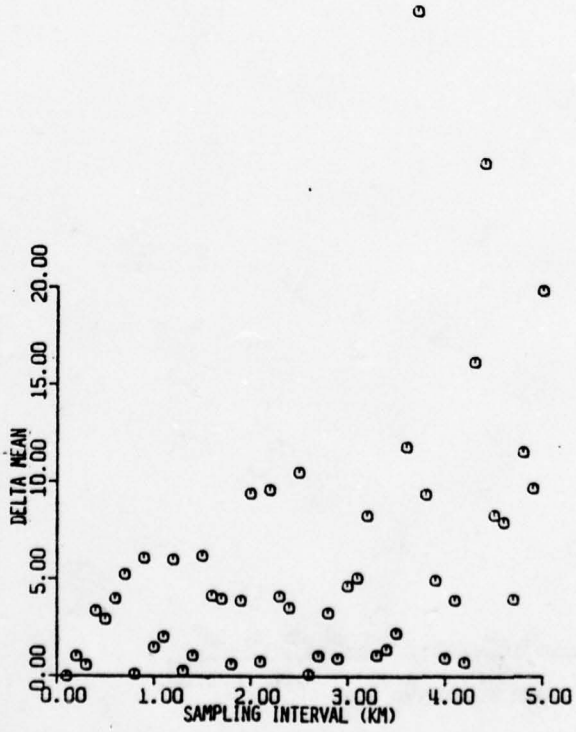

8B

CORE BANKS

MEAN SHORELINE RATE ($\overline{SL}$)

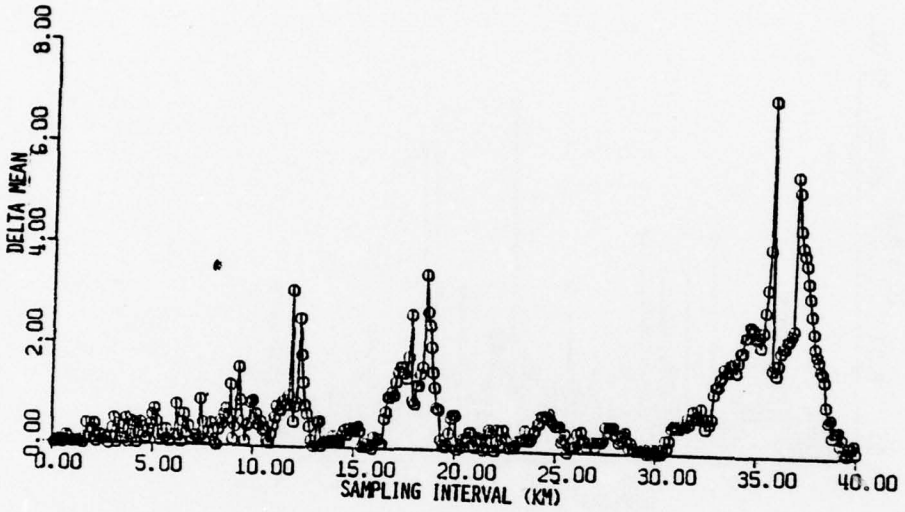

9A

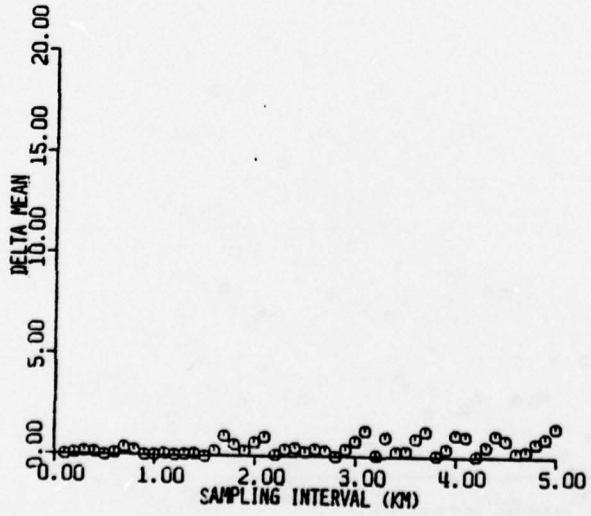

9B

CORE BANKS

SHORELINE RATE STANDARD DEVIATION (σ_{SL})

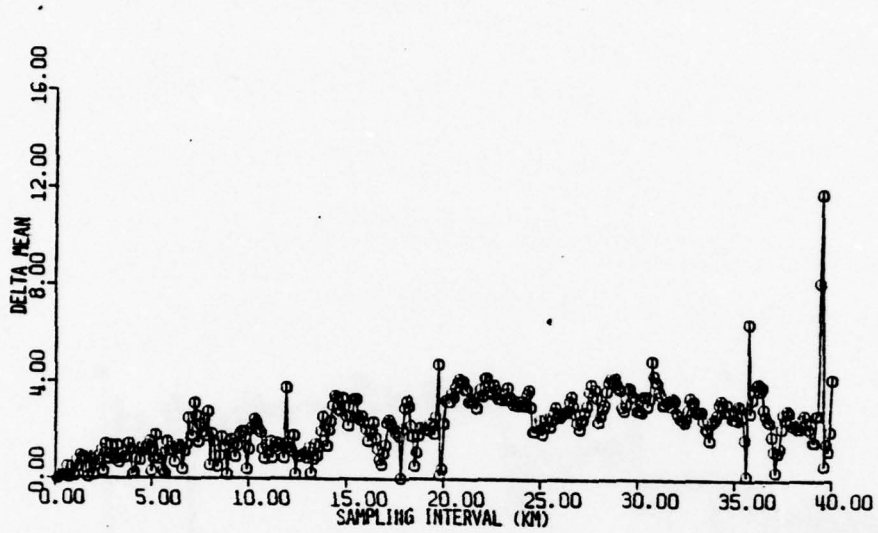

10A

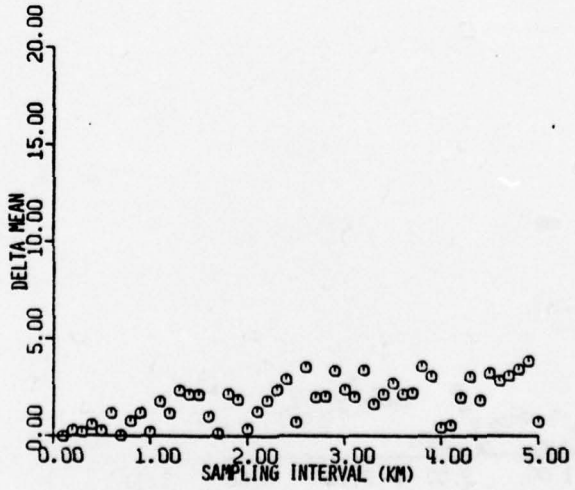

10B

CORE BANKS

MEAN STORM SURGE PENETRATION ($\overline{SP}$)

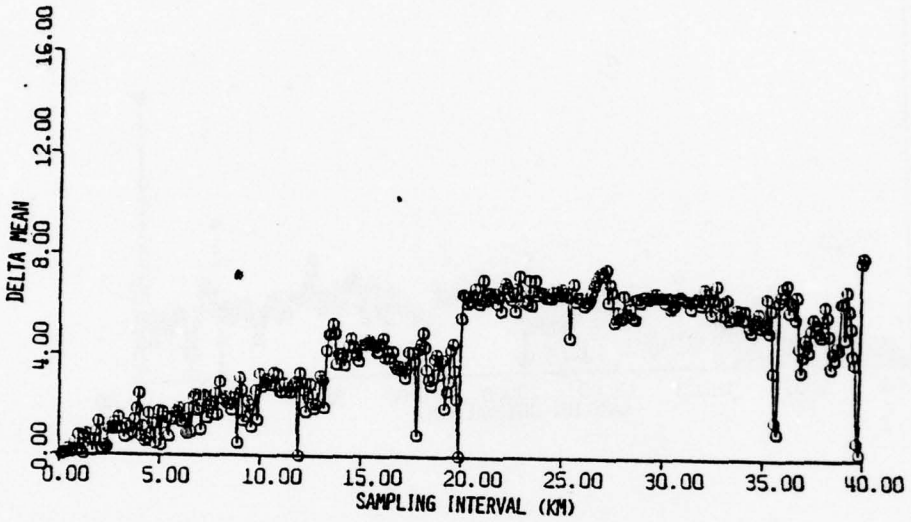

11A

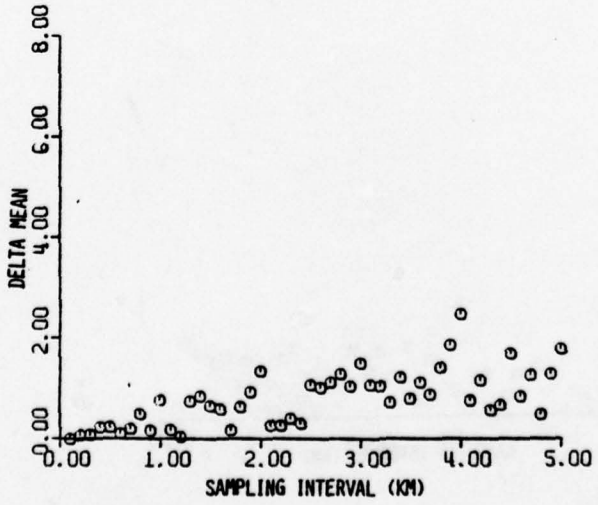

11B

CORE BANKS

STORM SURGE PENETRATION STANDARD DEVIATION (σ_{SP})

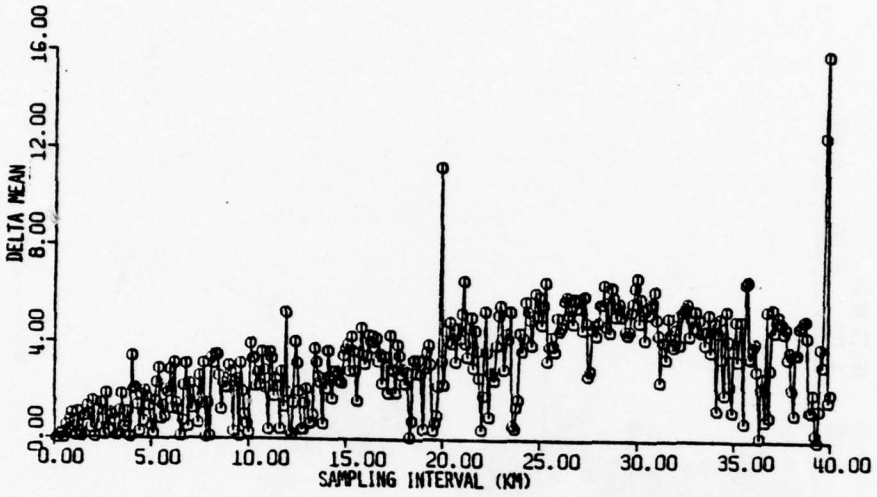

12A.

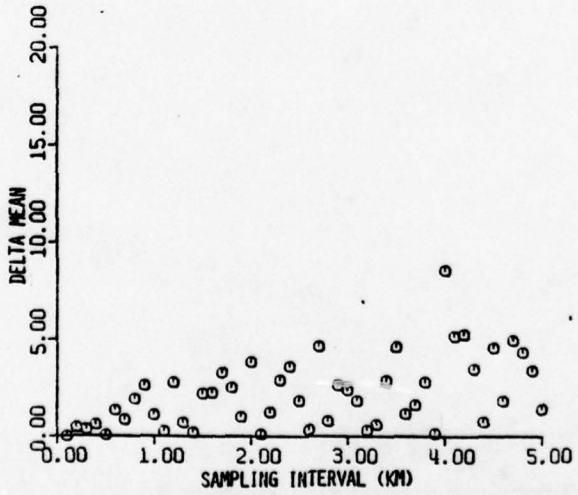

12B

OCRACOKE ISLAND

MEAN SHORELINE RATE ($\overline{SL}$)

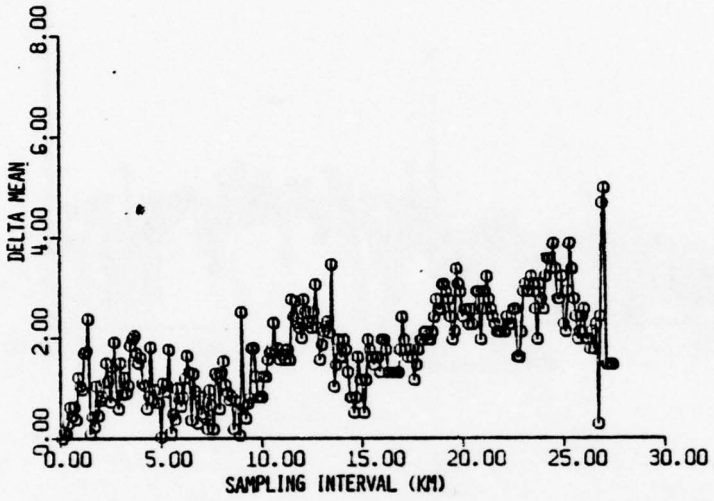

13A

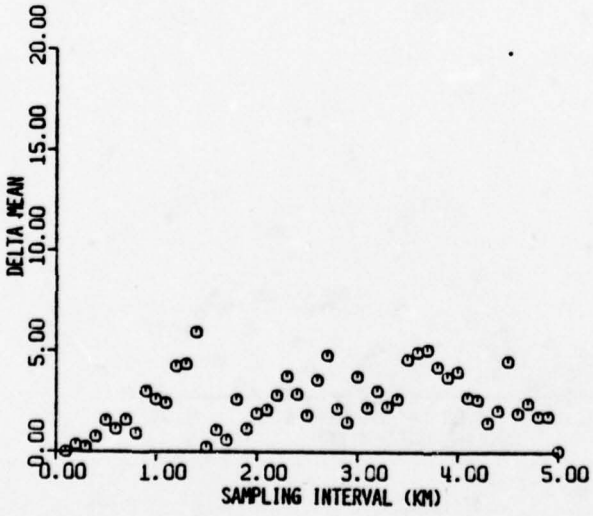

13B

OCRACOKE ISLAND

SHORELINE RATE STANDARD DEVIATION (σ_{SL})

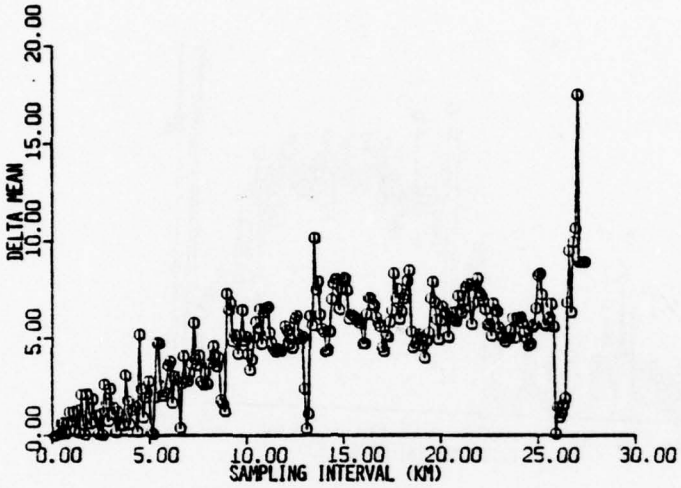

14A

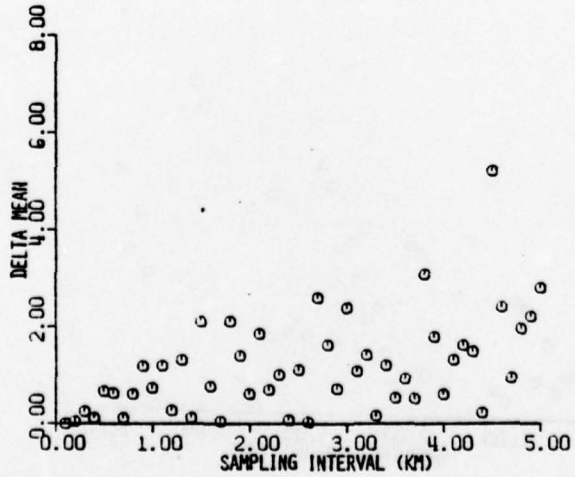

14B

OCRACOKE ISLAND

MEAN STORM SURGE PENETRATION ($\overline{SP}$)

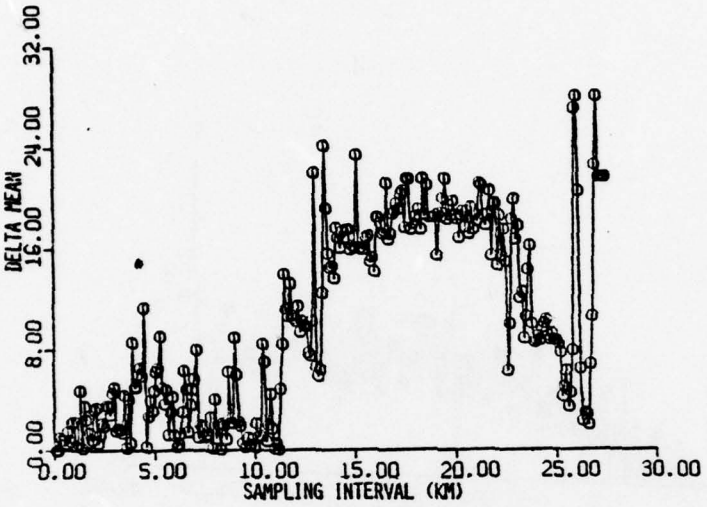

15A

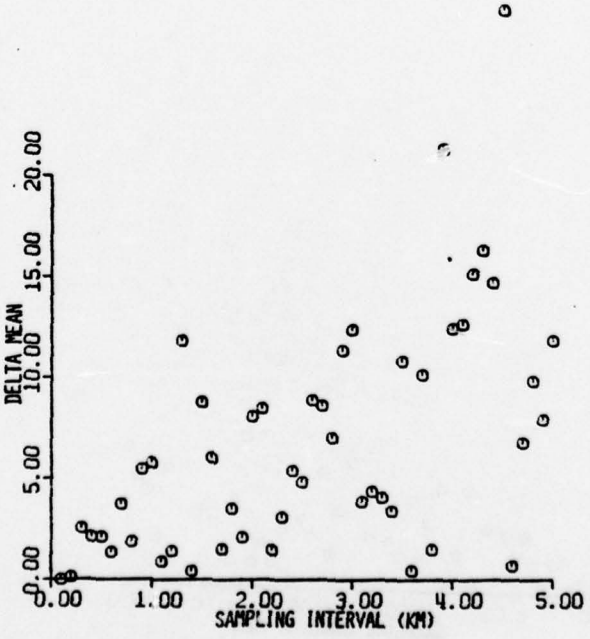

15B

OCRACOKE ISLAND

STORM SURGE PENETRATION STANDARD DEVIATION (σ_{SP})

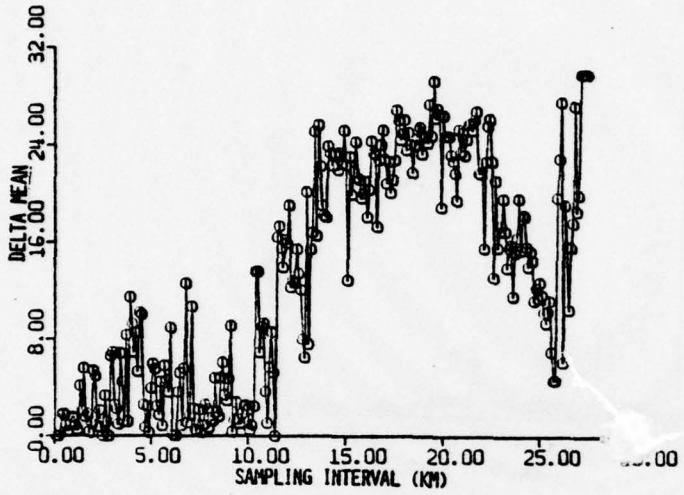

16A

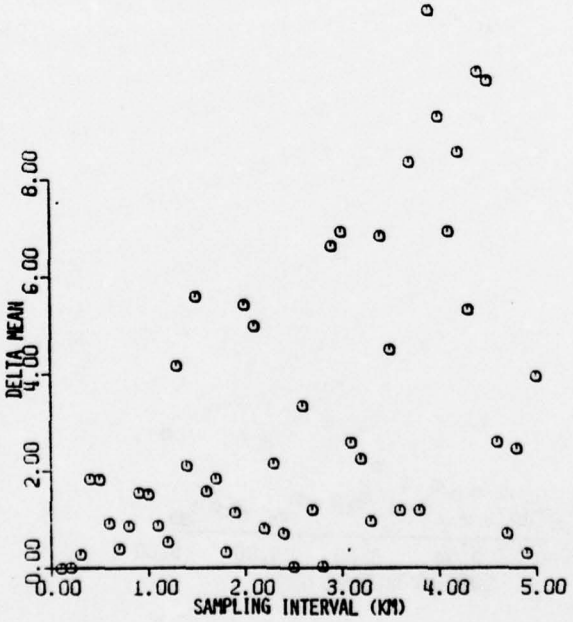

16B

SOUTH HATTERAS ISLAND

MEAN SHORELINE RATE ($\overline{SL}$)

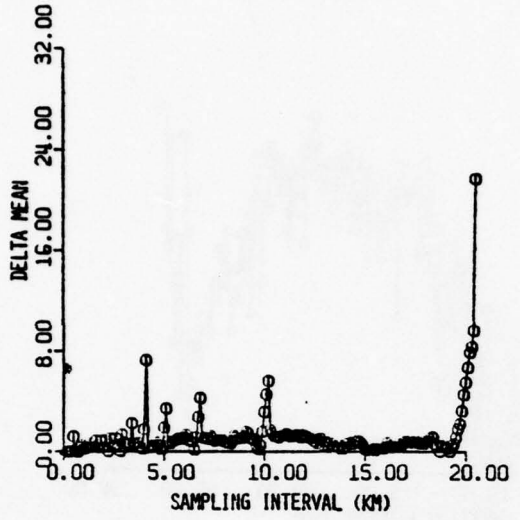

17A

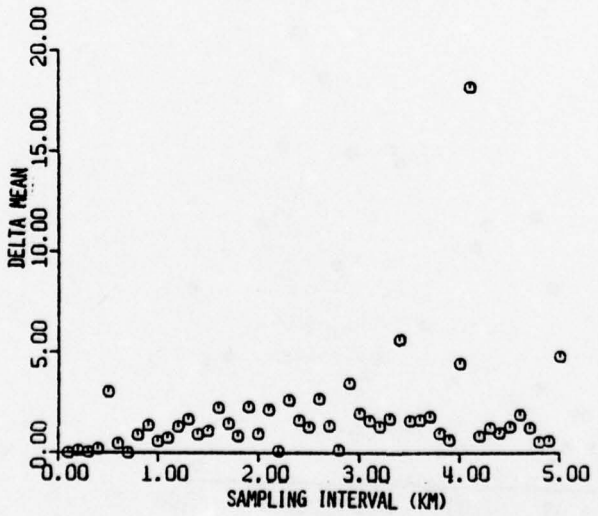

17B

SOUTH HATTERAS ISLAND

SHORELINE RATE STANDARD DEVIATION (σ_{SL})

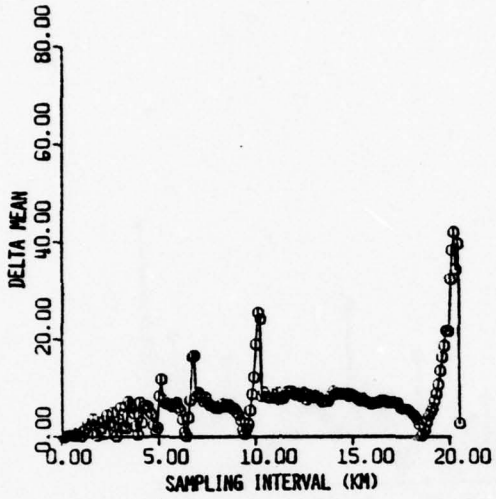

18A

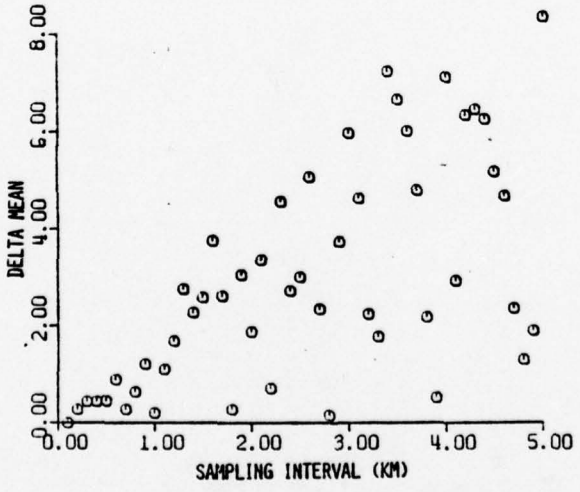

18B

SOUTH HATTERAS ISLAND

MEAN STORM SURGE PENETRATION ($\overline{SP}$)

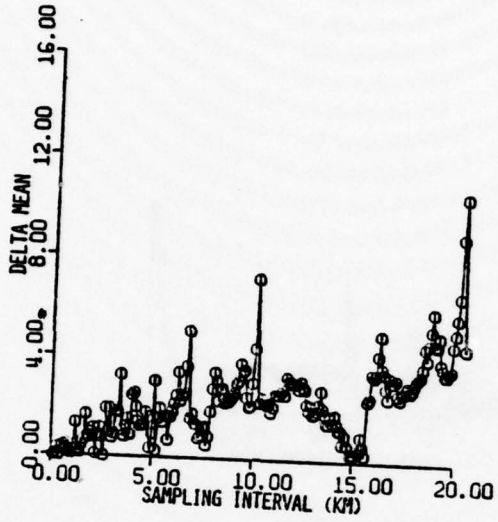

19A

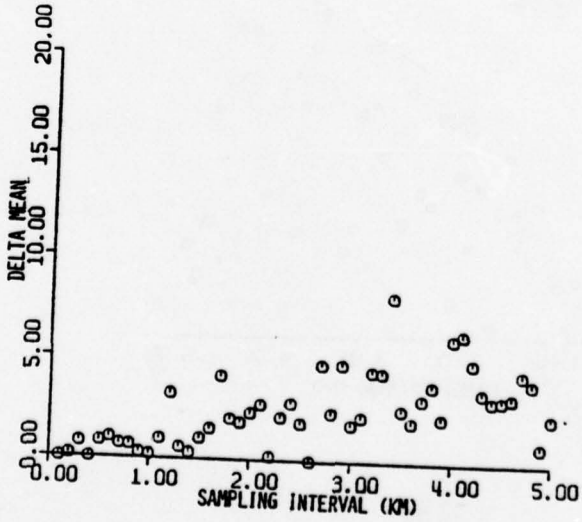

19B

SOUTH HATTERAS ISLAND

STORM SURGE PENETRATION STANDARD DEVIATION (σSP)

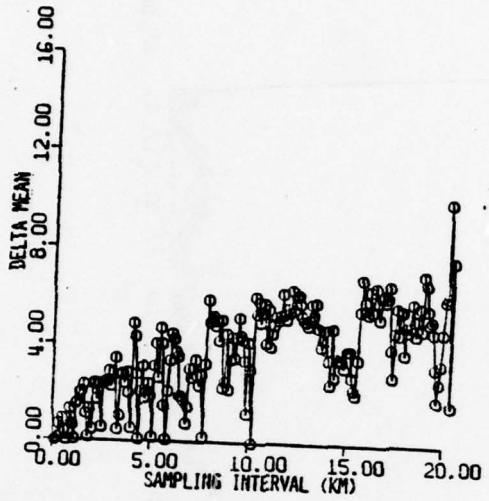

20A

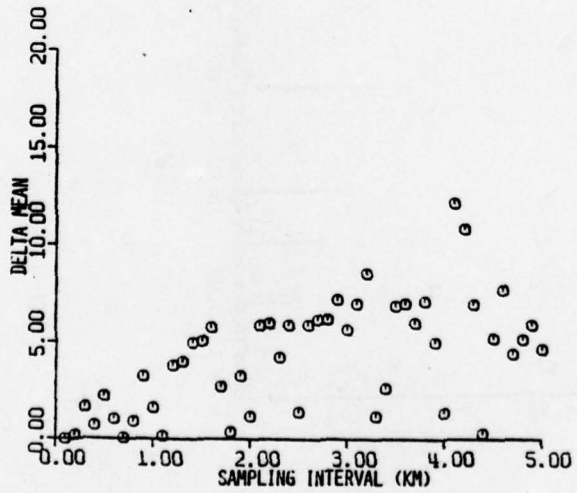

20B

NORTH HATTERAS ISLAND

MEAN SHORELINE RATE ($\overline{SL}$)

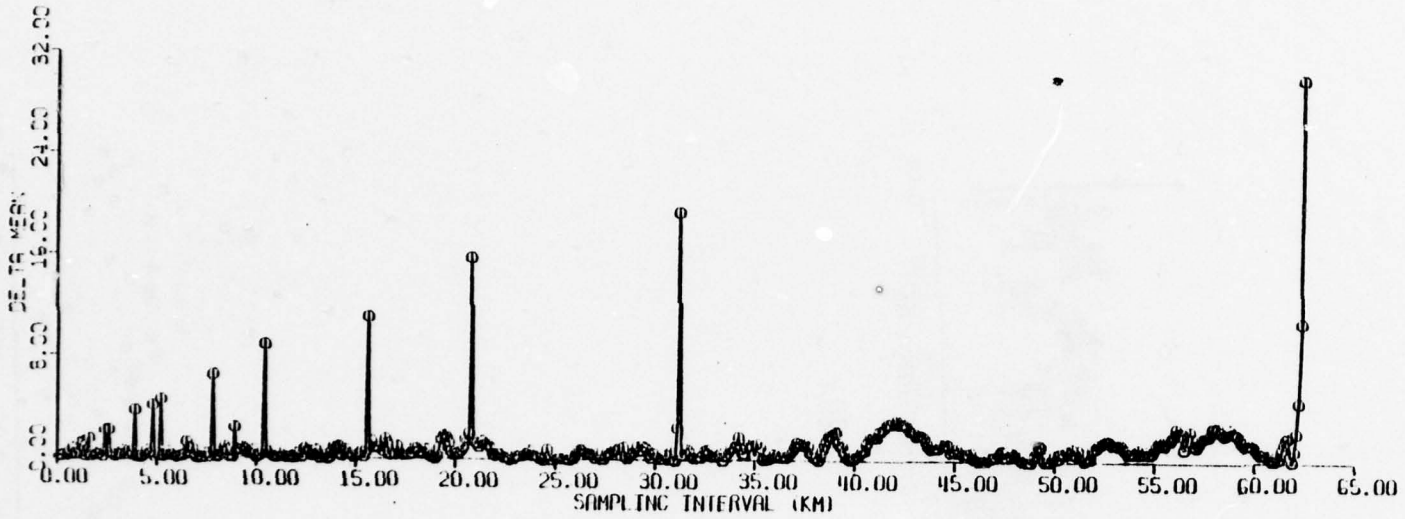

NORTH HATTERAS ISLAND

MEAN SHORELINE RATE ($\overline{SL}$)

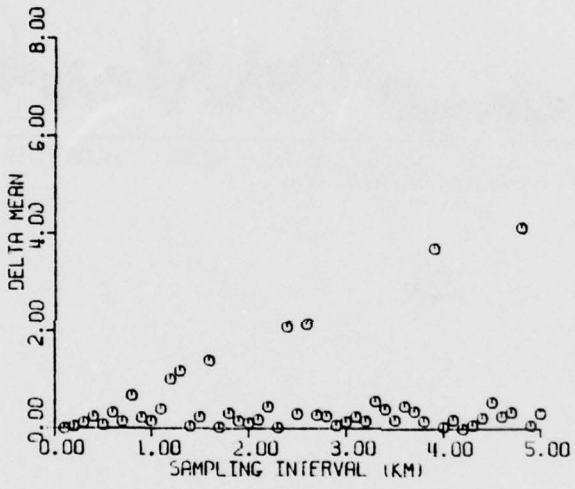

21B

NORTH HATTERAS ISLAND

SHORELINE RATE STANDARD DEVIATION (σ_{SL})

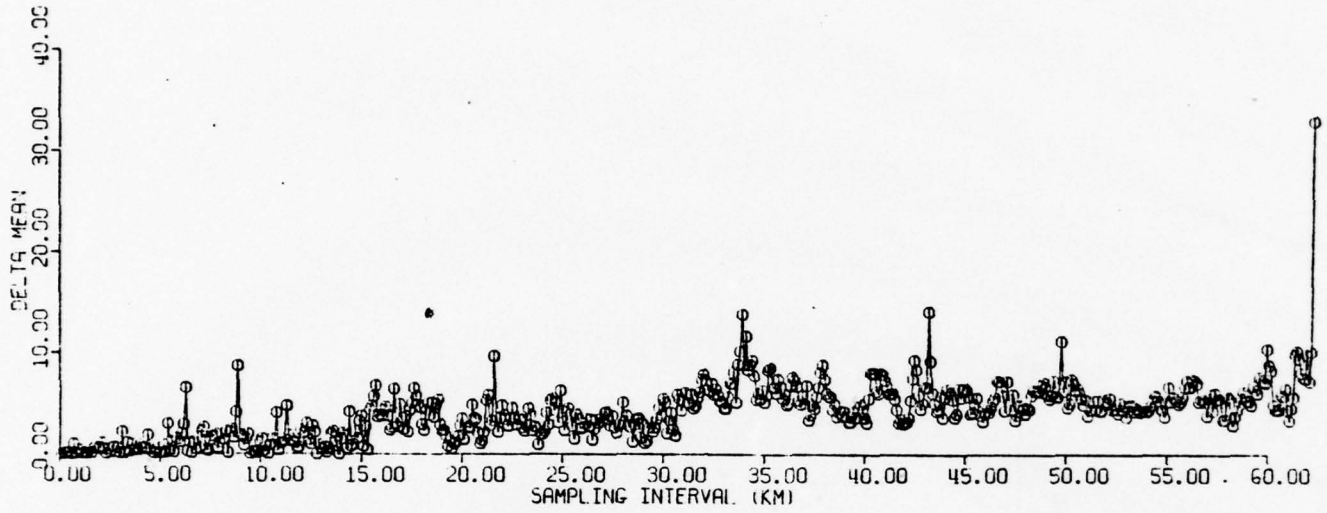

22A

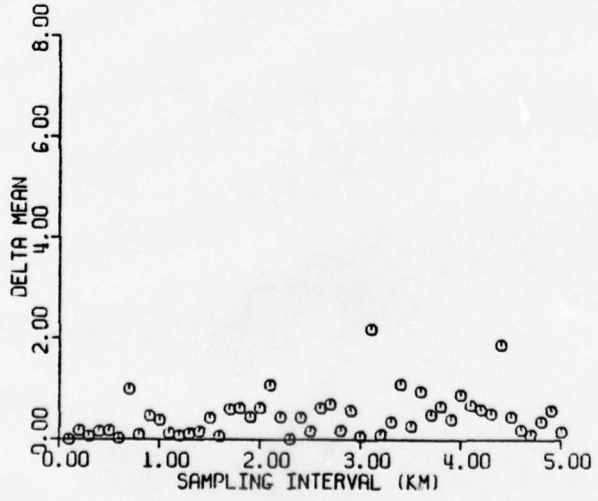

22B

NORTH HATTERAS ISLAND

MEAN STORM SURGE PENETRATION ($\overline{SP}$)

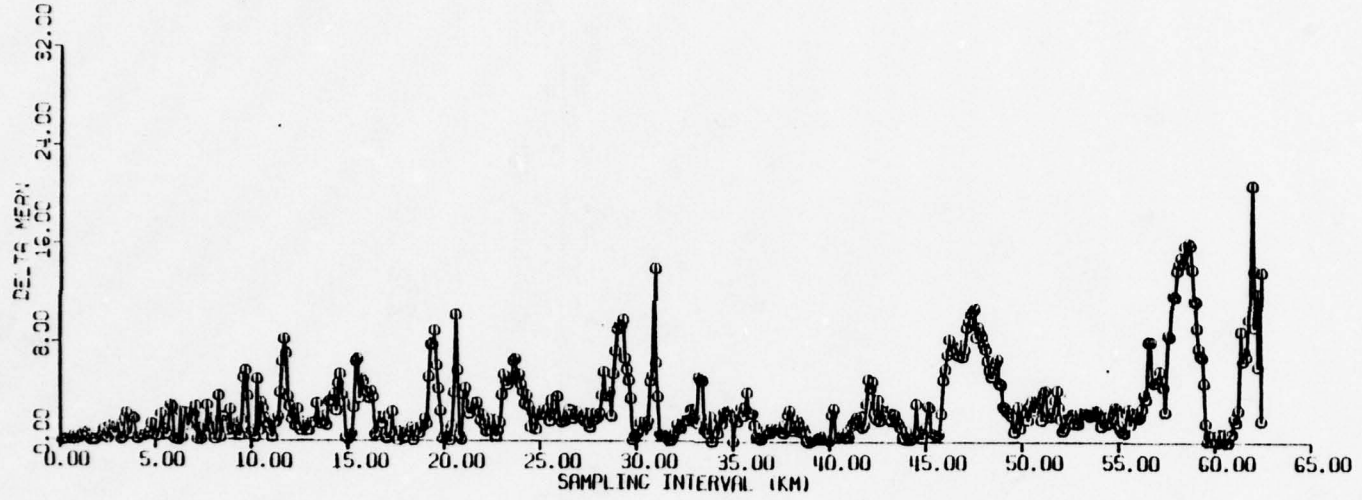

NORTH HATTERAS ISLAND

MEAN STORM SURGE PENETRATION ($\overline{SP}$)

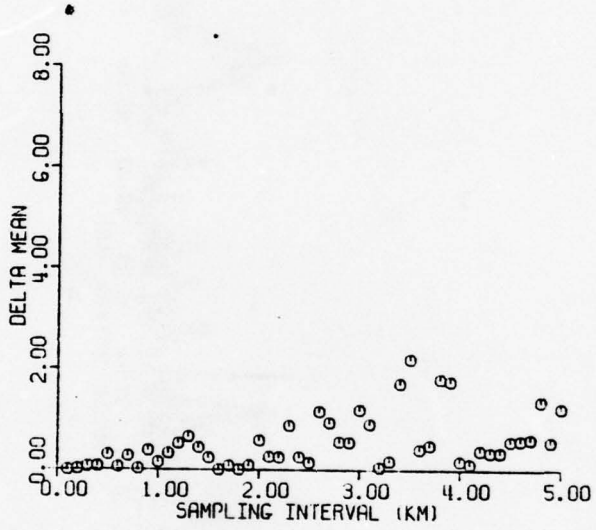

23B

NORTH HATTERAS ISLAND

STORM SURGE PENETRATION STANDARD DEVIATION (σ_{SP})

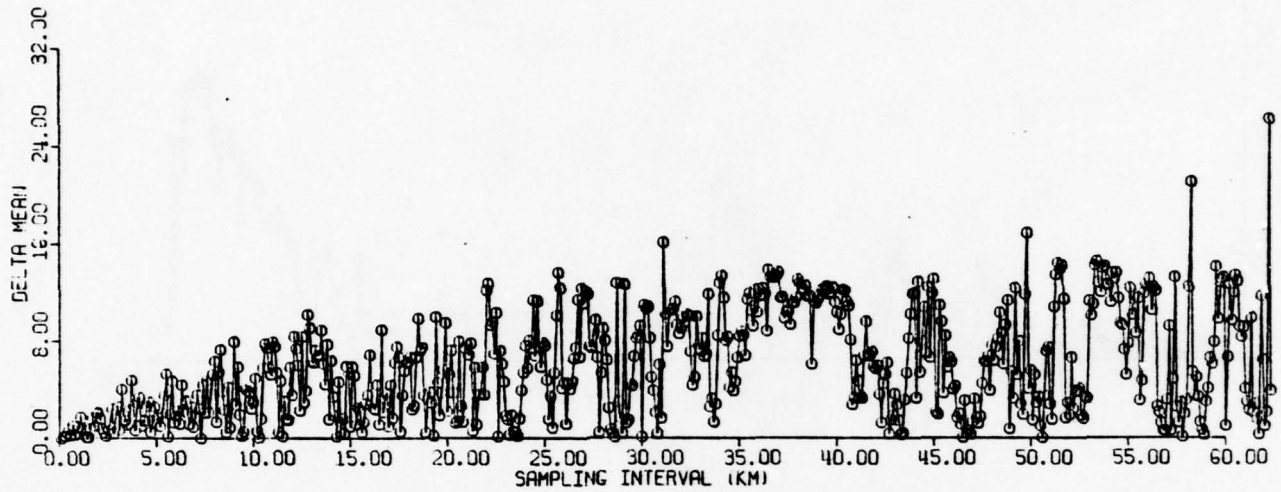

24A

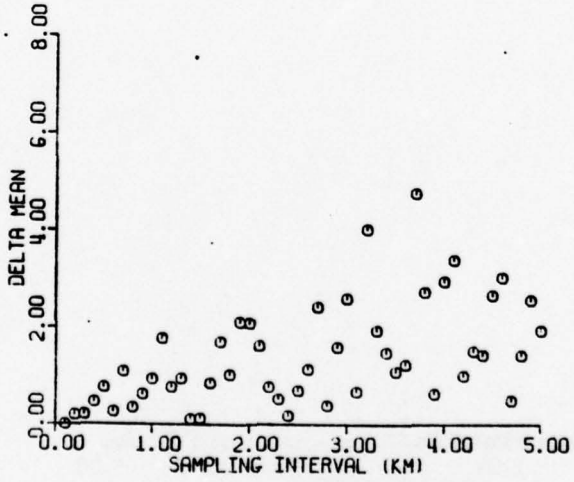

24B

ASSATEAGUE ISLAND

MEAN SHORELINE RATE ($\overline{SL}$)

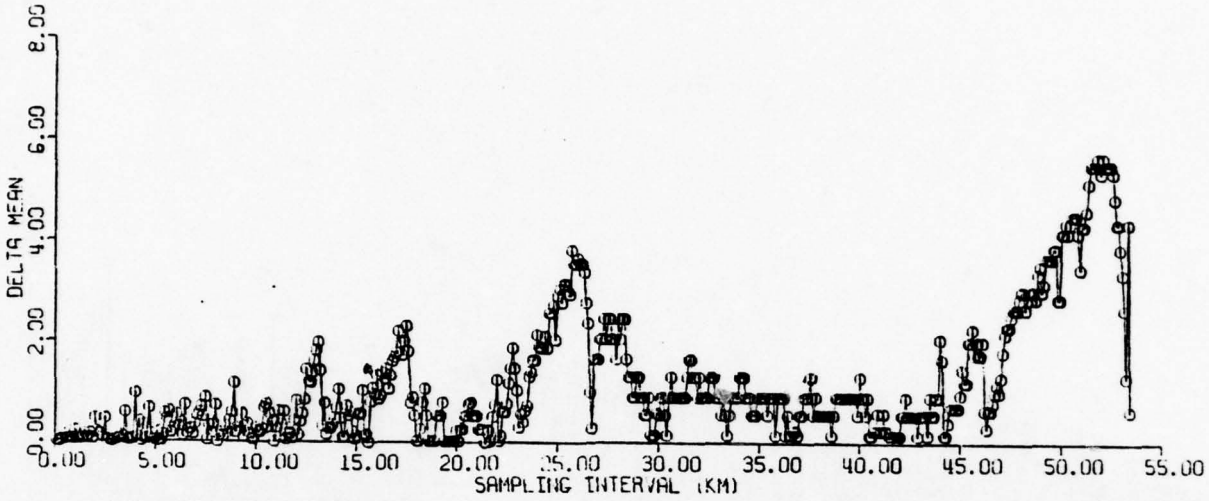

25A

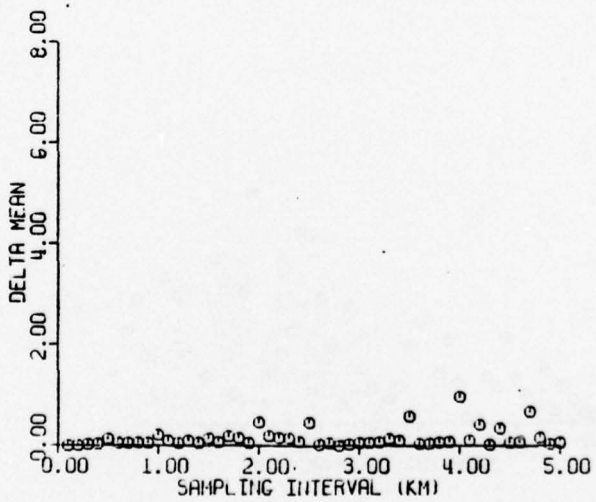

25B

ASSATEAGUE ISLAND

SHORELINE RATE STANDARD DEVIATION (σ_{SL})

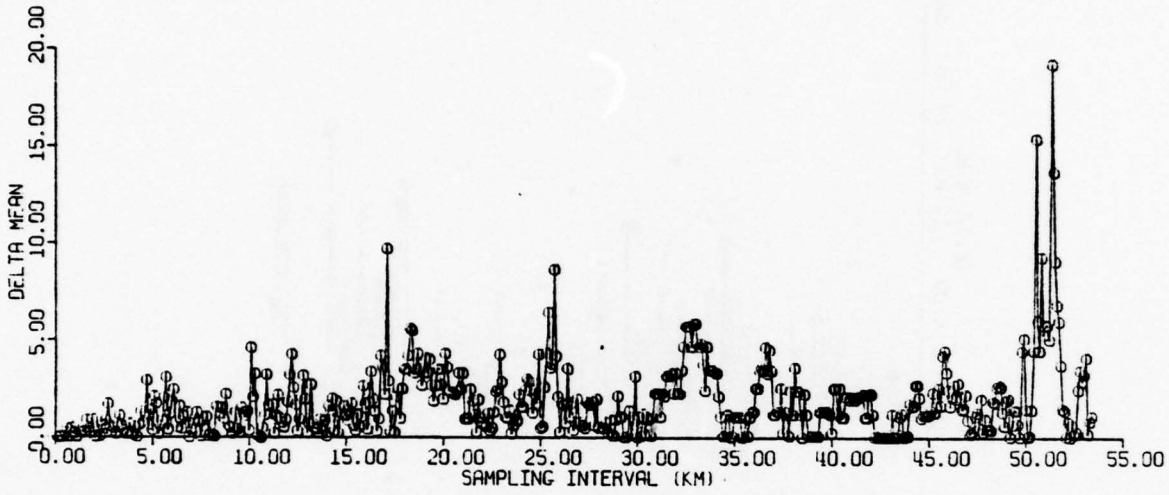

26A

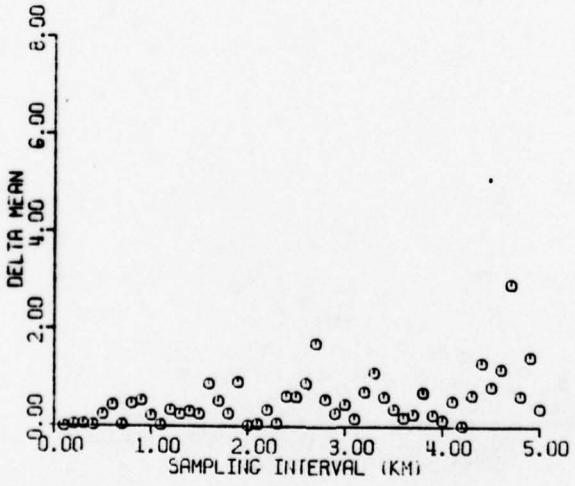

26B

ASSATEAGUE ISLAND

MEAN STORM SURGE PENETRATION ($\overline{SP}$)

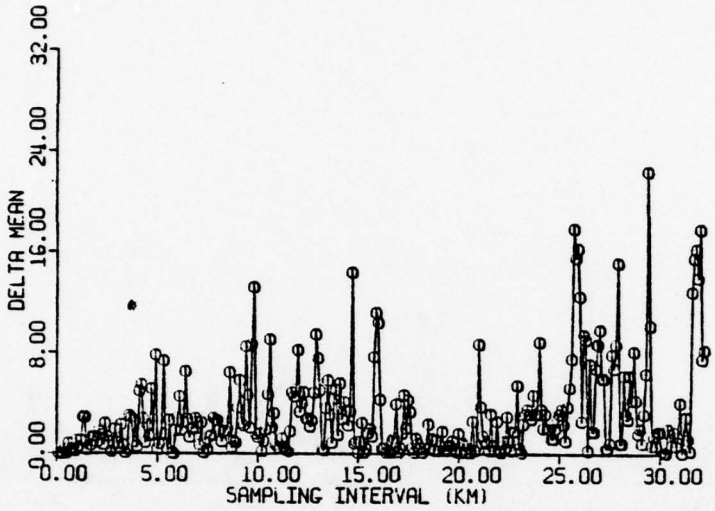

27A

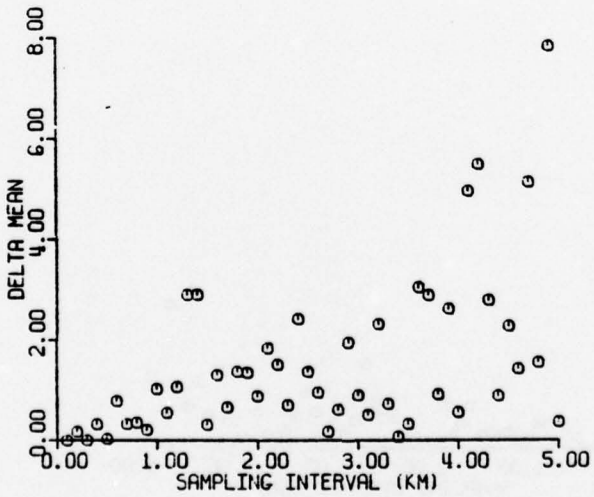

27B

ASSATEAGUE ISLAND

LITTLE TOM'S COVE TO SMITH HAMMOCKS

STORM SURGE PENETRATION STANDARD DEVIATION (σ SP)

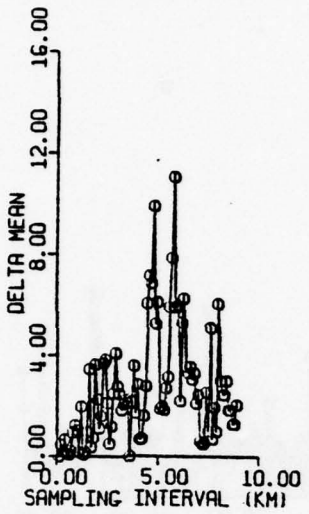

28A

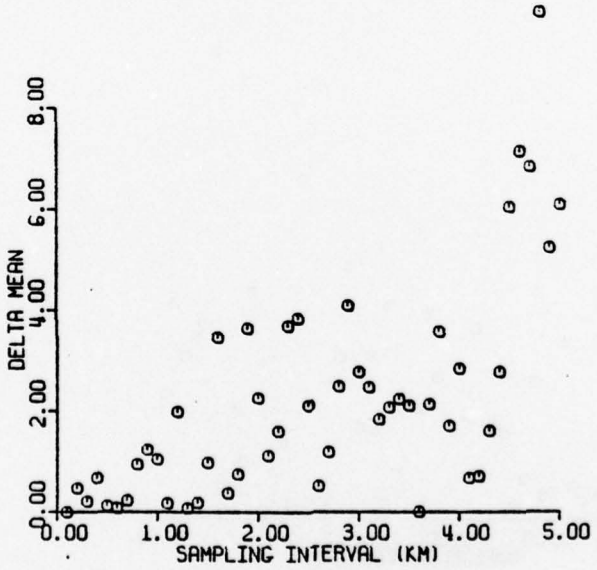

28B

ASSATEAGUE ISLAND

CHERRY TREE HILL TO FOX HILL LEVEL

STORM SURGE PENETRATION STANDARD DEVIATION (σ_{SP})

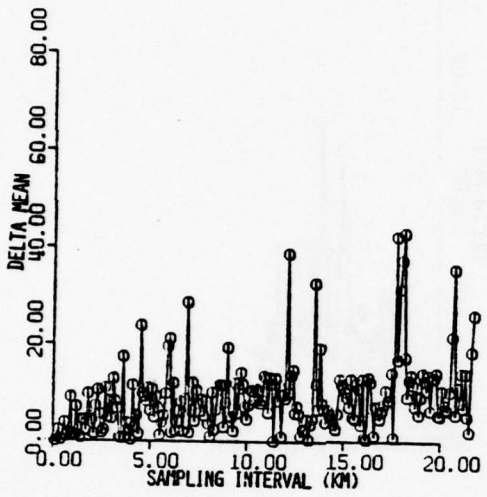

29A

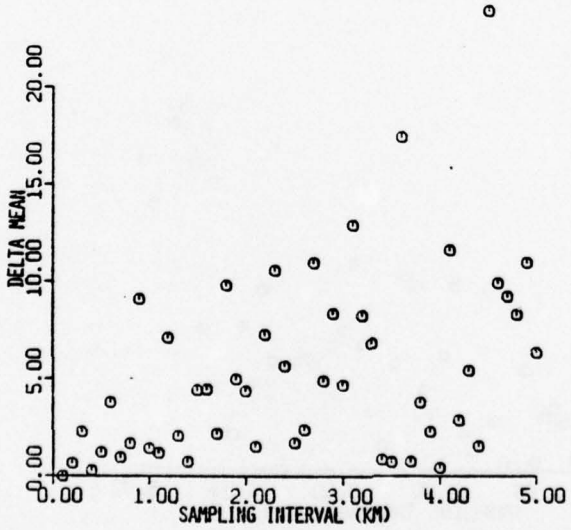

29B

ASSATEAGUE ISLAND

FOX HILL LEVEL TO OCEAN CITY INLET

STORM SURGE PENETRATION STANDARD DEVIATION (σSP)

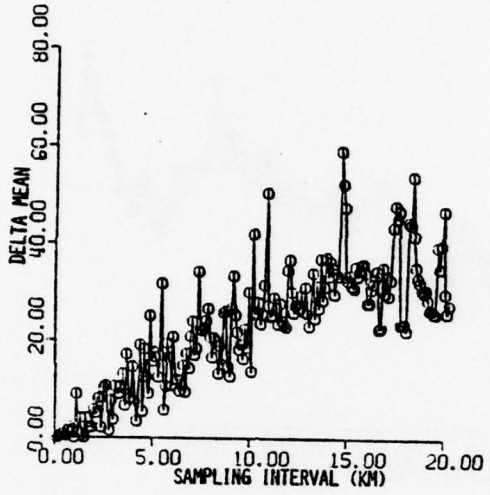

30A

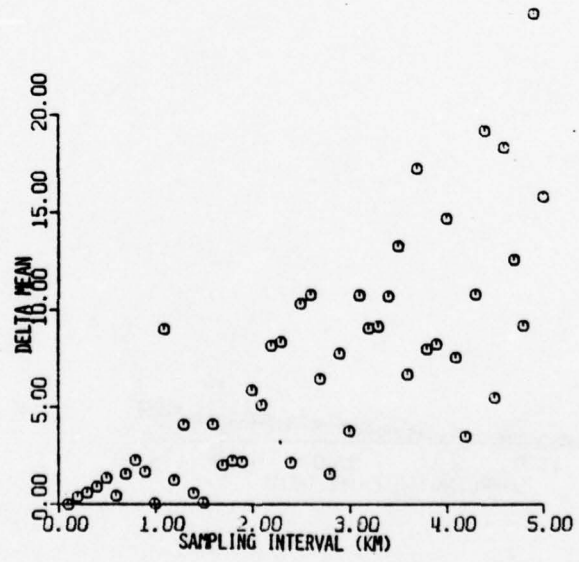

30B

FENWICK ISLAND

SOUTH OF INDIAN RIVER INLET

MEAN SHORELINE RATE ($\overline{SL}$)

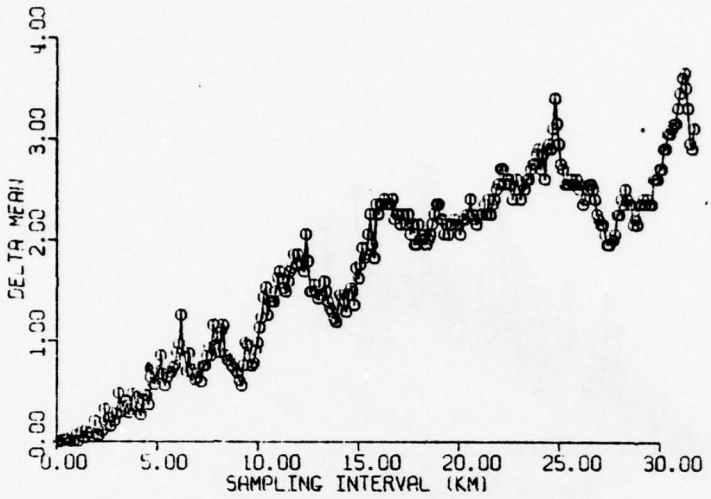

31A

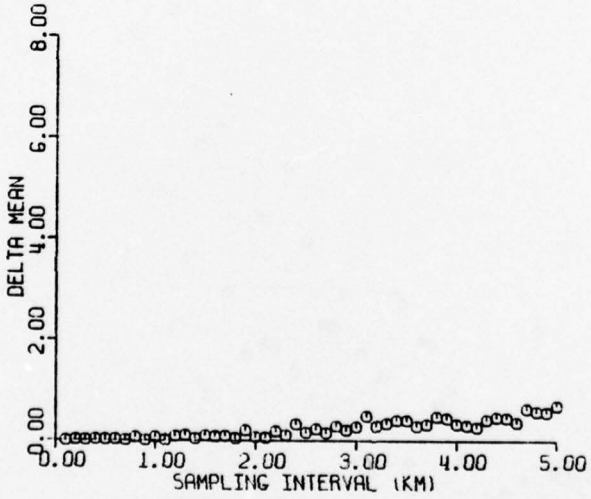

31B

FENWICK ISLAND

NORTH OF INDIAN RIVER INLET

MEAN SHORELINE RATE ($\overline{SL}$)

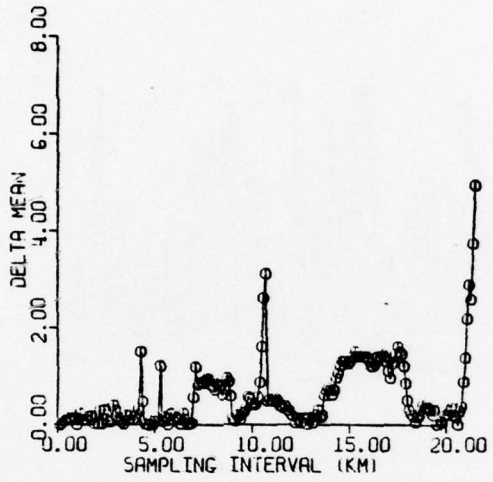

32A

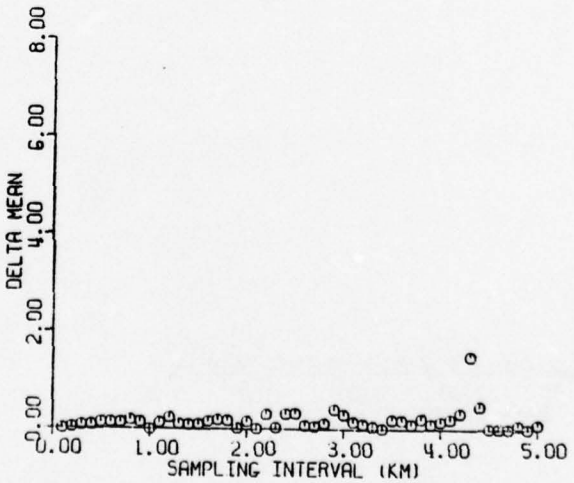

32B

FENWICK ISLAND

SOUTH OF INDIAN RIVER INLET

SHORELINE RATE STANDARD DEVIATION (σSL)

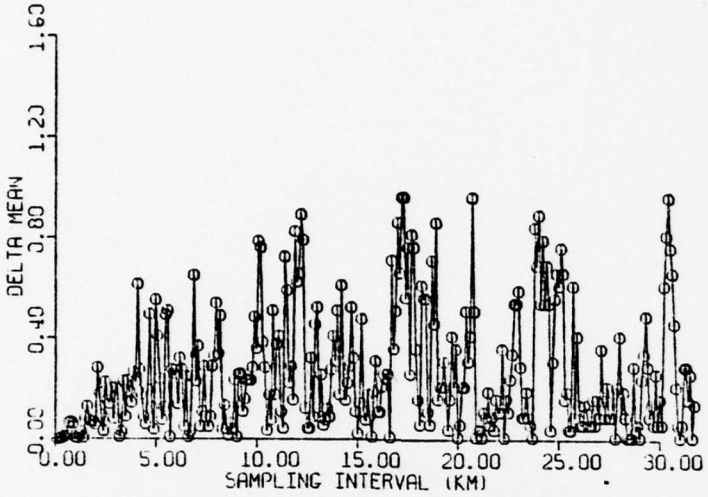

33A

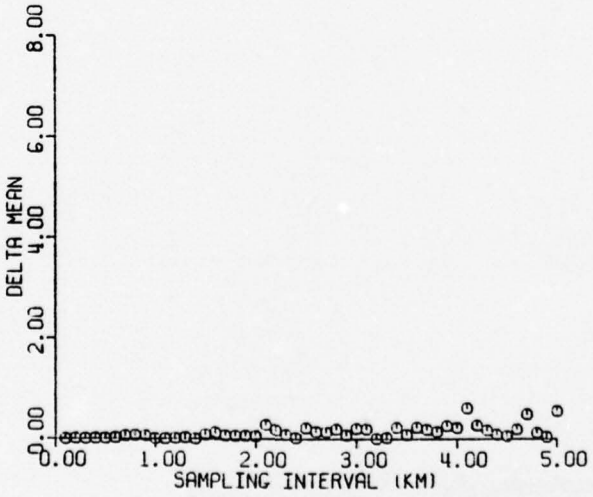

33B

FENWICK ISLAND

NORTH OF INDIAN RIVER INLET

SHORELINE RATE STANDARD DEVIATION (σ_{SL})

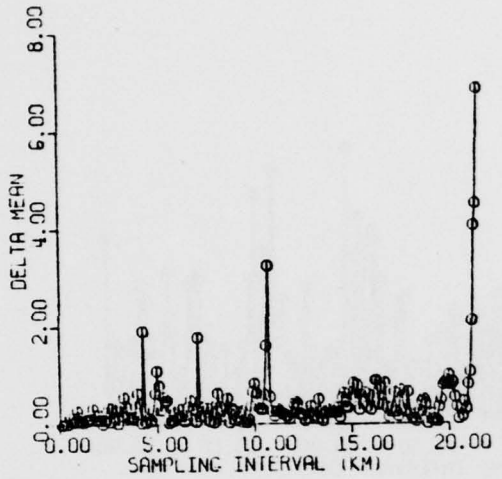

34A

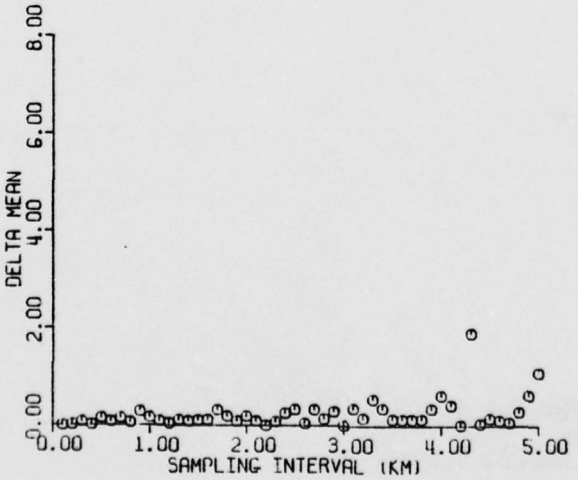

34B

SOUTH OF INDIAN RIVER INLET

MEAN STORM SURGE PENETRATION ($\overline{SP}$)

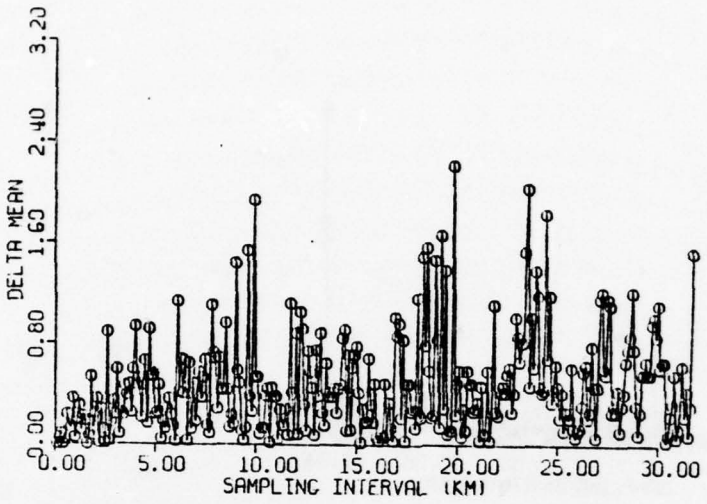

35A

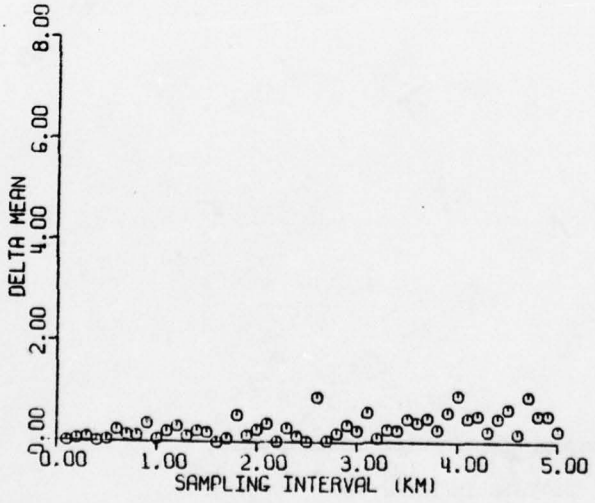

35B

FENWICK ISLAND

NORTH OF INDIAN RIVER INLET

MEAN STORM SURGE PENETRATION ($\overline{SP}$)

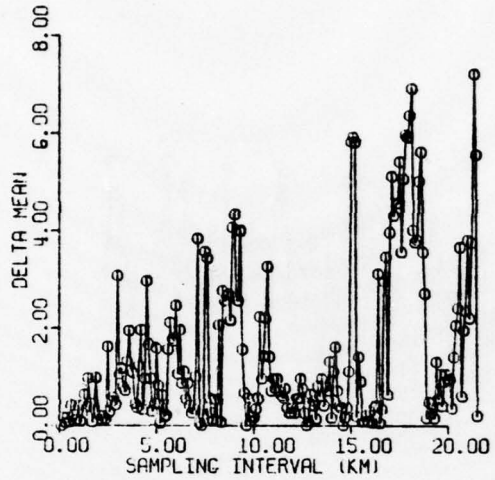

36A

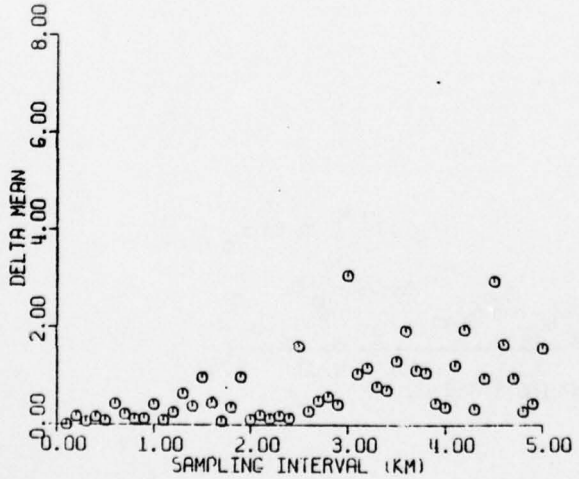

36B

FENWICK ISLAND

SOUTH OF INDIAN RIVER INLET

STORM SURGE PENETRATION STANDARD DEVIATION (σ_{SP})

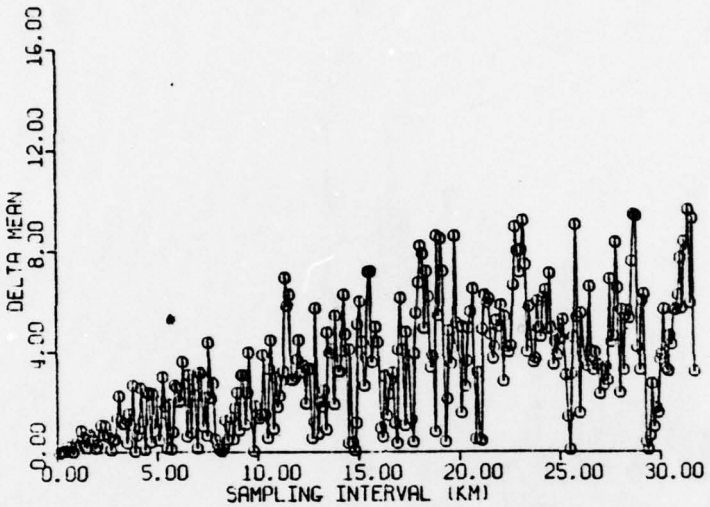

37A

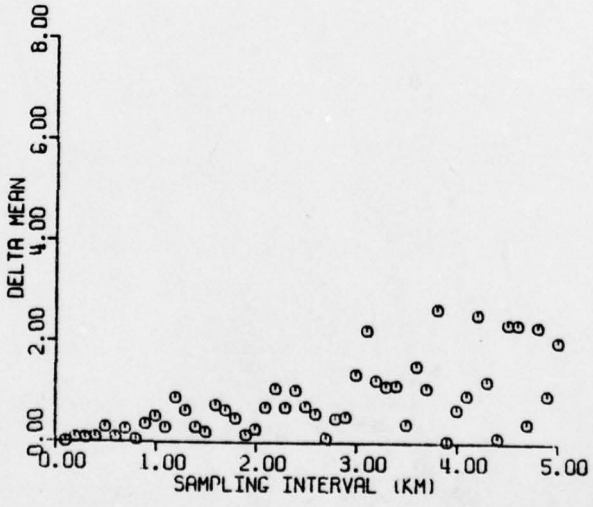

37B

FENWICK ISLAND

NORTH OF INDIAN RIVER INLET

STORM SURGE PENETRATION STANDARD DEVIATION (σ_{SP})

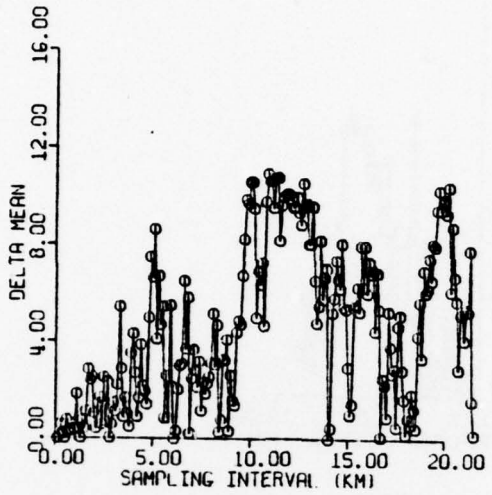

38A

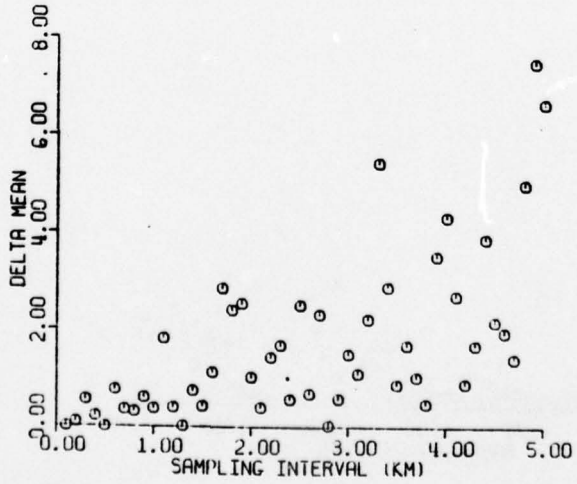

38B

CAPE MAY

SOUTH NEW JERSEY

MEAN SHORELINE RATE ($\overline{SL}$)

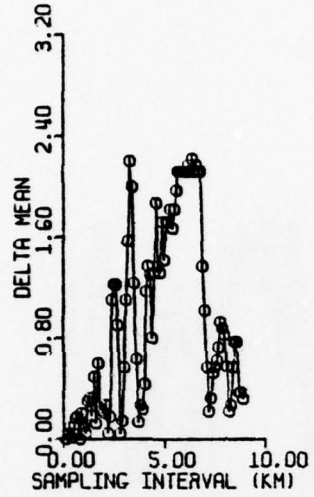

39A

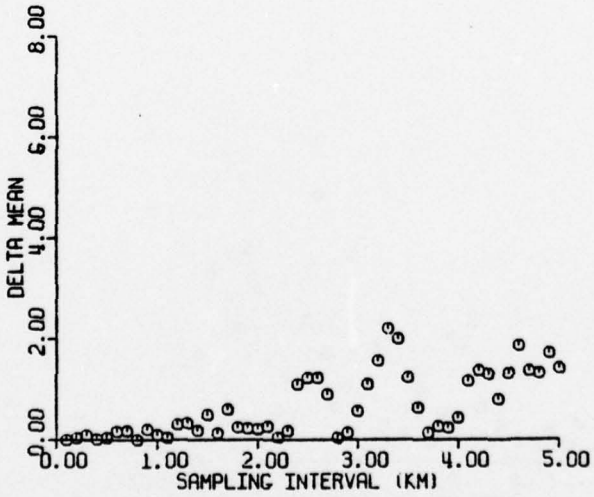

39B

CAPE MAY

SOUTH NEW JERSEY

SHORELINE RATE STANDARD DEVIATION (σ_{SL})

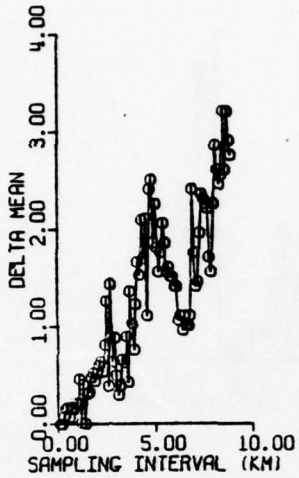

40A

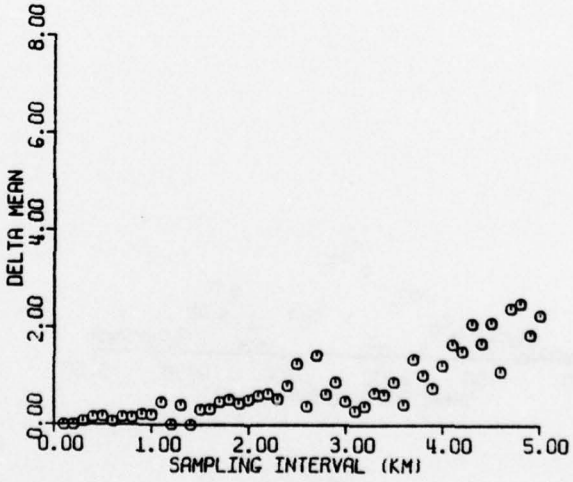

40B

CAPE MAY

SOUTH NEW JERSEY

MEAN STORM SURGE PENETRATION ($\overline{SP}$)

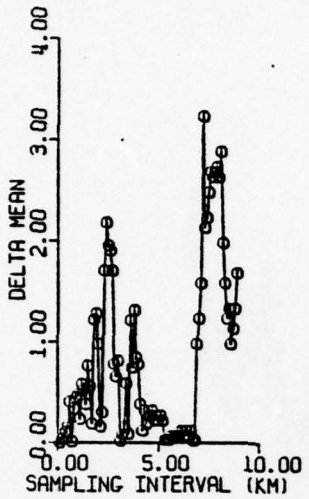

41A

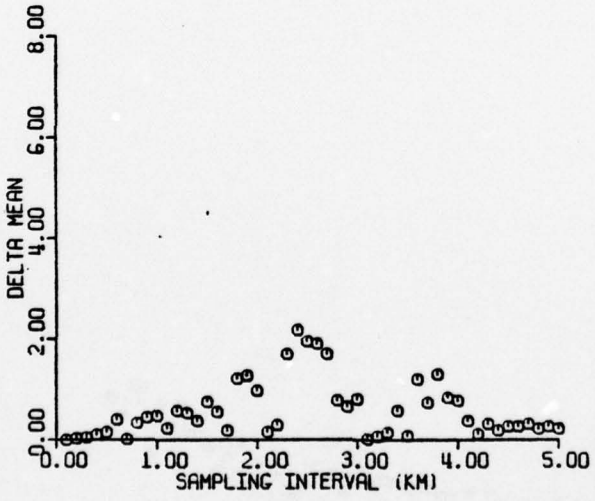

41B

CAPE MAY

SOUTH NEW JERSEY

STORM SURGE PENETRATION STANDARD DEVIATION ($\sigma_{\bar{SP}}$)

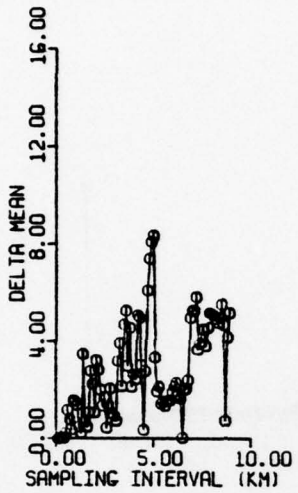

42A

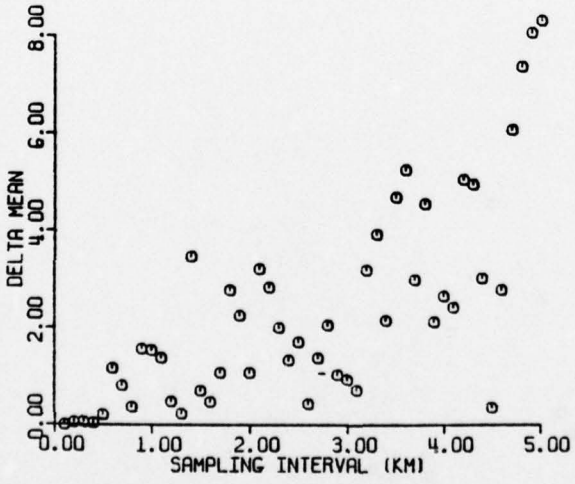

42B

SEVEN MILE BEACH

SOUTH NEW JERSEY

MEAN SHORELINE RATE ($\overline{SL}$)

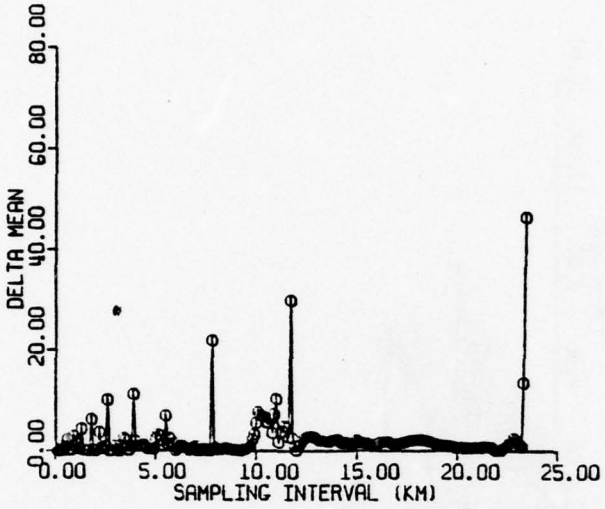

43A

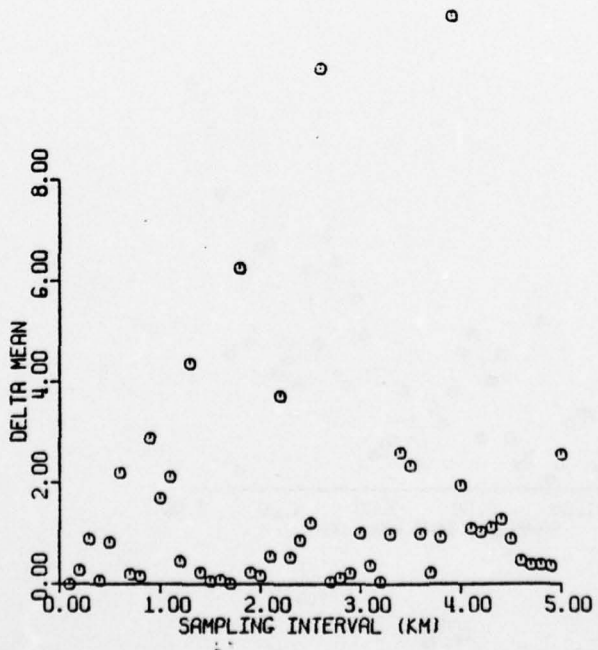

43B

SEVEN MILE BEACH SOUTH OF HEREFORD INLET

SOUTH NEW JERSEY

SHORELINE RATE STANDARD DEVIATION (σ_{SL})

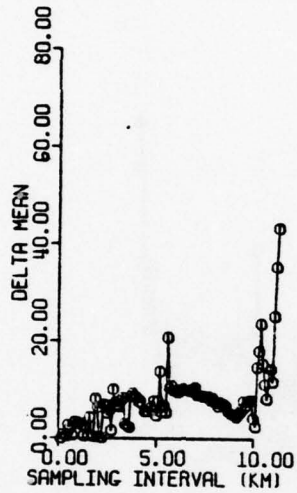

44A

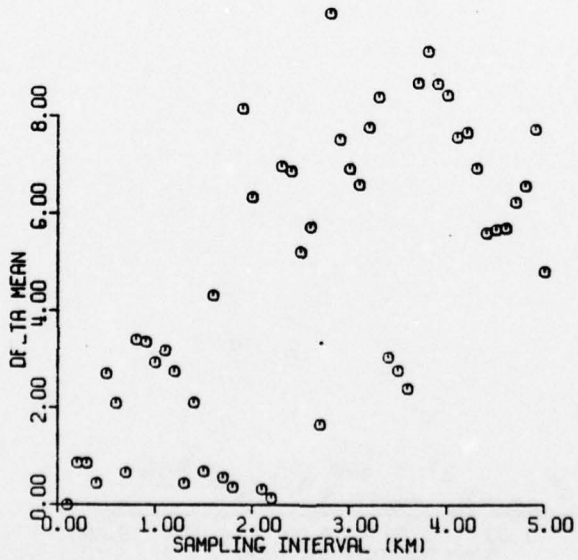

44B

SEVEN MILE BEACH NORTH OF HEREFORD INLET

SOUTH NEW JERSEY

SHORELINE RATE STANDARD DEVIATION (σ_{SL})

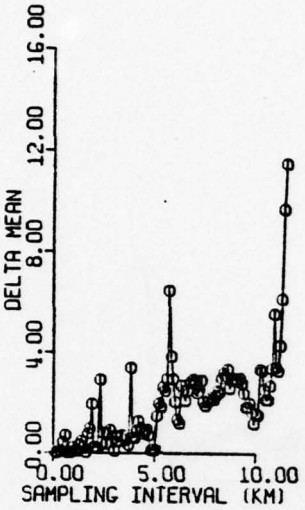

45A

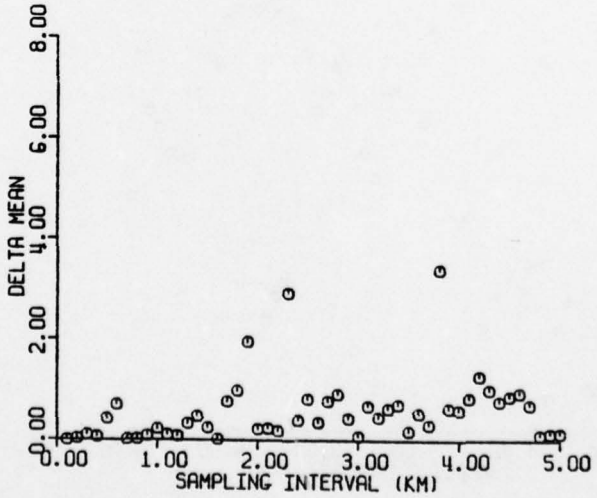

45B

SEVEN MILE BEACH

SOUTH NEW JERSEY

MEAN STORM SURGE PENETRATION ($\overline{SP}$)

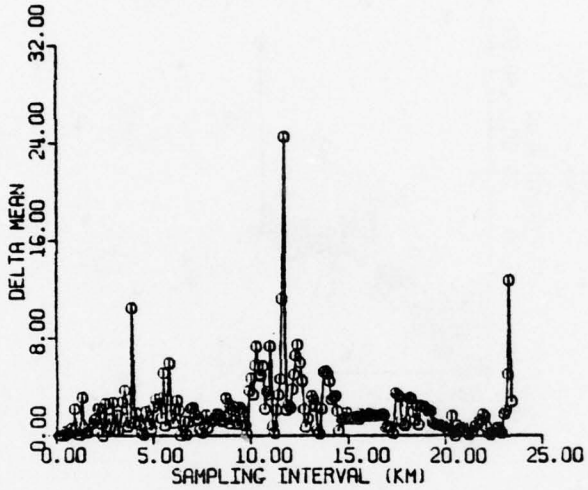

46A

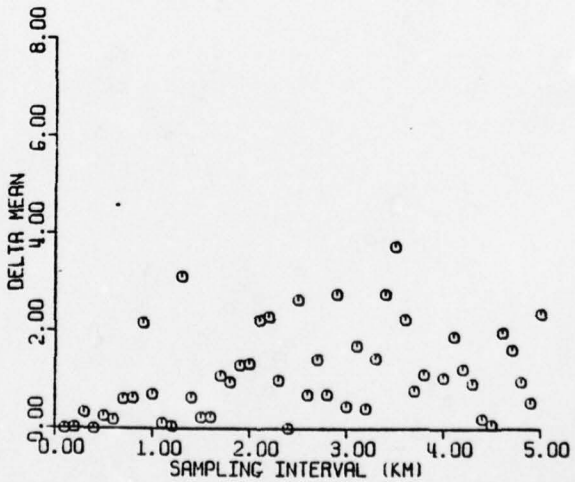

46B

SEVEN MILE BEACH SOUTH OF HEREFORD INLET

SOUTH NEW JERSEY

STORM SURGE PENETRATION

STANDARD DEVIATION (σ_{SP})

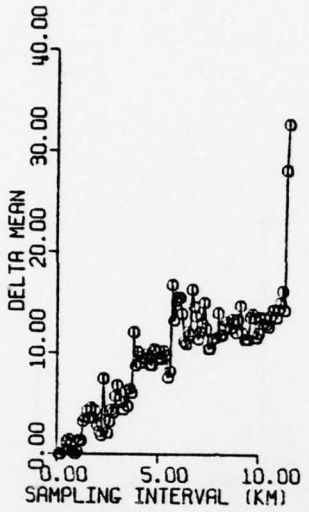

47A

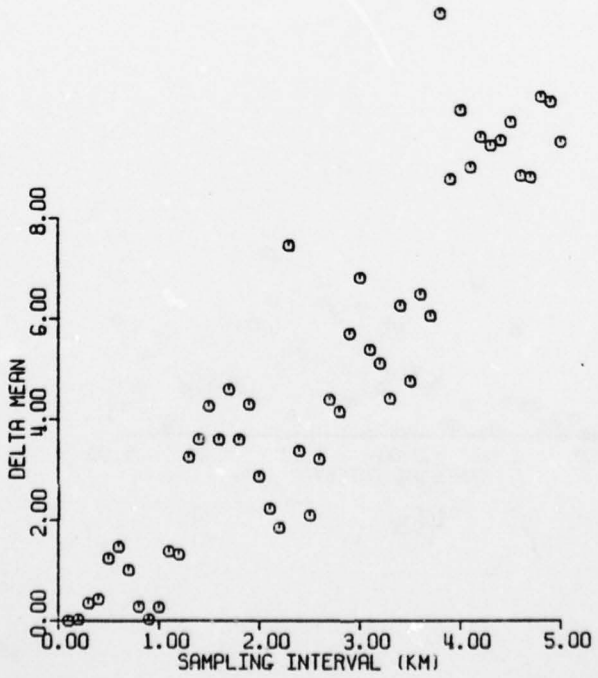

47B

AD-A058 636 VIRGINIA UNIV CHARLOTTESVILLE DEPT OF ENVIRONMENTAL --ETC F/G 8/3
ANALYSIS OF SPATIAL AND TEMPORAL SHORELINE VARIATIONS ALONG THE--ETC(U)
SEP 78 R DOLAN, B HAYDEN, W FELDER, J HEYWOOD N00014-75-C-0480

UNCLASSIFIED TR-19 NL

2 OF 2
AD
A058636

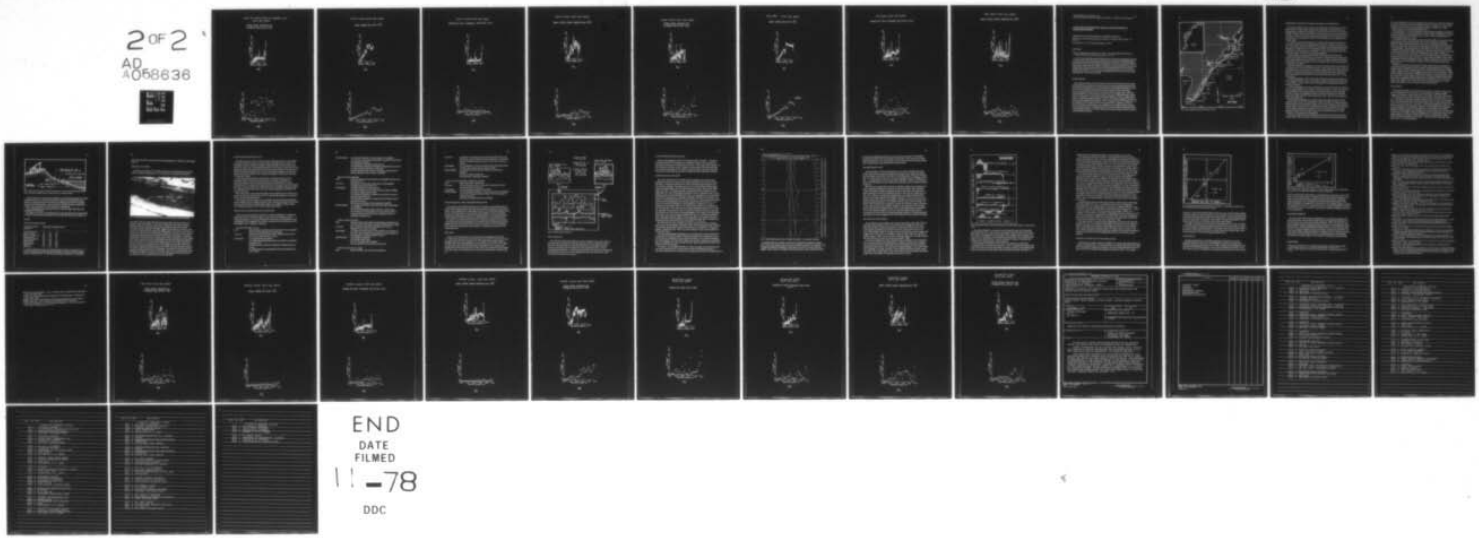

END
DATE
FILMED
11-78
DDC

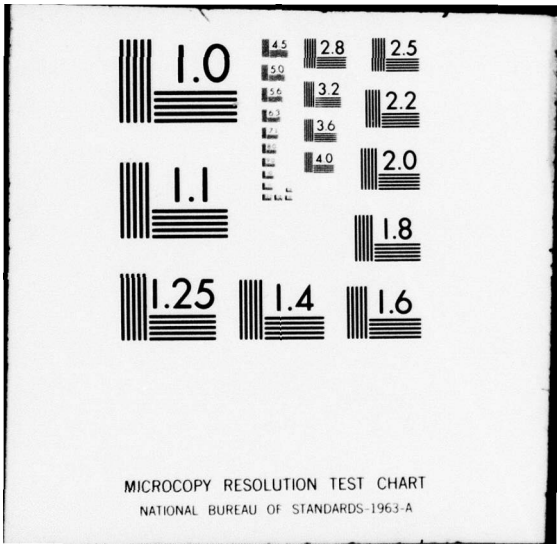
1.0
1.1
1.25
1.4
1.6
1.8
2.0
2.2
2.5
2.8
3.2
3.6
4.0
4.5
5.0
5.6
MICROCOPY RESOLUTION TEST CHART
NATIONAL BUREAU OF STANDARDS-1963-A

SEVEN MILE BEACH NORTH OF HEREFORD INLET

SOUTH NEW JERSEY

STORM SURGE PENETRATION
STANDARD DEVIATION (σ_{SP})

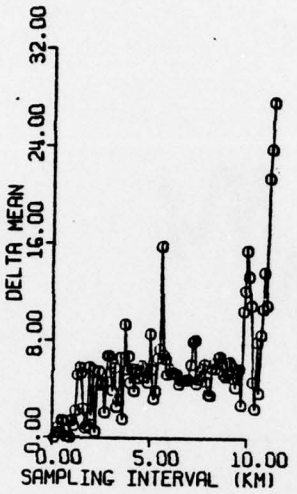

48A

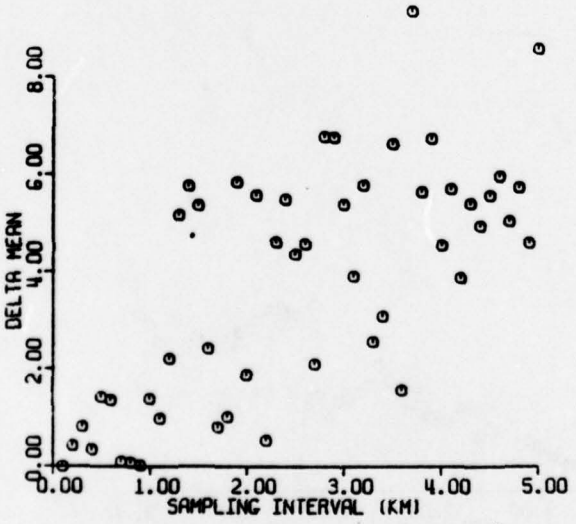

48B

LUDLAM ISLAND SOUTH NEW JERSEY

MEAN SHORELINE RATE ($\overline{SL}$)

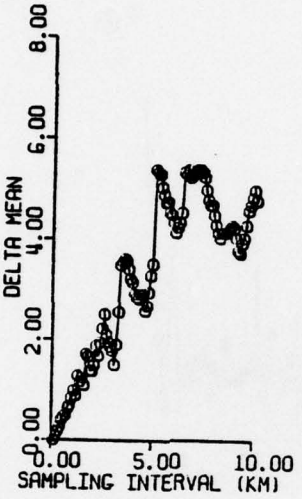

49A

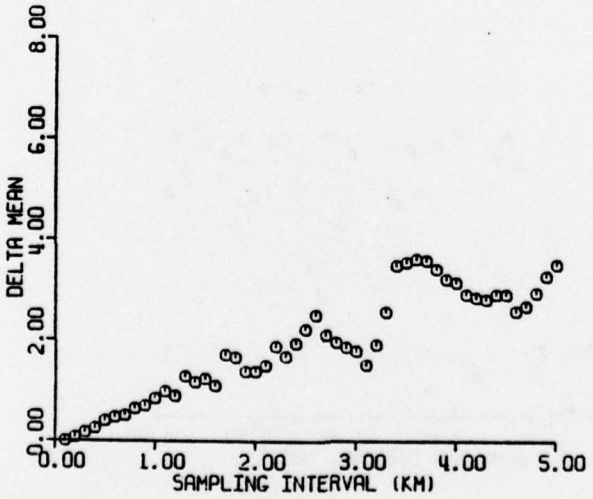

49B

LUDLAM ISLAND SOUTH NEW JERSEY

SHORELINE RATE STANDARD DEVIATION (σSL)

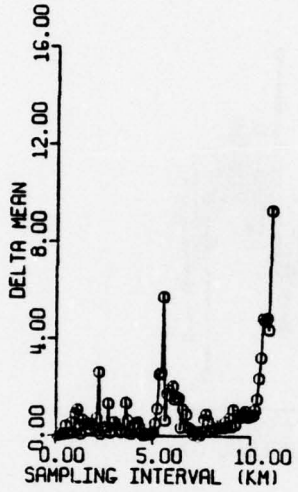

50A

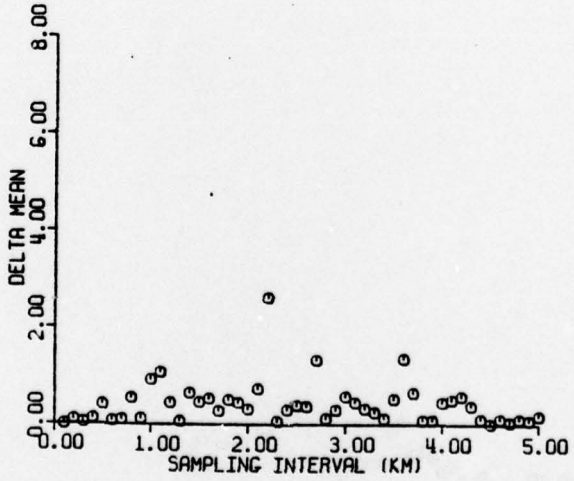

50B

LUDLAM ISLAND SOUTH NEW JERSEY

MEAN STORM SURGE PENETRATION ($\overline{SP}$)

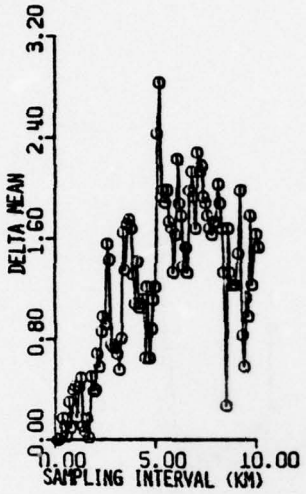

51A

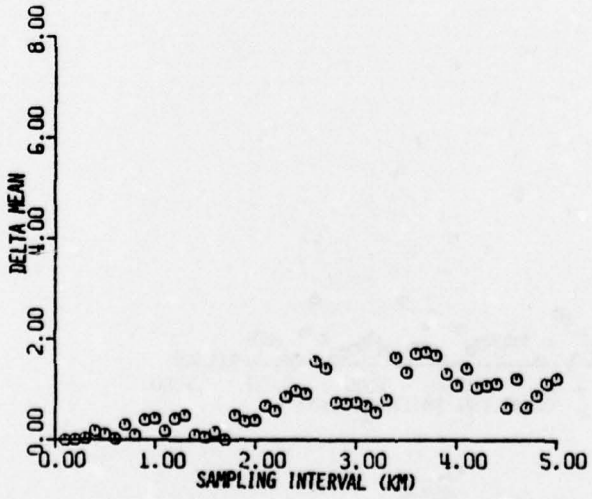

51B

LUDLAM ISLAND SOUTH NEW JERSEY

STORM SURGE PENETRATION
STANDARD DEVIATION (σ_{SP})

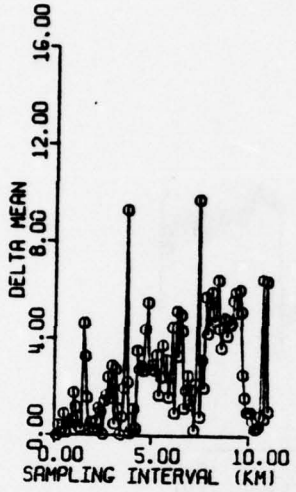

52A

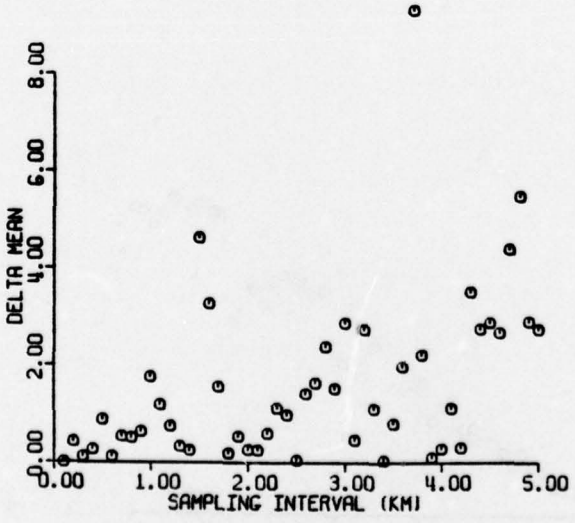

52B

PECK BEACH SOUTH NEW JERSEY

MEAN SHORELINE RATE ($\overline{SL}$)

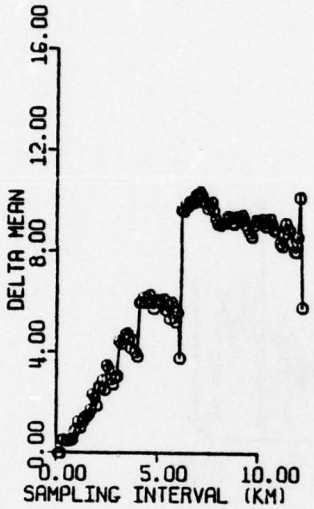

53A

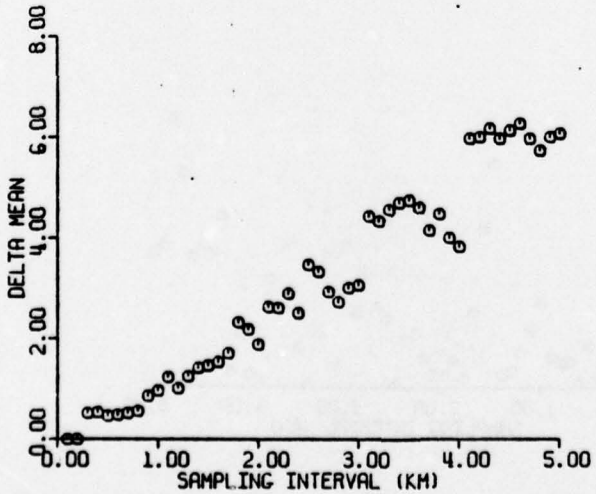

53B

PECK BEACH SOUTH NEW JERSEY

SHORELINE RATE. STANDARD DEVIATION (σ_{SL})

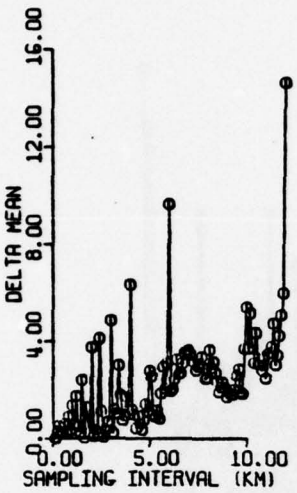

54A

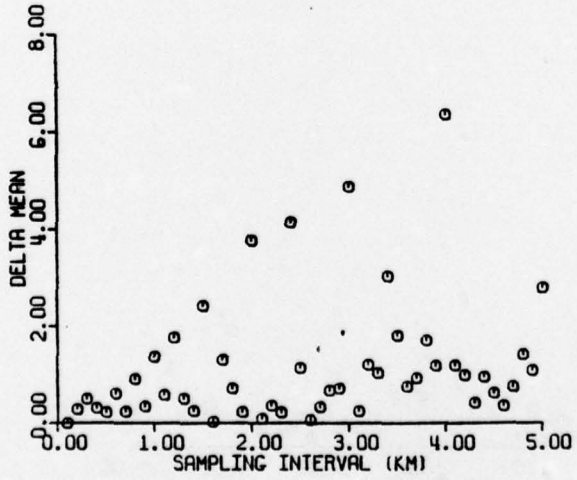

54B

PECK BEACH SOUTH NEW JERSEY

MEAN STORM SURGE PENETRATION ($\overline{SP}$)

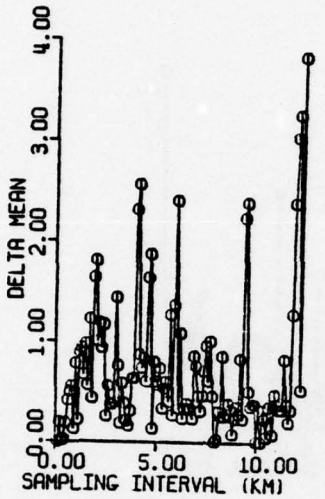

55A

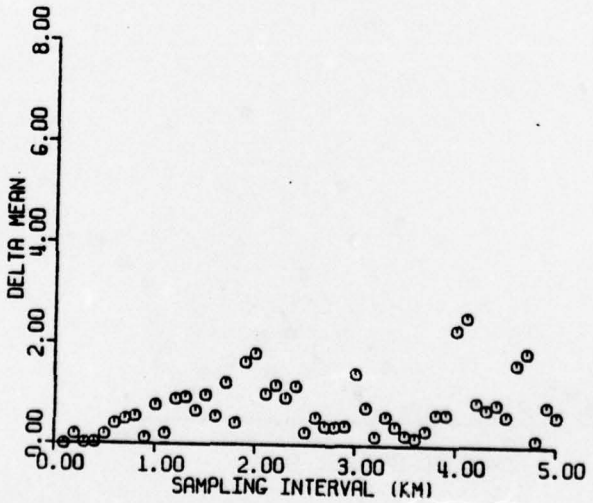

55B

Coastal Engineering, 2 (1978) 21—39

A NEW PHOTOGRAMMETRIC METHOD FOR DETERMINING SHORELINE EROSION

ROBERT DOLAN, BRUCE HAYDEN and JEFFREY HEYWOOD

Department of Environmental Sciences, University of Virginia, Charlottesville, Va. (U.S.A.)

(Received July 11, 1977; accepted December 1, 1977)

ABSTRACT

Dolan, R., Hayden, B. and Heywood, J., 1978. A new photogrammetric method for determining shoreline erosion. Coastal Eng., 2: 21—39.

In order to systematically measure shoreline erosion and storm surge penetration along extensive reaches of the United States Atlantic coast, a common-scale mapping method was developed using historical aerial photography as the data base. Aerial photography of the southern New Jersey coast covering four decades is used to demonstrate the methodology and to provide long-term baseline information on shoreline dynamics. The data sets include mean erosion rates and variance at 100-m intervals along the coast. Shoreline recession rates along the New Jersey coast are generally less than 1 m/yr. but for several locations rates exceed 5 m/yr., and they vary considerably both within and between the island segments of the New Jersey coast.

INTRODUCTION

The Atlantic coast of North America is one of the world's most dynamic sedimentary environments. Extratropical and tropical storms generate waves and surge that frequently alter the subaqueous and subaerial portions of the shore zone. During the past several decades there has been a net trend toward coastal recession (erosion) along the Atlantic coast. This trend has been attributed to a recent rise in sea level (Bruun, 1962; Hicks and Crosby, 1974), a reduction in new fluvial sediments (Wolman, 1971), human alterations of coastal morphology (Dolan, 1972), and secular changes in storm frequencies and magnitudes (Hayden, 1975). Changes along New Jersey (Fig. 1) are typical for the Atlantic coast; the average rate of recession is about 1 m/yr. This paper summarizes a new method of recording shoreline changes over extensive reaches of sedimentary coasts using aerial photography and an orthogonal grid system. A 90-km section of the New Jersey coast is used for a demonstration project.

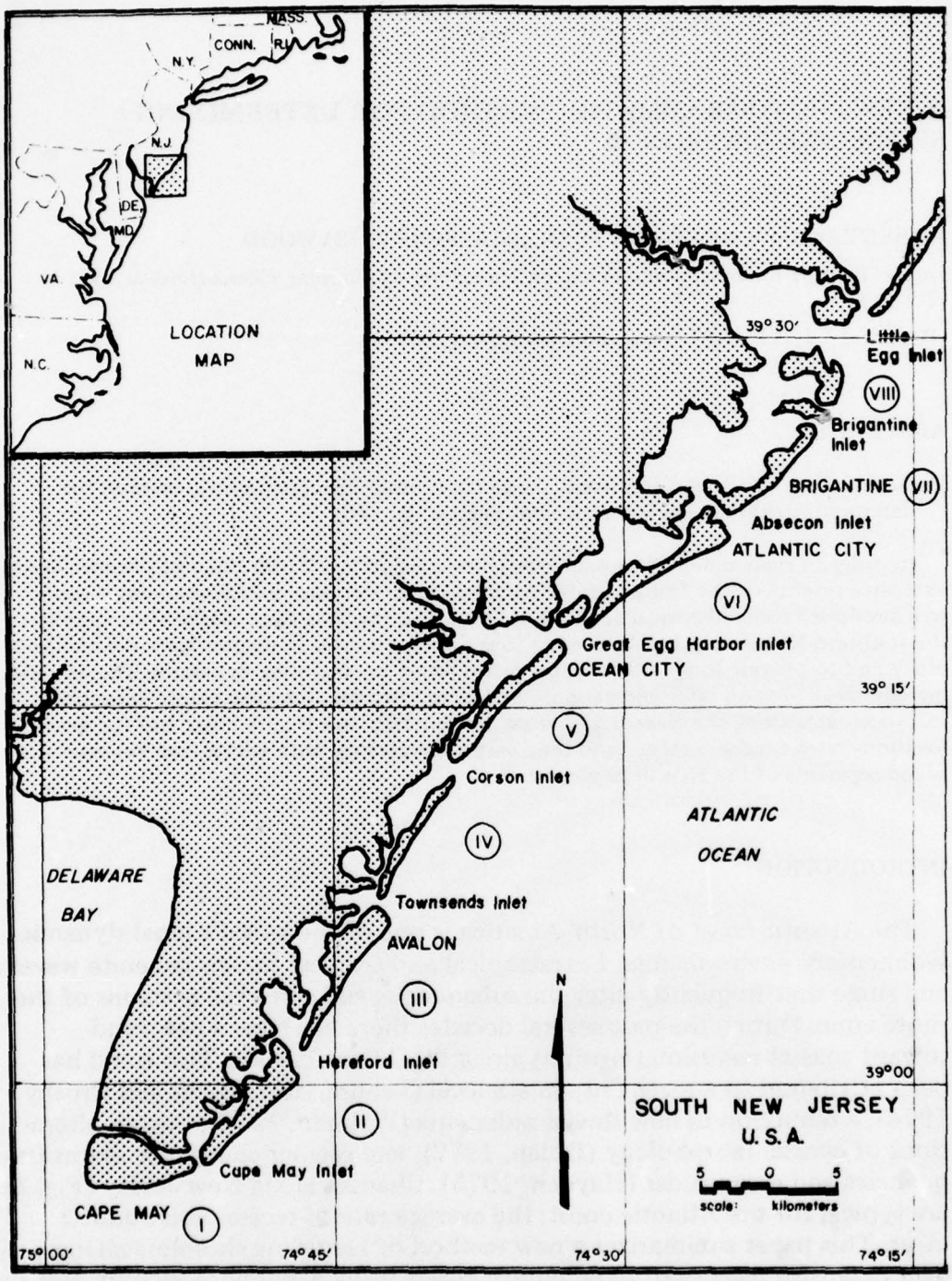

Fig. 1. The southern coast of New Jersey, U.S.A.

DETERMINING TRENDS IN SHORELINE EROSION AND DEPOSITION

Along the Atlantic coast, storms cause landscape modification at a wide range of scales. Private land holdings are destroyed, communication and transportation facilities are disrupted, and the loss of life is not uncommon. In spite of these obvious problems in coastal areas where extreme storms are common, with few exceptions management strategy has been based on the concept that the landscape is stable or at least that it can be engineered to remain stable.

To marine scientists, managers, and coastal engineers the shoreline and beach-face have long been recognized as elements of a highly dynamic system. The information base needed for good planning and engineering design includes the current state of the system and rates of change through time. Information of this type can be obtained: (1) by ground surveys; (2) from maps and charts; and (3) from aerial photographs.

Ground survey methods provide data of the highest resolution but accurate historical records that can be used for comparisons are lacking for most coastal areas and the generation of new surveys is expensive and time consuming. With the exception of a few scattered sites, ground information is generally unavailable.

Maps and charts are available for numerous coastal locations and frequently extend back to the mid-1800's; however, while charts are useful, most are of questionable accuracy and are frequently restricted to areas immediately adjacent to major shipping lanes and port facilities. Maps and charts best serve as supplemental information in determining historical trends in shoreline change.

Aerial photographs, taken with metric mapping cameras, are available for most coastal locations in the United States. Earliest photographs date back to the 1930's or early 1940's, and photographs for subsequent decades are generally available.

Aerial photography has many advantages over the other types of information in coastal mapping. In a matter of hours hundreds of miles of coast can be photographed: an instantaneous record rather than a survey spanning months or years. Photographs include a measure of detail over extended areas unavailable with any other information base, and they are permanent and easily duplicated.

While aerial photographs are usually taken with high resolution metric cameras, they are not the equivalent of maps. This lack of orthogonal equivalence results in scale variance within and between images. Scale variations are generally of four types: (1) differences caused by changes in the altitude of the camera platform; (2) variations due to camera tilt; (3) radial scale variations away from the image center; and (4) distortions due to relief variations of the surface photographed.

The scale variation due to land relief is the least serious error along low sedimentary coasts, resulting in insignificant errors in measurements (Staf-

ford and Langfelder, 1971), and radial scale distortion is also well within the potential error associated with mapping shoreline changes. Tilt error within images and scale error between images is usually minimal and is easily rectified using correcting enlarging projectors.

Early attempts to obtain information from aerial photographs focused on the identification of coastal landforms (Lucke, 1934); illustration of coastal processes (Eardley, 1941; Shepard et al., 1941), and the classification of coastal features (Smith, 1943).

In 1947 McCurdy identified the high water line (HWL) as a major recognizable feature of the subaerial beach face. Later, McCurdy (1950) and McBeth (1956) indicated that there was only an insignificant difference between the water line of the previous high tide and the HWL line recognized on photographs. The stable nature of the HWL over a tidal cycle was later confirmed by Stafford (1968). During the 1950's several attempts were made to assess beach erosion with aerial photographs (Rib, 1957; Zeigler and Ronne, 1957; Chieruzzi and Baker, 1958). In 1960, Williams recommended several procedures to insure accuracy in extracting information from aerial photography, and subsequently Tanner (1961) attempted to calculate from a sequence of aerial photographs changes in beach sand volume caused by storm action.

Efforts to quantify local shoreline changes using aerial photography increased following the great Atlantic coast Ash Wednesday storm of March, 1962 (El Ashry, 1963; Athearn and Ronne, 1963; Harris and Jones, 1964). Larger coastal reaches were investigated subsequently by Plusquellec (1966), Gawne (1966), and El Ashry (1966), using common scale planimetric maps generated from aerial photo interpretation. Shoreline change measurements were made by Stafford (1968), Stafford and Langfelder (1971) and Langfelder et al. (1968, 1970). They also assess the errors inherent in metric aerial photographs as well as errors in their interpretation.

The shoreline

The simple definition of a shoreline is the edge of a body of water; however, the position of the shoreline on the beach face is highly variable because of changes in water level due to lunar tides, waves, and wind tides.

The slopes on the beaches along the mid-Atlantic coast vary from 1 : 10 to 1 : 50. With a tidal range of approximately 1.0 m to 1.25 m the intersection of the beach and ocean has a horizontal variation range over the tidal cycle of 10 m to 60 m for 1 : 10 and 1 : 50 slopes, respectively (Fig. 2). This level of variation of the shoreline interface is unacceptable for a mapping program designed to characterize changes in the shoreline over several decades. Two alternatives are available: (1) correct all data sets for tidal stage at the time of the flight of the photography; or (2) define some other more stable marker of the shore which is less sensitive to tidal stage. In these studies the latter strategy was followed — the alternative is the high water line as seen on the photography.

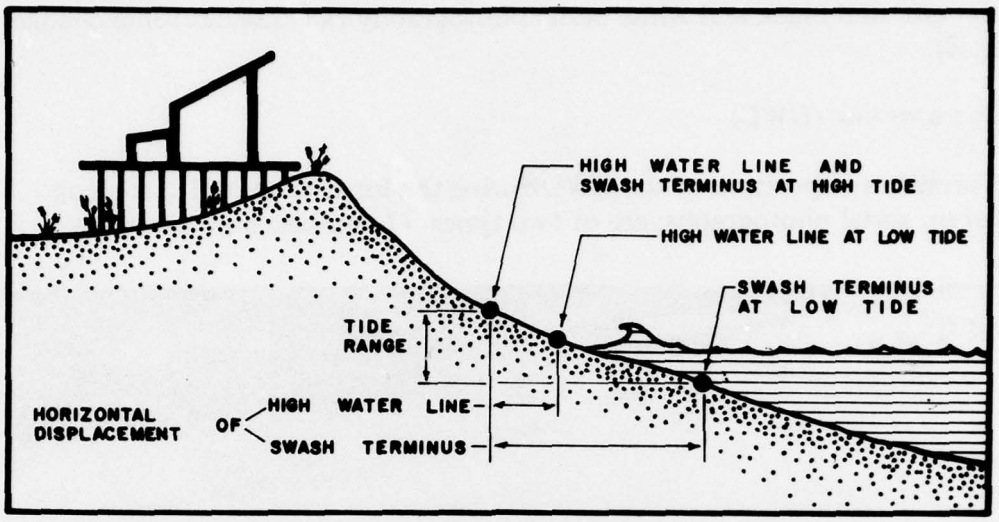

Fig. 2. Horizontal displacement of high water line vs. swash terminus.

For the purposes of shoreline recognition on aerial photographs, the major requirements are: (1) that the shoreline be easily and consistently recognizable on both black and white and color imagery; (2) that it be linearly continuous along-the-beach; and (3) that the across-the-beach variations in position due to changes in water level be at a minimum.

Nine possibilities were assessed (Table I); only the high water line was favorable for all criteria.

The high water line is re-established with each high tide as the upper beach is wetted. The resulting boundary between moist and dry sand is evident on

TABLE I

Criteria for shoreline selection

Possible operational shorelines	Criteria for shoreline selection.* 1	2	3
Line of inshore bars	no	no	yes
Mean low water	no	yes	yes
Bottom of swash zone	yes	yes	no
Mid-swash zone	yes	yes	no
Swash terminus (ST)	yes	yes	no
Mean sea level	no	yes	yes
High water line	yes	yes	yes
High tide line	no	yes	yes
Berm line	no	no	yes

*1 = That the beach-face feature (shoreline) defined be easily and consistently recognizable on both black and white and color IR imagery; 2 = that the feature be linearly continuous along-the-beach; 3 = that the across-the-beach variations be at a minimum.

both color and black and white aerial photography as a distinct tonal change (Fig. 3).

High water line (HWL)

Variations in position of the HWL during the lunar tidal cycle, as recognized on aerial photographs, are of two types: (1) up-beach movement

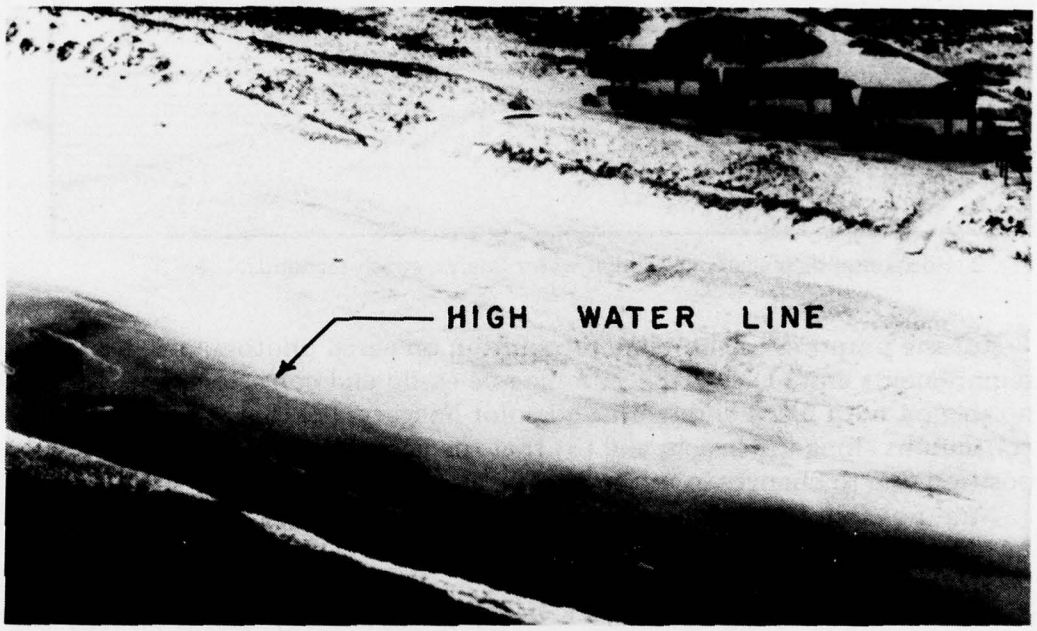

Fig. 3. Current high water line as seen on black and white oblique aerial photograph.

associated with the rising tide; and (2) down-beach movement forced by drying of the sand surface. At the time of high tide, the swash terminus (ST) and HWL are the same (Fig. 2); as the high tide falls both the ST and HWL migrate seaward. The HWL migrates much slower, however, than the ST. The extent of the horizontal displacement of the ST is a function of the slope of the beach, the tidal range, roughness of the beach face, and the wave height and period at the time of wave runup. In addition, occasional variations in water level due to longer period tidal components, storm surges and wind set-up and set-down may further increase the horizontal displacement. The extent of the horizontal displacement of the HWL landward is a function of the same factors, since on the rising tide, the HWL equals the ST. But the horizontal displacement of the HWL seaward during the falling tide has the additional factor of drying the beach sand. The drying process retards the seaward movement of the HWL, and it never retreats as far as the ST. Thus, the HWL has a smaller horizontal displacement than the ST and is, therefore, a more suitable choice for the shoreline.

STORM SURGE PENETRATION (VL)

During periods of extreme storm activity (high waves and/or wind surge) low lying coastal areas may be flooded and overwashed by sea waters. The overwash is a bore of highly turbulent, sediment-laden water which moves across the beach and onto subaerial portions of the coast. As this flow moves inland, its velocity is reduced so that at some point the flow of water can no longer transport sediments. Thus a zone of sediment transport is produced between the beach and the line of inland penetration of the bore: the zone of overwash deposit.

In the months immediately following an overwash event the newly deposited sand is clearly evident against the contrast of vegetated or developed surfaces. As time passes, vegetation encroaches on the sand deposit and the overwash zone begins to narrow. Thus there are two separate processes that give definition to the width of the overwash penetration zone: (1) overwash events that widen the zone; and (2) vegetation regrowth that narrows the zone.

The width of the overwash penetration zone is defined as the distance between the shoreline and the line (VL) of encroaching vegetation (or development) on the overwash deposit.

The width of the overwash zone is variable over time and the magnitude of this variability also changes along-the-coast. Along the Atlantic coast areas that experienced deep overwash penetration in the 1940's usually experienced deep penetration in the 1950's, 1960's and 1970's.

Measurement of shoreline and storm penetration

There are several methods available to coastal investigators to determine historical trends in shoreline change. These range from highly accurate engineering surveys to very general patterns detected by comparisons of old photographs. The paragraphs that follow summarize the advantages and disadvantages of the "standard" methods.

Repeated shoreline surveys

Cost: Data acquisition based upon field survey is very expensive because of the high man hours required.

Accuracy: Survey data are the most accurate available with resolution on the order of 0.01 m or less.

Advantages:

(1) Measurements are direct.

(2) Individual measurements may be updated at relatively moderate cost.

(3) Measurement method commonly understood by the public.

(4) Measurement commensurate with local property survey records.

Disadvantages:
(1) Historical timeline of data usually not available.
(2) Accuracy of measurement greatly exceeds the resolution of shoreline definition.
(3) Along-the-coast data density is poor.
(4) Systematic updating of extensive coastal reaches would be very expensive and time-consuming.
(5) Because surveying is time-consuming, measurements differ markedly with sea state conditions.

Metric aerial photography

Cost: Given the along-the-coast density of available data the cost is rated as low.

Accuracy: Resolution of data varies with scale of photography, normal errors are less than 5 m.

Advantages:
(1) High along-the-coast resolution.
(2) Historical data for the last 40 years usually available.
(3) Data is highly time-specific.
(4) Shoreline definition is within the resolution error of systems being analyzed.
(5) Repeated coverage is inexpensive if extensive coastal areas are included.
(6) Frequent coverage in time generally available.

Disadvantages:
(1) Longer time lines than the last 40 years are generally not available.
(2) Photointerpretation skills needed to reduce data.
(3) Variation in photography type may result in errors.
(4) Some historic photo series are classified and not available for general use.

Historic maps and charts

Cost: Map and chart derived data are generally inexpensive but cost associated with data to produce original maps is high.

Accuracy: Map accuracy is generally unavailable but may be estimated in the tens of meters.

Advantages:
(1) Maps and charts from the mid-1800's are available in the USA, thus providing an unusually long time frame for determination of mean shoreline erosion.

Disadvantages:
(1) Irregular availability.
(2) Unstable map bases.
(3) Low accuracy and resolution.
(4) No correction for sea state or tide level.

Property survey and tax maps

Cost: Where available, such data are inexpensive.

Accuracy: In general, such maps are as accurate as field survey, but definition of the shoreline is rarely defined in a systematic way and therefore errors may be on the order of tens of meters.

Advantages: (1) Availability for most commercial and residential areas.
(2) Map base understood by public at large.

Disadvantages: (1) Historical survey and tax maps are in general unavailable.
(2) Poor shoreline definition.
(3) Systematic updating unrealistic.

Non-metric photography (hand-held cameras)

Cost: Data is generally inexpensive.

Accuracy: At best, accuracy is poor with little information about either sea state or tide cycle.

Advantages: (1) Historical information is possible.

Disadvantages: (1) No systematic archives of such information is available.
(2) Photos are almost always oblique views requiring extensive correction.
(3) Scale is usually difficult to estimate.

THE ORTHOGONAL GRID ADDRESS SYSTEM (OGAS)

The analysis of shoreline dynamics for the purpose of specifying rates of erosion and coastal hazard zones requires repetitive sampling of the coastal system, both spatially and temporally. Review of the methods available leads to the conclusion that the use of metric photography is the only feasible solution to a regional or nation-wide mapping effort. The Orthogonal Grid Address System (OGAS) method has been designed to meet these needs.

In essence, the method provides for the rapid and systematic acquisition of shoreline and storm penetration information from historical aerial photographs at 100-m intervals along the coast. Comparison of the data derived from different years permits the definition of statistical properties of the coastal data sets.

Base maps

Prior to the interpretation of historical aerial photographs, standard 1 : 5,000 scale base maps of the study region are prepared. These base maps are produced by photo enlargement of 7½ minute series USGS maps (1 : 24,000). Each base map represents an area 3,500 m by 2,100 m. The frame of each base map is oriented with long side parallel to the coastline and positioned over the active portion of the coast. The long axis, lying entirely over the ocean, is the baseline from which all measurements are made (Fig. 4).

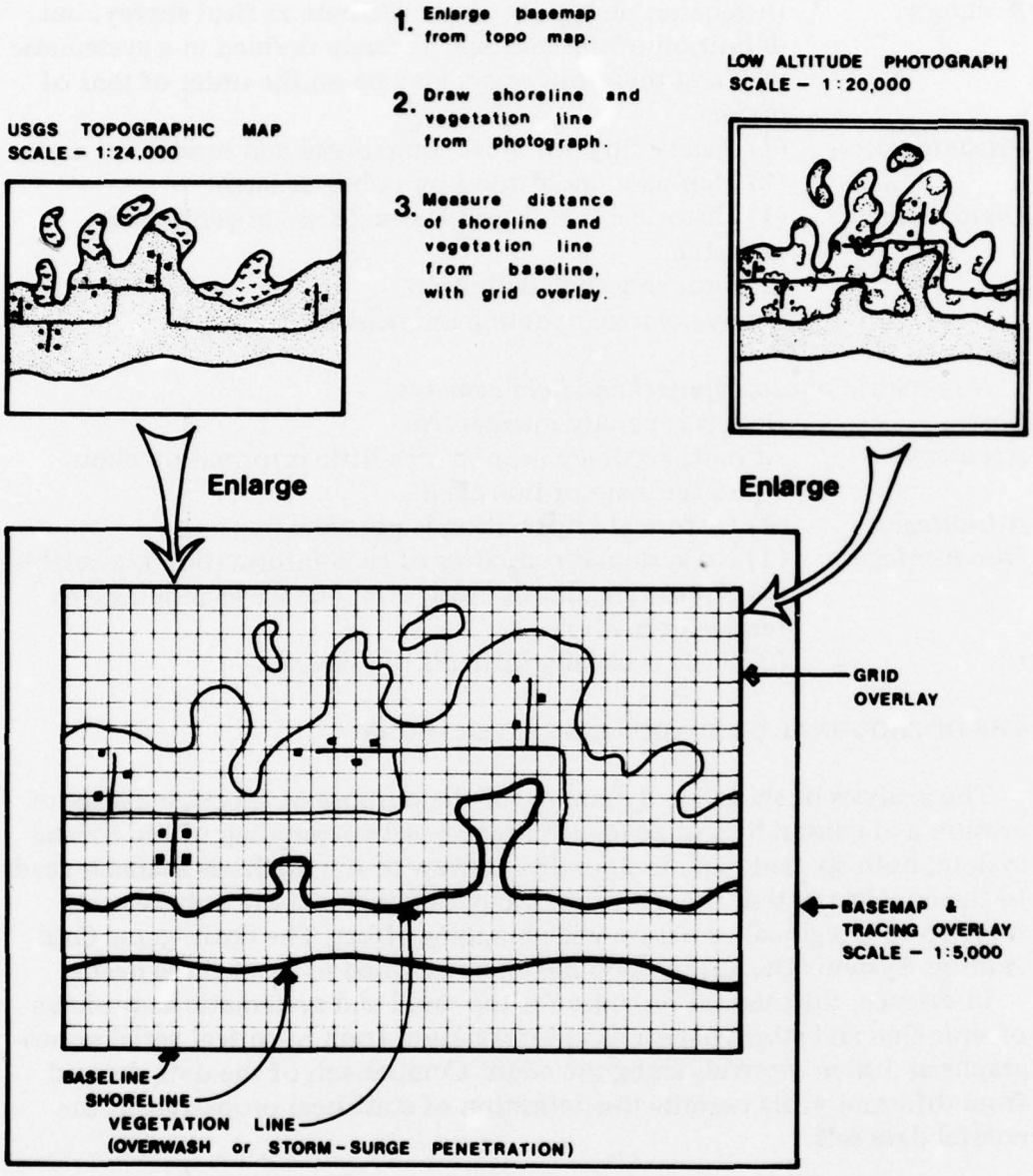

Fig. 4. Method of data collection.

Photo projection

The historical aerial photographs are then enlarged to the exact scale of the base map by projection onto the base map. On a transparent overlay placed on the base map, the shoreline (HWL) and active sand zone line (storm penetration line) are traced from the projection (Fig. 4). Such tracings prepared from 1 : 5,000 scale projections of a sequence of historical photographs constitute the raw cartographic data base from which subsequent measurements are extracted.

Grid addressing and data extraction

On each photographic tracing a transparent grid is overlaid — the grid is rectilinear with 100-m spacings. Any coastal location is thus specified by base map number and co-ordinates of the 100 × 100 m grid. The position of the shoreline and other lines of interest, with respect to the base map base line, are then measured to the nearest 5 m with a high-resolution movable cursor grid. These data are punched on IBM cards for subsequent analyses.

Computer printout of OGAS

The data contained in our OGAS output represents the location and change in location-over-time of the storm penetration line (VL) and shoreline (SL) on transects positioned at 100-m intervals perpendicular to the trend of the shoreline. The data source for our New Jersey demonstration was aerial photography for the following time periods: 1930, 1940, 1949, 1962, and 1971. As indicated earlier, the shoreline (SL) is defined as the high water line. The storm-surge penetration line (or vegetation line, VL) is defined as the line that separates the active, non-vegetated or non-developed sand areas (including non or sparsely vegetated sand dunes which show evidence of overwash penetration), from the areas of continuous stands of grass and shrub (including grass-covered dune masses that show little or no evidence of overwash penetration or development). In absence of such a vegetated or developed area, the VL in the barrier island case is defined as the bay shoreline. The values on the OGAS computer printouts for VL and SL represent the distances to the VL and SL, in meters, from the map base line located over the ocean and running parallel to the trend of the shoreline. Also listed is the storm-surge penetration distance or overwash penetration (OP). This represents the width of the active sand zone between the shoreline and the line of development or the vegetation line, and is calculated by subtracting the value for SL from the value for VL (Fig. 4).

The New Jersey coast is divided into map sections of 3.5 km in length, with a base map associated with each section. Each OGAS base map contains 36 transects, spaced 100 m apart. Each transect is identified by a map and transect number (M-TR). Thus, any point along the coast can be located to the nearest 100 m.

The computer program presently in use provides data output divided into 11 sections of tables and graphs. Tables are valuable as a permanent historical data bank; the graphs are most useful stretched out and spliced together for visual analysis. For each set of dates over all maps, changes are calculated, listed, and graphed for time periods between adjacent dates and between the first date and the last date.

The mean ± one standard deviation of rate of change of the shoreline and the storm penetration line are the most useful for determining areas of the coast which have been subjected to the greatest extremes of change (Fig. 5).

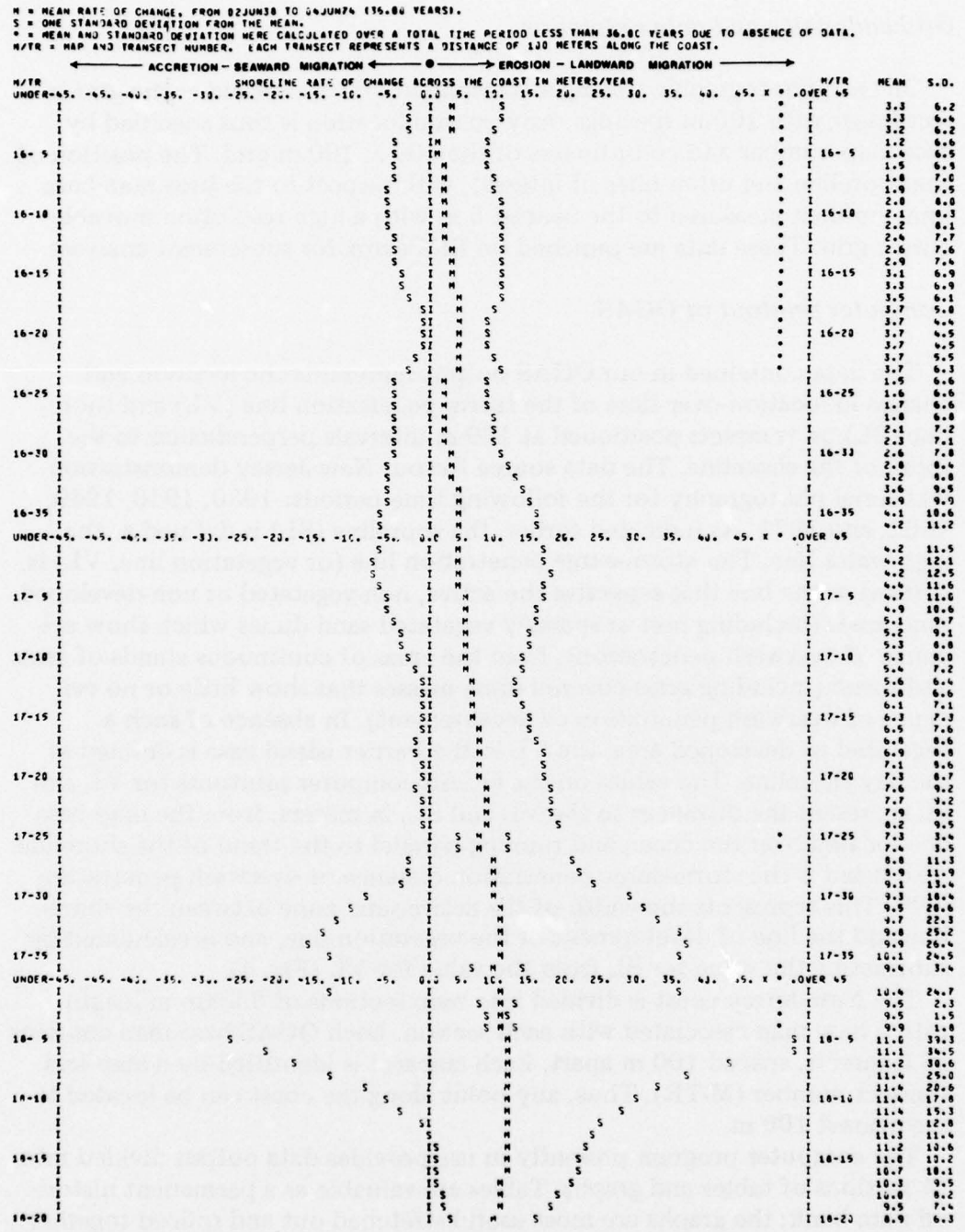

Fig. 5. Graph showing mean rate of change of shoreline ± one standard deviation.

It visually presents a measure of shoreline variability and gives an indication of the more stable versus the more vulnerable parts of the coastline. The standard deviations calculated, while based upon only five sets of photography, were found to be highly uniform along the coast. Numerical values

for mean and standard deviation at each transect are listed. The standard deviation lines that form an envelope on each side of the mean are of great value because they are a combination of the historical trend of mean change and of episodically occurring extreme storm events.

THE NEW JERSEY COAST

A demonstration of the applicability of this newly developed shoreline erosion and storm penetration measurement system was carried out along the New Jersey coast from Cape May to Little Egg Inlet, a distance of 90 km (Fig. 1). This section of the coast is not an unbroken reach of straight shoreline — it is segmented, however, into eight individual "islands" by a series of inlets. For this reason we have divided our discussion into an island-by-island treatment.

Fig. 6 shows the generalized trends of shoreline change for the eight individual segments making up the 90 km of the New Jersey coast. The wide range of shoreline dynamics suggested by these along-the-coast patterns is clear justification for not treating the 90 km of the coast as a single unit. In fact, one could even question generalizations on an island-by-island basis. Again, Fig. 6 helps evaluate this problem. Islands IV and VI have very low variance along the coast so the averages of shoreline erosion and storm penetration are good estimators. In extreme contrast, mean rates of erosion for island VIII would give poor estimates because the along-the-coast variation is is very high and the mean statistics would be representative of but a small portion of the island. Islands II and VII also have high variances; islands III and V have modest variation. Thus it is clear that island means are not necessarily the best choices for planning, design criterion or establishing risk and hazard zones for programs such as the Federal Flood Insurance Program.

The eight New Jersey islands

The shoreline at the southern end of New Jersey from Cape May Point to Cape May Inlet (Island I, Fig. 1) has eroded at an average rate of 3 m/yr. This rate has been constant during the 41 years from 1930 to 1971. The storm-surge penetration line for this reach has receded at the rate of 2.7 m/yr. The average width of the active sand zone was 60 m over 41 years, and ranged from a low of 21 m in 1949 to a high of 159 m after the Ash Wednesday storm in 1962. At one location near Cape May, the overwash penetration was 425 m as a result of the storm of March, 1962.

The coast of Wildwood from Cape May Inlet to Hereford Inlet (Island II, Fig. 1) has responded very differently to coastal processes when compared with the section south to Cape May. Both the shoreline and the overwash penetration line showed a net accretion of approximately 1 m/yr since 1930. The variability in change over time was moderate and fairly uniform along the beach. The average width of the active sand zone has remained unusually stable both temporally and spatially at just above 150 m.

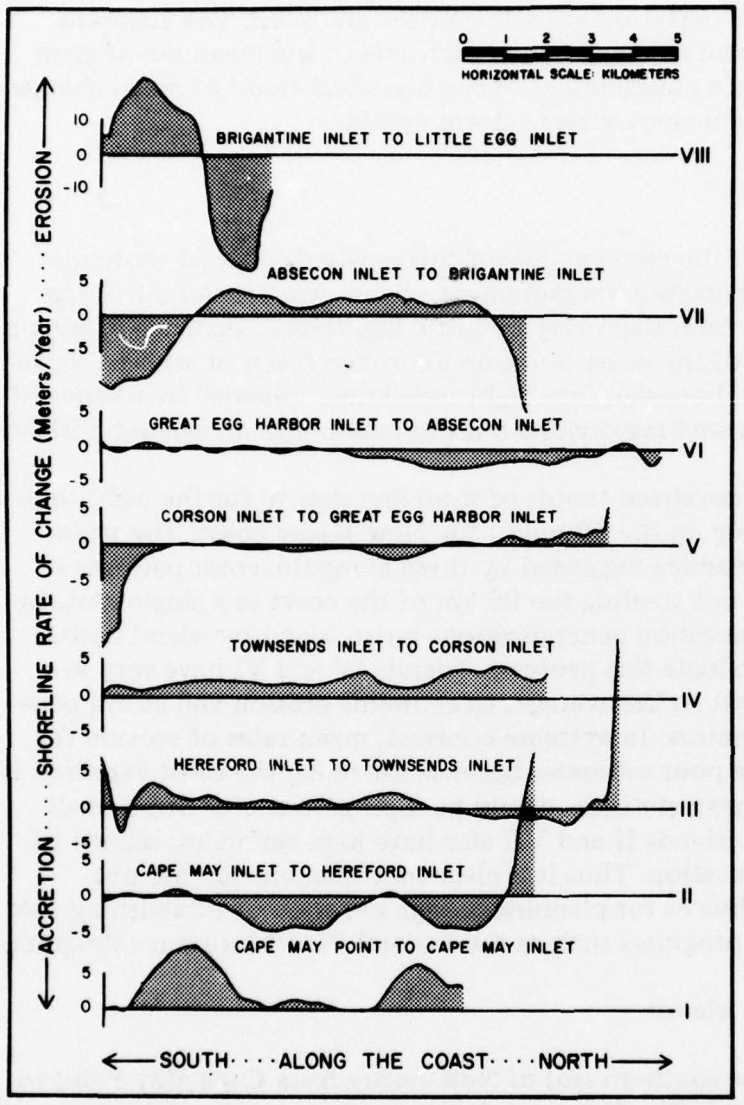

Fig. 6. Generalized trend of shoreline change for the eight barrier islands of southern New Jersey.

From Stone Harbor to Avalon between Hereford Inlet and Townsends Inlet (Island III, Fig. 1) the pattern of change is similar to that in the Cape May section. The shoreline is more stable with a mean rate of erosion of 0.7 m/yr and low variability, both spatially and temporally. The overwash penetration line is relatively low, 1.4 m/yr recession, because of massive engineering works, including sea walls and groins.

In the period from 1930 to 1971, the 11 km section of coast from Townsend Inlet to Corson Inlet (Island IV, Fig. 1) experienced erosion rates of 2.5 m/yr and overwash penetration recession of 2 m/yr. The spatial variability was very low in both cases, with a standard deviation less than 1.5.

Furthermore, the temporal variation of the shoreline was very low.

The shoreline from Corson Inlet to Great Egg Harbor Inlet including Ocean City (Island V, Fig. 1) has been stabilized by engineering works since 1930. Unlike the islands to the south, the Ocean City shoreline showed a net accretion of 26 m from 1930 to 1971, for a rate of 0.6 m/yr. This stability and minimal amount of shoreline change can be attributed in part to the extensive system of groins and sea walls on the island. The average width of the overwash penetration zone during the period 1930 to 1971 was 80 m. This nearly tripled to 217 m following the Ash Wednesday storm of 1962.

The most notable features of the coastline between Great Egg Harbor Inlet and Absecon (Island VI, Fig. 1), are its extreme vulnerability at Margate City and its extreme stability at Ventnor City and Atlantic City. The net rate of change in the overwash penetration line along this 13 km island was 0 m/yr between 1930 and 1971. Due primarily to the Ash Wednesday storm of 1962, however, the standard deviation of the rate of change of this line as measured from the five sets of photography exceeded 40 m/yr in Margate City. In Ventnor and Atlantic cities, the maximum standard deviation was 5 m/yr. Stated in other terms, the extent of storm surge penetration in Margate City due to the Ash Wednesday storm was as great as 670 m; whereas in Ventnor and Atlantic cities, the penetration seldom exceeded 100 m. The net average change in shoreline in 41 years was 27 m accretion (0.7 m/yr).

Approximately half of the shoreline between Absecon Inlet and Brigantine Inlet (Island VII, Fig. 1) is developed at the town of Brigantine. Although there are numerous groins, very little of Brigantine Beach is protected by a sea wall. The shoreline has experienced an average net accretion of 0.6 m/yr since 1930. This has, however, been highly variable. For example, a 1-km stretch of shoreline in Brigantine has been eroding at a rate of 3 m/yr; whereas the southern 2 km of the island have been accreting as much as 12 m/yr since 1930. The net change in the overwash penetration line has been seaward at a rate of 1.6 m/yr since 1930.

The 4-km section of coast between Brigantine Inlet and Little Egg Inlet (Island VIII, Fig. 1) is entirely undeveloped. The shoreline at the northern half of the island has accreted at rates higher than 30 m/yr from 1930 to 1971, while that at the sourthern half is eroding at rates in excess of 20 m/yr. The overwash penetration distance is greater than anywhere along the southern New Jersey coast, averaging 333 meters over the time periods studied.

Summary of hazards for the New Jersey islands

Along the New Jersey coast the shoreline and storm-surge penetration line covary in areas that have not been stabilized by engineering works. The mean rates of shoreline change and changes in the storm-surge penetration line for each of the 8 New Jersey study islands are plotted in Fig. 7. The nearly

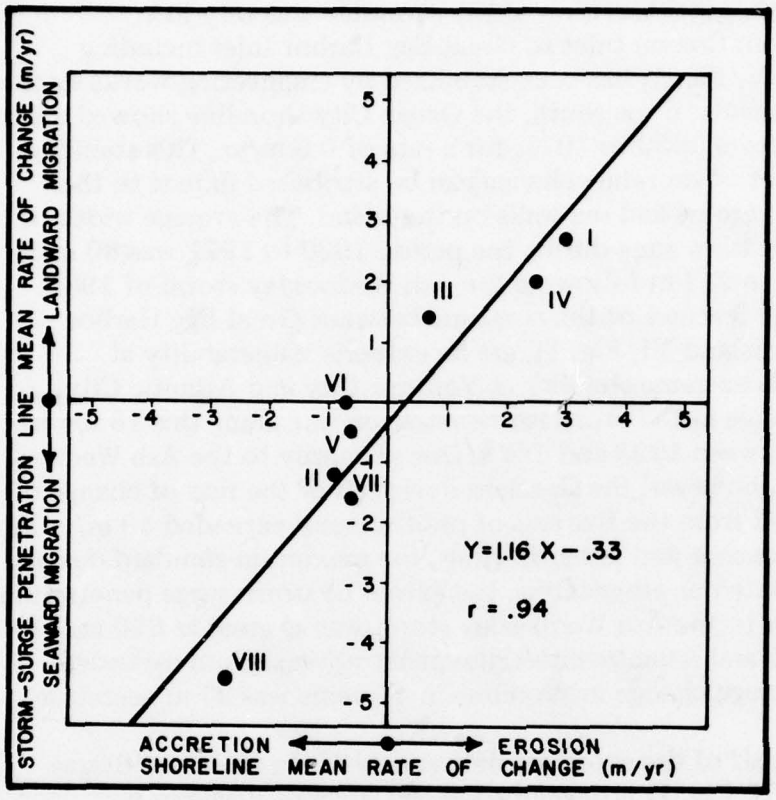

Fig. 7. Scatter plot of mean rate of change in shoreline vs. storm-surge penetration line for eight barrier islands in southern New Jersey.

linear fit of the points clearly indicates that the zone of storm-surge damage is rather constant in time and space. As the shoreline erodes, the storm-surge penetration line likewise recedes. This relationship is of practical significance because coefficients for insurance rates based on hazard probabilities would apply equally well to both erosion and storm-surge hazards.

It is also of interest to note that the standard deviations of rate of change in shoreline and storm-surge penetration line likewise covary (Fig. 8). That is, areas of highly unstable shoreline, with large excursions of the shoreline in the erosive and accretive directions, are also areas with similarly large variations in location of the storm-surge penetration line.

CONCLUSIONS

Detailed information on shoreline dynamics is required by coastal engineers, planners, and in the United States, for various sections of the National Environmental Policy Act of 1969, Coastal Zone Management Act of 1972 with 1976 amendments, and the Flood Disaster Protection Act of 1973. Since there is no program for systematic data collection in the United

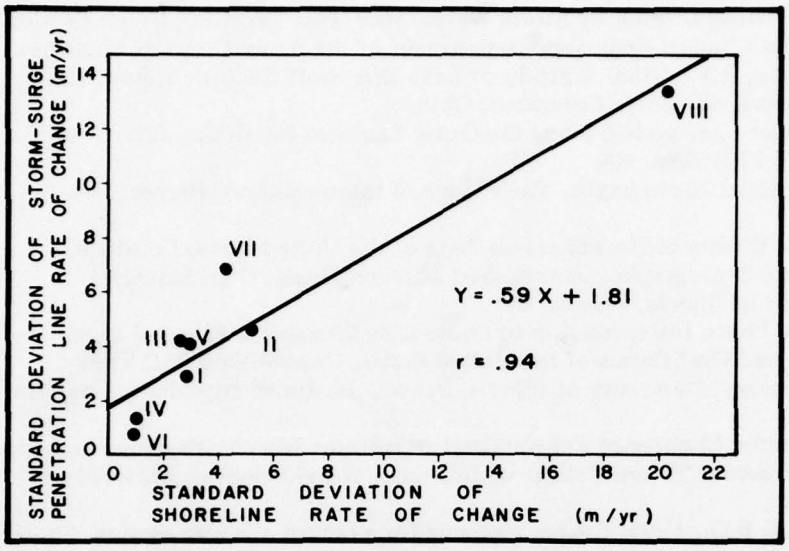

Fig. 8. Scatter plot of standard deviation of rate of change in shoreline vs. storm-surge penetration line for eight barrier islands in southern New Jersey.

States to provide this information, existing historical data must serve as the base. Of the available types of historical data only aerial photography provides a record with sufficient spatial and temporal detail for a national mapping program. The orthogonal grid address system described in this paper is designed to maximize the usefulness of the existing imagery. Finally, this research has led to the conclusion that an annual photographic record of all sections of the U.S. coastline is essential for research, planning, and shorezone management.

ACKNOWLEDGEMENTS

We wish to give special acknowledgement to our research assistant, Ms. Kathy Schroeder, who performed the aerial photograph interpretation for the historical erosion and storm-surge penetration data. The research was made possible through funding from the Department of Housing and Urban Development, NASA-Goddard Space Flight Center, and the National Park Service. Aerial photography for the New Jersey study was provided by the New Jersey Office of Shore Protection. Finally we wish to thank the Chesapeake Bay Ecological Program Office for providing services and imagery essential to the development of our method of measuring coastal change.

REFERENCES

Athearn, W.C. and Ronne, F.C., 1963. Shoreline change at Cape Hatteras: an aerial photographic study of a 17-year period. Naval Res. Rev., 17(6): 17—24.

Bruun, P., 1962. Sea-level rise as a cause of shore erosion. J. Waterways Harbors Div., 2-15.

Caldwell, J.M., 1959. Shore Erosion by Storm Waves. Misc. Pap. No. 1-59, Beach Erosion Board, Office of the Chief of Engineers, Department of the Army Corps of Engineers.

Chieruzzi, R. and Baker, R.F., 1958. A Study of Lake Erie Bluff Recession. Bull. 172, Eng. Exp. Stat. Ohio State Univ., Columbus, Ohio.

Dolan, R., 1972. Barrier dune system along the Outer Banks of North Carolina: a reappraisal. Science, V (176): 286—88.

Eardley, A.J., 1941. Aerial Photographs: Their Use and Interpretation. Harper, New York, N.Y.

El-Ashry, M.T., 1963. Effects of Hurricanes on Parts of the United States Coast Line as Illustrated by Aerial Photographs. Unpublished Master's Thesis, Department of Geology, University of Illinois, Urbana, Ill.

El-Ashry, M.T., 1966. Photo Interpretation of Shore Line Changes in Selected Areas along the Atlantic and Gulf Coasts of the United States. Unpublished PhD Thesis, Department of Geology, University of Illinois, Urbana, Ill. University Microfilms, Ann Arbor, Mich.

Gawne, C.E., 1966. Shore Changes of Fenwick and Assateague Islands, Maryland and Virginia. Unpublished Senior Thesis, College of Liberal Arts and Sciences, University of Illinois, Urbana, Ill.

Harris, W.D. and Jones, B.G., 1964. Repeat mapping for a record of shore erosion. Shore Beach, 32(2): 31—34.

Hayden, B.P., 1975. Storm wave climates at Cape Hatteras, North Carolina: recent secular variations. Science, V(190): 981—983.

Hicks, S.D. and Crosby, J.E., 1974. Trends and Variability of Yearly Mean Sea Level. NOAA Tech. Memo NOS 13, National Oceanic and Atmospheric Administration, National Ocean Survey, Rockville, Md.

Kraft, J.C., 1971. Sedimentary facies patterns and geologic history of a Holocene marine transgression. Geol. Soc. Am. Bull., V(82): 2131—2158.

Langfelder, J., Stafford, D. and Amein, M., 1968. A reconnaissance of coastal erosion in North Carolina, Project ERD — 238. Department of Civil Eng., North Carolina State University at Raleigh, 126 pp.

Langfelder, J., Stafford, D. and Amein, M., 1970. Coastal erosion in North Carolina. J. Waterw., Harbors Coastal Eng. Div., WW2, pp. 531—545.

Lucke, J.B., 1934. A study of Barnegat Inlet, New Jersey and related shore line phenomena. Shore Beach, 2(2): pp. 98—111.

McBeth, F.H., 1956. A method of shore line delineation. Photogram. Engr., 22(2): 400—405.

McCurdy, P.G., 1947. Manual of Coastal Delineation from Aerial Photographs. U.S. Navy Hydro Off. Pub. No. 592, U.S. Navy Hydrographic Office, Washington, D.C.

McCurdy, P.G., 1950. Coastal delineation from aerial photographs. Photogram. Eng., 16(4): 550—555.

Milliman, J.D. and Emery, K.O., 1968. Sea levels during the past 35,000 years. Science, V (162): 1121—1123.

Plusquellec, P.L., 1966. Coastal Morphology and Changes of an Area between Brigantine and Beach Haven Heights, New Jersey. Unpublished Master's Thesis, Department of Geology, University of Illinois, Urbana, Ill.

Rib, H.T., 1957. The Application of Aerial Photography to Beach Erosion Studies. Unpublished Master's Thesis, Department of Civil Engineering, Cornell University, Ithaca, New York, N.Y.

Shepard, F.P., Emery, K.O. and LaFond, E.D., 1941. Rip currents: a process of geological importance. J. Geol., 49(4): 337—369.

Smith, H.T.U., 1943. Aerial Photographs and Their Application. Appleton-Century-Crofts, Inc., New York, N.Y.

Stafford, D.B., 1968. Development and Evaluation of a Procedure for Using Aerial Photographs to Conduct a Survey of Coastal Erosion. Report prepared for the State of North Carolina, Dept. of Civil Engineering, North Carolina State University, Raleigh, North Carolina. (Also unpublished PhD Thesis).

Stafford, D.B., and Langfelder, J., 1971. Air photo survey of coastal erosion. Photogram. Eng., V (37):565—575.

Tanner, W.F., 1961. Mainland beach changes due to hurricane Donna. J. Geophys. Res., 66(7): 2265—2266.

Williams, W.W., 1960. Coastal Changes. Routledge and Kegan Paul, Limited, London.

Wolman, Gordon M., 1971. The nation's rivers. Science, V (174): 905—918.

Zeigler, J.M. and Ronne, F.C., 1957. Time-lapse photography — an aid to the studies of the shoreline. Naval Res. Rev., (4): 1—6.

PECK BEACH SOUTH NEW JERSEY

STORM SURGE PENETRATION
STANDARD DEVIATION (σ_{SP})

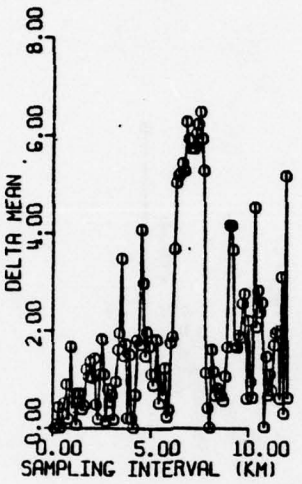

56A

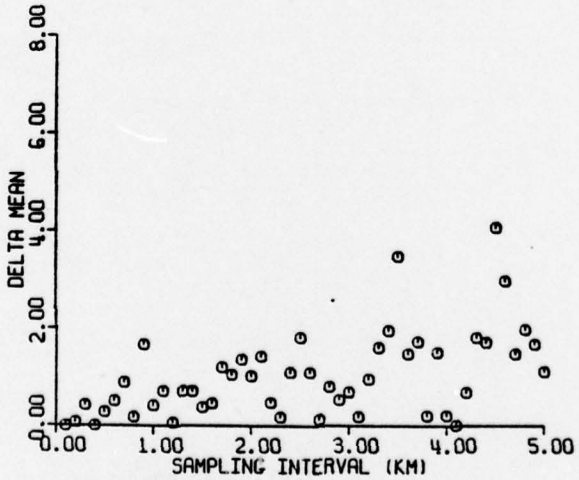

56B

VENTNOR ISLAND SOUTH NEW JERSEY

MEAN SHORELINE RATE ($\overline{SL}$)

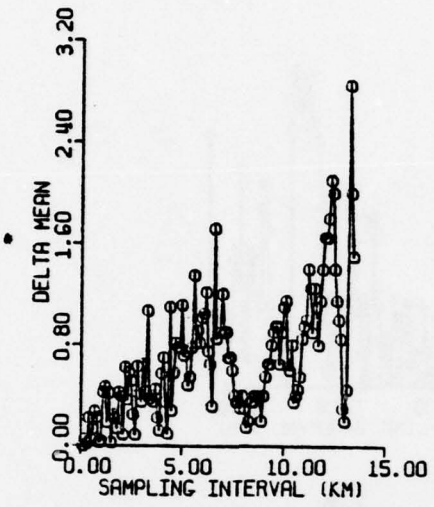

57A

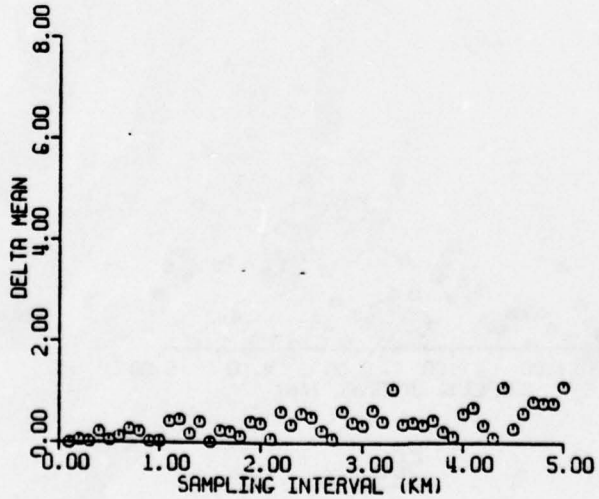

57B

VENTNOR ISLAND SOUTH NEW JERSEY

SHORELINE RATE STANDARD DEVIATION (σ_{SL})

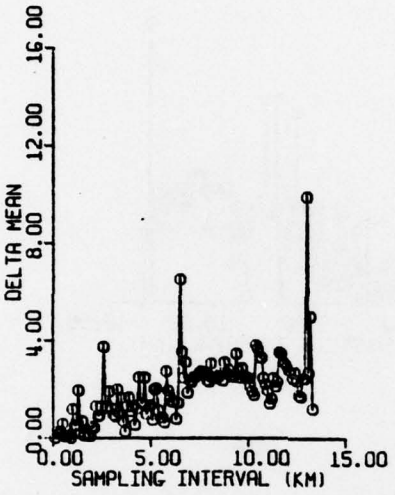

58A

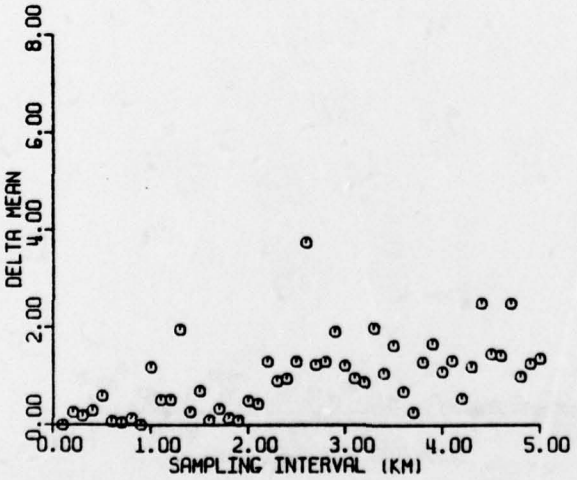

58B

VENTNOR ISLAND SOUTH NEW JERSEY

MEAN STORM SURGE PENETRATION ($\overline{SP}$)

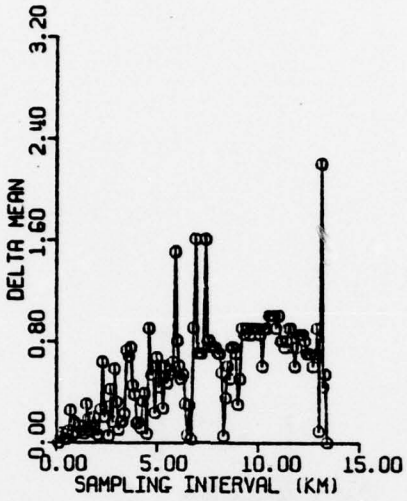

59A

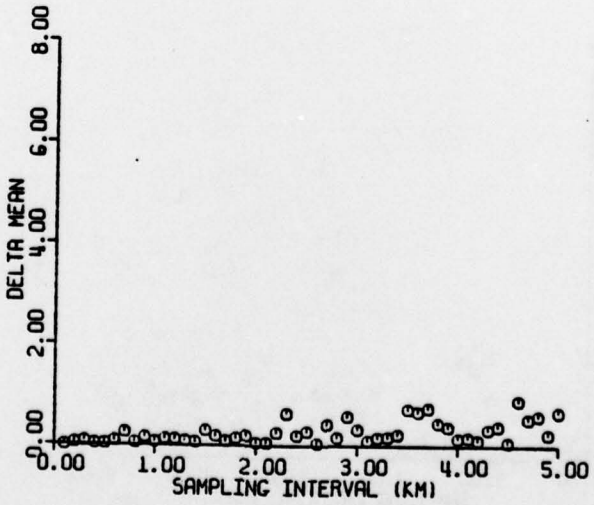

59B

VENTNOR ISLAND SOUTH NEW JERSEY

STORM SURGE PENETRATION
STANDARD DEVIATION (σ_{SP})

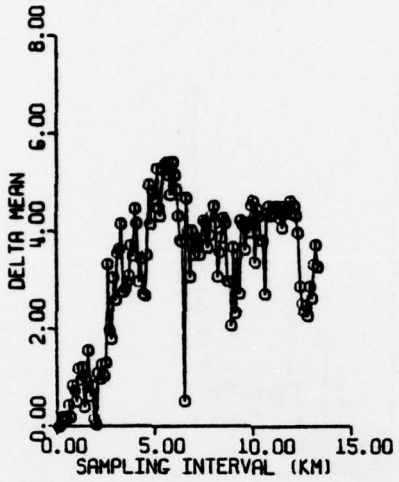

60A

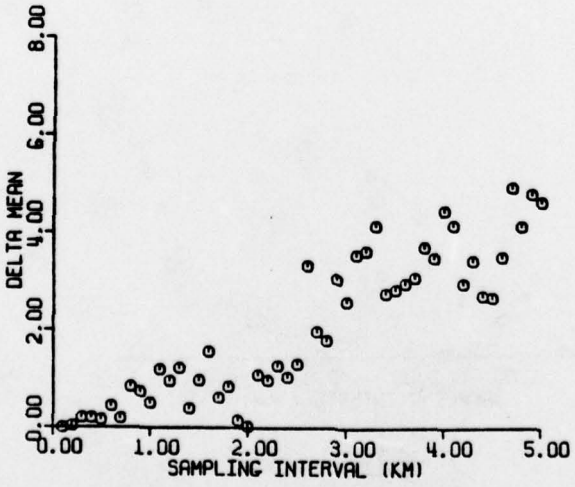

60B

BRIGANTINE ISLAND
SOUTH NEW JERSEY

SHORELINE MEAN RATE ($\overline{SL}$)

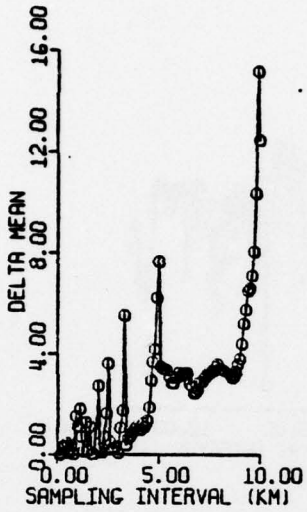

61A

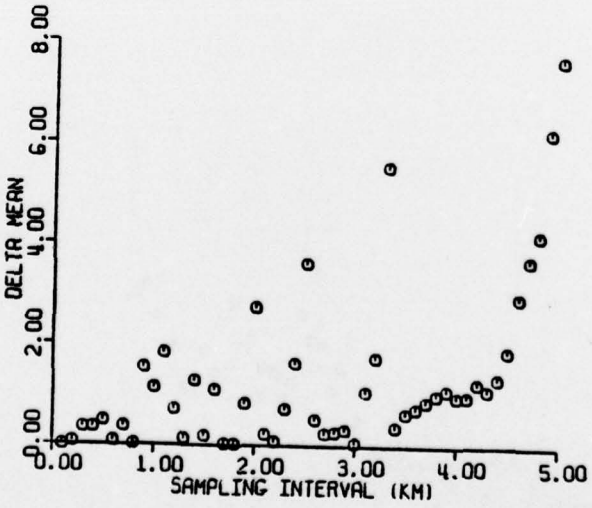

61B

BRIGANTINE ISLAND
SOUTH NEW JERSEY

SHORELINE RATE STANDARD DEVIATION
(σ_{SL})

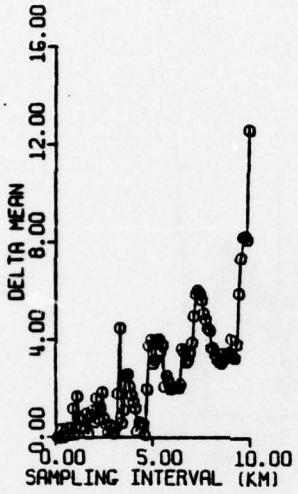

62A

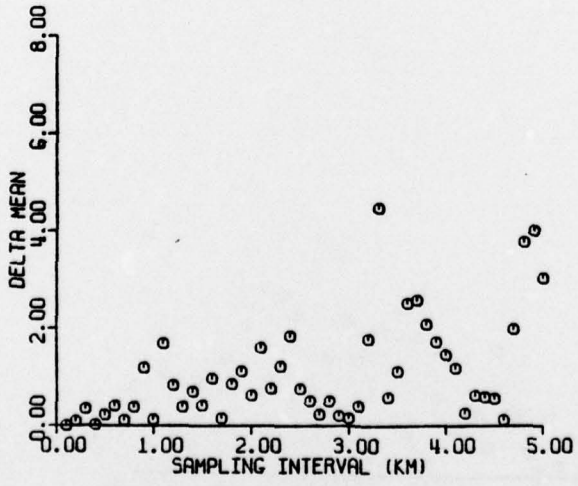

62B

BRIGANTINE ISLAND
SOUTH NEW JERSEY

MEAN STORM SURGE PENETRATION ($\overline{SP}$)

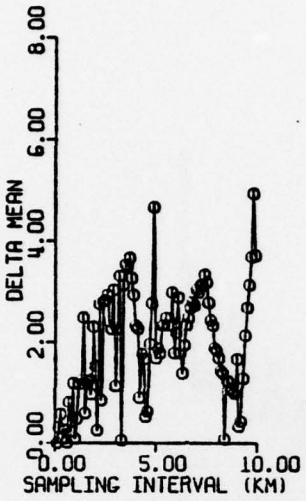

63A

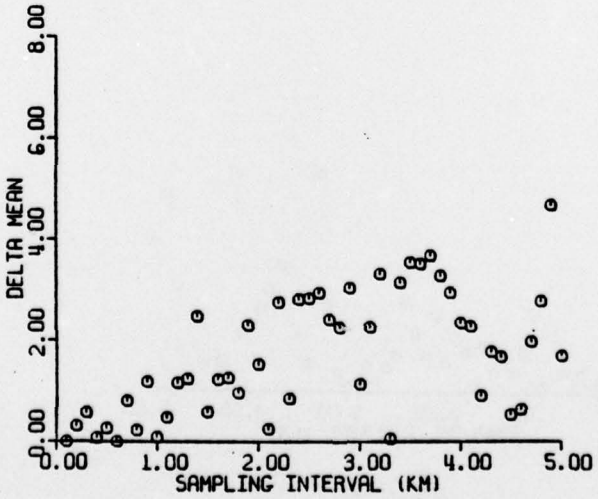

63B

BRIGANTINE ISLAND
SOUTH NEW JERSEY

STORM SURGE PENETRATION
STANDARD DEVIATION (σ_{SP})

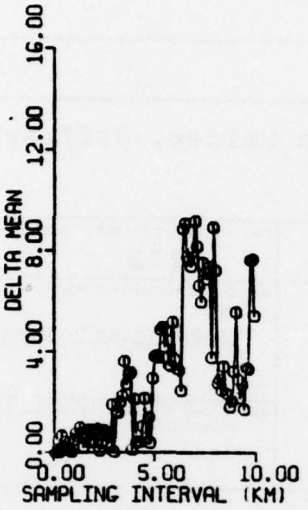

64A

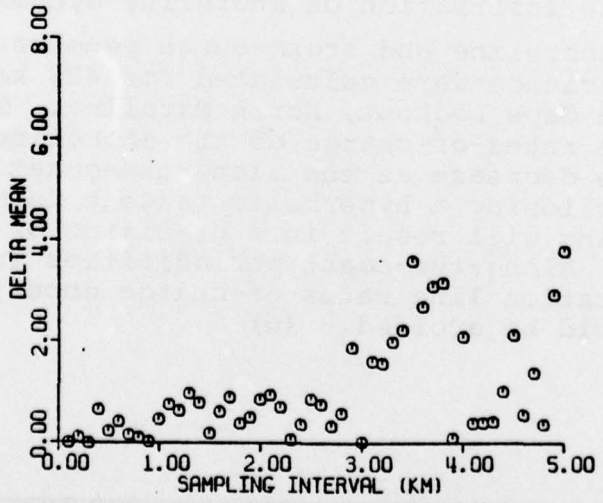

64B

Security Classification

DOCUMENT CONTROL DATA - R & D

(Security classification of title, body of abstract and indexing annotation must be entered when the overall report is classified)

1. ORIGINATING ACTIVITY *(Corporate author)*
Department of Environmental Sciences
University of Virginia
Charlottesville, Virginia 22903

2a. REPORT SECURITY CLASSIFICATION
Unclassified

2b. GROUP
Unclassified

3. REPORT TITLE
Analysis of Spatial and Temporal Shoreline Variations Along the United States Atlantic Coast

4. DESCRIPTIVE NOTES *(Type of report and inclusive dates)*

5. AUTHOR(S) *(First name, middle initial, last name)*
Robert Dolan, Bruce Hayden, Wilson Felder, Jeffrey Heywood, Phyllis Ross

6. REPORT DATE
September, 1977

7a. TOTAL NO. OF PAGES
122

7b. NO. OF REFS
35

8a. CONTRACT OR GRANT NO.
N00014-75-C-0480

b. PROJECT NO.
NR 389-170

c.

d.

9a. ORIGINATOR'S REPORT NUMBER(S)
Technical Report No. 19

9b. OTHER REPORT NO(S) *(Any other numbers that may be assigned this report)*

10. DISTRIBUTION STATEMENT
Approved for public release-distribution unlimited

11. SUPPLEMENTARY NOTES

12. SPONSORING MILITARY ACTIVITY
Office of Naval Research
Geography Programs
Arlington, VA 22217

13. ABSTRACT

An historical aerial photography methodology for deriving along- and across-the-coast risk probabilities is summarized.

Aerial photography of the southern New Jersey coast covering four decades is used to demonstrate this methodology and to provide long-term baseline information on shoreline dynamics.

High resolution shoreline and storm-surge penetration line rates-of-change and variance were calculated for 428 km of coast between New Jersey and Cape Lookout, North Carolina. The precision of measurements of the rates-of-change of the shoreline and storm-surge penetration line decrease as the along-the-coast sampling interval increases, following a hyperbolic tangent form of decline. A 500-m sampling spacing will result in a precision of $\pm$ .75 m/yr for shoreline change. Along-the-coast periodicities in shoreline and storm-surge penetration line rates-of-change occur; a constant interval sampling should be avoided. (u)

DD FORM 1 NOV 65 1473 (PAGE 1)

S/N 0101-807-6801

Unclassified
Security Classification

14. KEY WORDS	LINK A		LINK B		LINK C	
	ROLE	WT	ROLE	WT	ROLE	WT
Atlantic coast erosion accretion hyperbolic tangent photogrammetry shoreline variations						

OCT. 26, 1977 JOB 460-101

SYSTEMATIC GEOGRAPHY LISTING

0001 1 OFFICE OF NAVAL RESEARCH 2 COPIES
0001 2 GEOGRAPHY PROGRAMS
0001 3 CODE 462
0001 4 ARLINGTON, VIRGINIA 22217

0002 1 DEFENSE DOCUMENTATION CENTER 12 COPIES
0002 2 CAMERON STATION
0002 3 ALEXANDRIA, VIRGINIA 22314

0003 1 DIRECTOR, NAVAL RESEARCH LAB 6 COPIES
0003 2 ATTENTION TECHNICAL INFORMATION OFFICER
0003 3 WASHINGTON, D. C. 20375

0004 1 DIRECTOR
0004 2 OFFICE OF NAVAL RESEARCH BRANCH OFFICE
0004 3 1030 EAST GREEN STREET
0004 4 PASADENA, CALIFORNIA 91101

0005 1 DIRECTOR
0005 2 OFFICE OF NAVAL RESEARCH BRANCH OFFICE
0005 3 536 SOUTH CLARK STREET
0005 4 CHICAGO, ILLINOIS 60605

0006 1 DIRECTOR
0006 2 OFFICE OF NAVAL RESEARCH BRANCH OFFICE
0006 3 495 SUMMER STREET
0006 4 BOSTON, MASSACHUSETTS 02210

0007 1 COMMANDING OFFICER
0007 2 OFFICE OF NAVAL RESEARCH BRANCH OFFICE
0007 3 BOX 39
0007 4 FPO NEW YORK 09510

0008 1 CHIEF OF NAVAL RESEARCH
0008 2 ASST. FOR MARINE CORPS MATTERS
0008 3 CODE 100M
0008 4 OFFICE OF NAVAL RESEARCH
0008 5 ARLINGTON, VIRGINIA 22217

0009 1 OFFICE OF NAVAL RESEARCH
0009 2 CODE 480
0009 3 NATIONAL SPACE TECHNOLOGY LABORATORIES
0009 4 BAY ST. LOUIS, MISSISSIPPI 39520

0010 1 OFFICE OF NAVAL RESEARCH
0010 2 OPERATIONAL APPLICATIONS DIVISION
0010 3 CODE 200
0010 4 ARLINGTON, VIRGINIA 22217

OCT. 26, 1977 JOB 460-101

SYSTEMATIC GEOGRAPHY LISTING

0011	1	OFFICE OF NAVAL RESEARCH
0011	2	SCIENTIFIC LIAISON OFFICER
0011	3	SCRIPPS INSTITUTION OF OCEANOGRAPHY
0011	4	LA JOLLA, CALIFORNIA 92093
0012	1	DIRECTOR, NAVAL RESEARCH LABORATORY
0012	2	ATTN LIBRARY, CODE 2628
0012	3	WASHINGTON, D. C. 20375
0013	1	ONR SCIENTIFIC LIAISON GROUP
0013	2	AMERICAN EMBASSY - ROOM A-407
0013	3	APO SAN FRANCISCO 96503
0101	1	COMMANDER
0101	2	NAVAL OCEANOGRAPHIC OFFICE
0101	3	ATTN. LIBRARY CODE 1600
0101	4	WASHINGTON, D. C. 20374
0102	1	NAVAL OCEANOGRAPHIC OFFICE
0102	2	CODE 3001
0102	3	WASHINGTON, D. C. 20374
0103	1	CHIEF OF NAVAL OPERATIONS
0103	2	OP 987P1
0103	3	DEPARTMENT OF THE NAVY
0103	4	WASHINGTON, D. C. 20350
0104	1	OCEANOGRAPHER OF THE NAVY
0104	2	HOFFMAN II BUILDING
0104	3	200 STOVALL STREET
0104	4	ALEXANDRIA, VIRGINIA 22322
0105	1	NAVAL ACADEMY LIBRARY
0105	2	U. S. NAVAL ACADEMY
0105	3	ANNAPOLIS, MARYLAND 21402
0106	1	COMMANDING OFFICER
0106	2	NAVAL COASTAL SYSTEMS LABORATORY
0106	3	PANAMA CITY, FLORIDA 32401
0107	1	LIBRARIAN
0107	2	NAVAL INTELLIGENCE
0107	3	SUPPORT CENTER
0107	4	4301 SUITLAND ROAD
0107	5	WASHINGTON, D. C. 20390

OCT. 26, 1977 JOB 460-101

SYSTEMATIC GEOGRAPHY LISTING

0112 1 OFFICER IN CHARGE
0112 2 ENVIRONMENTAL RESEARCH PRDCTN FCLTY
0112 3 NAVAL POSTGRADUATE SCHOOL
0112 4 MONTEREY, CALIFORNIA 93940

0201 1 COMMANDING GENERAL
0201 2 MARINE CORPS DEVELOPMENT AND
0201 3 EDUCATIONAL COMMAND
0201 4 QUANTICO, VIRGINIA 22134

0202 1 DR. A. L. SLAFKOSKY
0202 2 SCIENTIFIC ADVISOR
0202 3 COMMANDANT OF THE MARINE CORPS
0202 4 CODE MC-RD-1
0202 5 WASHINGTON, D. C. 20380

1001 1 DEFENSE INTELLIGENCE AGENCY
1001 2 CENTRAL REFERENCE DIVISION
1001 3 CODE RDS-3
1001 4 WASHINGTON, D. C. 20301

1002 1 DIRECTOR
1002 2 DEFENSE MAPPING TOPOGRAPHIC CENTER
1002 3 ATTN= CODE 50200
1002 4 WASHINGTON, D. C. 20315

1003 1 COMMANDING OFFICER
1003 2 U.S. ARMY ENGINEERING
1003 3 TOPOGRAPHIC LABORATORY
1003 4 ATTN= ETL-ST
1003 5 FORT BELVOIR, VIRGINIA 22060

1005 1 CHIEF, WAVE DYNAMICS DIVISION
1005 2 USAE-WES
1005 3 P. O. BOX 631
1005 4 VICKSBURG, MISSISSIPPI 39180

2003 1 NATIONAL OCEANOGRAPHIC DATA
2003 2 CENTER ID764
2003 3 ENVIRONMENTAL DATA SERVICES
2003 4 NOAA
2003 5 WASHINGTON, D. C. 20235

2005 1 CENTRAL INTELLIGENCE AGENCY
2005 2 ATTENTION OCR/DD-PUBLICATIONS
2005 3 WASHINGTON, D. C. 20505

OCT. 26, 1977 JOB 460-101

SYSTEMATIC GEOGRAPHY LISTING

2007	1	DR. MARK M. MACOMBER
2007	2	ADVANCED TECHNOLOGY DIVISION
2007	3	DEFENSE MAPPING AGENCY
2007	4	NAVAL OBSERVATORY
2007	5	WASHINGTON, D. C. 20390
5001	1	MINISTERIALDIREKTOR DR. F. WEVER
5001	2	RUE/FO
5001	3	BUNDESMINISTERIUM DER VERTEIDIGUNG
5001	4	HARDTHOEHE
5001	5	D-5300 BONN, WEST GERMANY
5002	1	OBERREGIERUNGSRAT DR. ULLRICH
5002	2	RUE/FO
5002	3	BUNDESMINISTERIUM DER VERTEIDIGUNG
5002	4	HARDTHOEHE
5002	5	D-5300 BONN, WEST GERMANY
5003	1	MR. TAGE STRARUP
5003	2	DEFENCE RESEARCH ESTABLISHMENT
5003	3	OSTERBROGADES KASERNE
5003	4	DK-2100 KOBENHAVN O, DENMARK
5302	1	IR. M. W. VAN BATENBERG
5302	2	PHYSISCH LABORATORIUM TNO
5302	3	OUDE WAALSDORPER WEG 63, DEN HAAG
5302	4	NETHERLANDS
8002	1	COASTAL STUDIES INSTITUTE
8002	2	LOUISIANA STATE UNIVERSITY
8002	3	BATON ROUGE, LOUISIANA 70803
8003	1	DR. CHOULE J. SONU
8003	2	TETRA TECH, INC.
8003	3	630 NORTH ROSEMEAD BOULEVARD
8003	4	PASADENA, CALIFORNIA 91107
9001	1	DR. LESTER A. GERHARDT
9001	2	RENNSSELAER POLYTECHNIC INSTITUTE
9001	3	TROY, NEW YORK 12181
9002	1	MR. FRED THOMSON
9002	2	ENVIRONMENTAL RESEARCH INSTITUTE
9002	3	P.O. BOX 618
9002	4	ANN ARBOR, MICHIGAN 48107

OCT. 26, 1977 JOB 460-101

SYSTEMATIC GEOGRAPHY LISTING

9004 1 DR. THOMAS K. PEUCKER
9004 2 SIMON FRASER UNIVERSITY
9004 3 DEPARTMENT OF GEOGRAPHY
9004 4 BURNABY 2, B. C., CANADA

9005 1 DR. ROBERT DOLAN
9005 2 DEPARTMENT OF ENVIRONMENTAL SCIENCES
9005 3 UNIVERSITY OF VIRGINIA
9005 4 CHARLOTTESVILLE, VIRGINIA 22903